12-2011

MODELLING β2AR REGULATION

Sharat J. Vayttaden

Recommended Citation

Modelling β2AR Regulation

by

Sharat Jacob Vayttaden, MS

APPROVED:

Richard B. Clark, PhD (Chair)

Joseph L. Alcorn, PhD

Carmen W. Dessauer, PhD

Agnes Schonbrunn, PhD

Prahlad T. Ram, PhD

APPROVED:

Dean, The University of Texas
Health Science Center at Houston,
Graduate School of Biomedical Sciences

Modelling β2AR Regulation

A Dissertation

Presented to the Faculty of

The University of Texas Health Science Center at Houston

And

The University of Texas M.D. Anderson Cancer Center

Graduate School of Biomedical Sciences

In Partial Fulfillment of

The Requirements for the Degree of

Doctor of Philosophy

By

Sharat Jacob Vayttaden, MS

Houston, Texas

December 2011

Modelling β2AR Regulation

Publication No._____

Sharat J. Vayttaden, M.S.

Supervisory Professor: Richard B. Clark, Ph.D.

The β2 adrenergic receptor (β2AR) regulates smooth muscle relaxation in the
vasculature and airways. Long- and Short-acting β-agonists (LABAs/SABAs) are
widely used in treatment of chronic obstructive pulmonary disorder (COPD) and
asthma. Despite their widespread clinical use we do not understand well the dominant
β2AR regulatory pathways that are stimulated during therapy and bring about
tachyphylaxis, which is the loss of drug effects. Thus, an understanding of how the
β2AR responds to various β-agonists is crucial to their rational use. Towards that end
we have developed deterministic models that explore the mechanism of drug- induced
β2AR regulation. These mathematical models can be classified into three classes; (i)
Six quantitative models of SABA-induced G protein coupled receptor kinase (GRK)-
mediated β2AR regulation; (ii) Three phenomenological models of salmeterol (a
LABA)-induced GRK-mediated β2AR regulation; and (iii) One semi-quantitative,
unified model of SABA-induced GRK-, protein kinase A (PKA)-, and
phosphodiesterase (PDE)-mediated regulation of β2AR signalling. The various models
were constrained with all or some of the following experimental data; (i) GRK-mediated
β2AR phosphorylation in response to various LABAs/SABAs; (ii) dephosphorylation of
the GRK site on the β2AR; (iii) β2AR internalisation; (iv) β2AR recycling; (v) β2AR
desensitisation; (vi) β2AR resensitisation; (vii) PKA-mediated β2AR phosphorylation in

response to a SABA; and (viii) LABA/SABA induced cAMP profile ± PDE inhibitors. The models of GRK-mediated β2AR regulation show that plasma membrane dephosphorylation and recycling of the phosphorylated β2AR are required to reconcile with the measured dephosphorylation kinetics. We further used a consensus model to predict the consequences of rapid pulsatile agonist stimulation and found that although resensitisation was rapid, the β2AR system retained the memory of prior stimuli and desensitised much more rapidly and strongly in response to subsequent stimuli. This could explain tachyphylaxis of SABAs over repeated use in rescue therapy of asthma patients. The LABA models show that the long action of salmeterol can be explained due to decreased stability of the arrestin/β2AR/salmeterol complex. This could explain long action of β-agonists used in maintenance therapy of asthma patients. Our consensus model of PKA/PDE/GRK-mediated β2AR regulation is being used to identify the dominant β2AR desensitisation pathways under different therapeutic regimens in human airway cells. In summary our models represent a significant advance towards understanding agonist-specific β2AR regulation that will aid in a more rational use of the β2AR agonists in the treatment of asthma.

Acknowledgements

Table of Contents

List of Figures

6.   **Conclusions and Future Work**

List of Tables

Introduction

1.1. GPCRs

The G protein-coupled, seven-transmembrane receptors (GPCRs or 7TM receptors) are encoded by one of the largest gene families (Vroling, Sanders et al. 2011). They are targeted by > 25% FDA approved drugs (Flower 1999; Overington, Al-Lazikani et al. 2006). Based on hydropathy profiles and the crystal structure of bovine rhodopsin (Palczewski, Kumasaka et al. 2000) and human β2 adrenergic receptor (β2AR) (Cherezov, Rosenbaum et al. 2007; Rasmussen, Choi et al. 2007; Rosenbaum, Cherezov et al. 2007) all GPCRs are thought to have the same molecular architecture, consisting of seven trans-membrane domains, three extra- and intra-cellular loops, an extracellular amino-terminal and an intracellular carboxyl-terminal domain. GPCRs are named thus due to their action as guanine-nucleotide exchange factors at the heterotrimeric G proteins (comprising of an α-, β- and γ-subunit) leading to the exchange of GDP for GTP bound to the α-subunit post GPCR activation (Gilman 1987; Johnston and Siderovski 2007). The GTP-bound α-subunit and the released βγ-dimer of the G protein can stimulate or inhibit effector molecules like adenylyl and guanylyl cyclases, phospholipases, phosphodiesterases and phosphoinositide 3-kinases (PI3Ks) (Rall and Sutherland 1962; Sutherland, Rall et al. 1962; Jelsema and Axelrod 1987; Tang and Gilman 1991; Camps, Carozzi et al. 1992). This in turn activates or inhibits the production of second messengers like cyclic adenosine monophosphate (cAMP), cyclic guanosine monophosphate (cGMP), diacylglycerol (DAG), inositol trisphosphate (IP3), phosphatidyl inositol trisphosphate (PIP3), arachidonic acid (AA) and

phosphatidic acid (PA), in addition to the opening or closing of a variety of ion channels (Sutherland and Robison 1966; Hardman, Robison et al. 1971; Goldberg, O'Dea et al. 1973; Lapetina and Michell 1973; Brindley and Waggoner 1996).

GPCRs can be classified into six families based on functional similarity and sequence homology (Attwood and Findlay 1994; Kolakowski 1994; Bjarnadottir, Gloriam et al. 2006). The similarity in 7TM topology across GPCR families is believed to be due to evolutionary convergence (Bockaert and Pin 1999). GPCR families have >20% amino acid sequence similarity within their trans-membrane helices (Kolakowski 1994; Kristiansen 2004). β2AR belongs to the family of Rhodospsin-like GPCRs. This Class A family is classified into 19 subgroups (A1-A19) based on phylogenetic analysis of 241 sequences (Joost and Methner 2002), and the β2AR which is a Gαs-coupled GPCR belongs to subfamily A17.

1.1.1. Adrenergic Receptor Classification

Adrenergic receptors are a Class A GPCR that are targetted by catecholamines like norepinephrine and epinephrine. They can be classified into two groups, α and β, with subtypes in each group. The α receptors are either α1 or α3 where they are coupled to Gq and Gi respectively. All three subtypes of β receptors – β1, β 2 and β3 are coupled to Gs and can activate adenylyl cyclases leading to cAMP-mediated downstream signalling. The major locale of β1AR is the cardiac muscle where it is involved in regulation of cardiac output by increasing speed and force of contraction. The β2AR is near ubiquitously expressed and regulates smooth muscle relaxation in uterus, GI

tract, bronchi and blood vessels. The β3AR is predominantly found in adipose tissue and regulates lipolysis and thermogenesis.

1.1.2. Role of β2AR in Smooth Muscle Relaxation

β2AR agonists increase cAMP levels in airway smooth muscle that is consistent with their relaxation response (Katsuki and Murad 1977; Wong and Buckner 1978; Rinard, Rubinfeld et al. 1979; Zhou, Newsholme et al. 1992). Phosphodiesterases degrade cAMP and abrogate cAMP-mediated signalling. Phosphodiesterase inhibitors (*4,5-dihydro-6-[4-(1H-imidazol-1-yl)phenyl]-5-methyl-3(2H)-pyridazinone (CI-930), 3-isobutyl-1-methylxanthine (IBMX), 4-(3-Butoxy-4-methoxybenzyl)-2-imidazolidinone (Ro 20-1724), rolipram, siguazodan, SK&F 94120* and *zaprinast*) mimic and increase the response to β2AR agonists (Harris, Connell et al. 1989; Torphy, Zhou et al. 1991; Qian, Naline et al. 1993; Torphy, Undem et al. 1993). cAMP analogues (*8-(4-chlorophenylthio)-cAMP, 8-bromo-cAMP, 8-(6-aminohexylamino)-cAMP, N6-benzoyl-cAMP, N6-2'-O-dibutyryl-cAMP* and *N6-monobutyryl cAMP*) mimic the relaxation effect of β2AR agonists (Bresnahan, Borowitz et al. 1975; Napoli, Gruetter et al. 1980; Heaslip, Giesa et al. 1987; Francis, Noblett et al. 1988). β2AR agonists regulate cAMP-dependent protein kinase A (PKA) in airway smooth muscle consistent with the relaxation response (Torphy, Freese et al. 1982; Giembycz and Diamond 1990; Zhou, Newsholme et al. 1992). Myosin Light Chain Phosphatase (MLCP) can be activated by cyclic GMP/AMP activated kinases (Janssen, Tazzeo et al. 2004). cAMP can also cross activate cyclic GMP activated kinase (PKG) in smooth muscle (Francis, Noblett et al.

3

1988). PKA phosphorylation of the IP3 receptor inhibits binding of IP3 to the receptor. This reduces release of calcium from internal pools in response to bronchioconstrictors (Schramm, Chuang et al. 1995).

Bronchioconstrictors can activate kinases like ROCK which inactivate MYPT1 a subunit of MLCP. This inhibitory phosphorylation on MYPT1 can be blocked by phosphorylation of MYPT1 by PKG/PKA (Wooldridge, MacDonald et al. 2004). MLCK can be activated by ERK1(Morrison, Sanghera et al. 1996). MAPK Phosphatase 1 (MKP1) dephosphorylates and inactivates ERK1. MKP1 can be activated by agonist activation of β2AR (Brondello, Brunet et al. 1997; Price, Chik et al. 2004). β2AR activation by agonists leads to membrane hyperpolarisation through activation of big conductance Ca^{2+} activated K channels (BKCa) in the plasma membrane counteracting electrical excitation and subsequent Ca^{2+} influx. Iberiotoxin mediated inhibition of BKCa prevents hyperpolarisation and β2AR mediated ASM relaxation (Jones, Charette et al. 1993). The α subunit of BKCa has been shown to interact with β2AR and AKAP79 in ASM (Liu, Shi et al. 2004). PKA phosphorylation of the BKCa channel subunits has an activating or inactivating effect based on the splice isoform (Tian, Coghill et al. 2004). PKG also differentially activates various splice isoforms of the BKCa channel (Zhou, Arntz et al. 2001). All this (Figure 1.1) provides compelling evidence that β2AR activation mediates smooth muscle relaxation through both cAMP-dependent and -independent signalling.
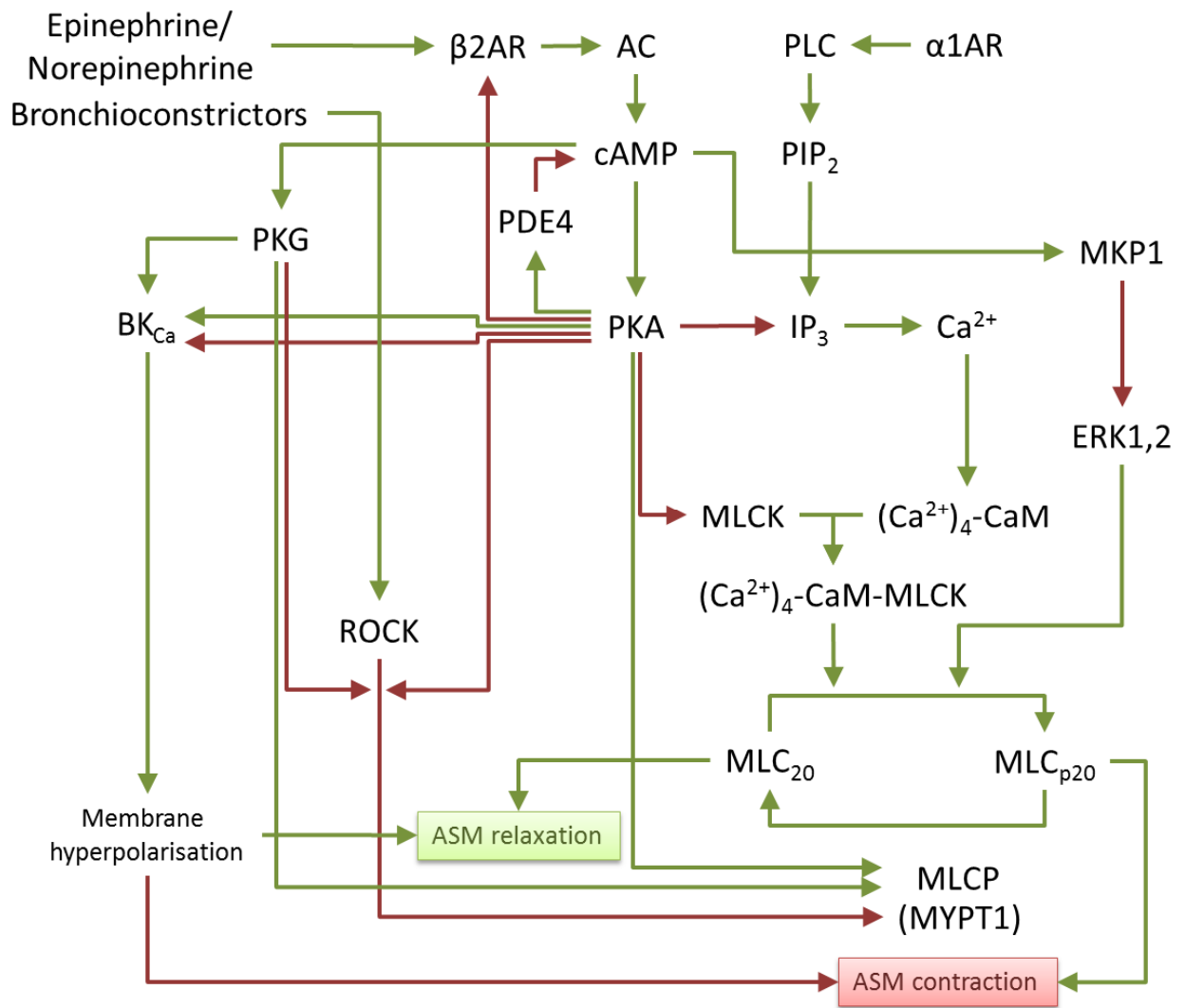
Figure 1.1 β2AR Agonist Induced ASM Relaxation/Contraction Pathways.

The arrows indicate a direct or indirect effect; green arrows indicate an activating effect and

the red arrows indicate an inhibitory effect.

In the light of the role of β2AR in ASM relaxation, β2AR agonists are used in the palliative treatment of inflammatorydiseases of the airways such as chronic obstructive pulmonary disease (COPD) and asthma (Connors, Dawson et al. 1996; Celli and MacNee 2004; Donohue 2004). These include short-acting (SABA) and long-acting (LABA) β-agonists. SABAs are generally used as required for immediate relief in the treatment of acute asthma while LABAs are recommended for longer term use in combination with an inhaled steroid. β-agonists have both bronchodilatory and bronchoprotective effects. Bronchodilation is the effect of lung inflation post airway smooth muscle relaxation. Bronchoprotection is the resistance to contraction on inhalation of a bronchioconstrictor like methacholine which acts on muscarinic receptors. Excessive and prolonged use of β2AR agonists leads to tachyphylaxis – which is the loss of both broncholdilatory and bronchoprotective effects of the drug (Keighley 1966; Van Metre 1969; Davis and Conolly 1980; Sears 2002; Abramson, Walters et al. 2003). It has been noted that repeated aerosolised administration of a β2AR agonist like salbutamol or isoproterenol leads to a decrease in spirometric measures like the forced vital capacity (FVC) and forced expiratory volume in 1 second (FEV1)in asthmatic patients within 180 min (isoproterenol) and beyond 300 min (salbutamol) (Choo-Kang, Simpson et al. 1969). There is an increased rebound in bronchoconstriction in asthmatics following a prolonged isoproterenol treatment (Paterson, Evans et al. 1971) where rebound is defined as a fall in mean peak flow below baseline after

stopping treatment with β-agonists. Even healthy individuals show reduced bronchodilatory effects (as measured by specific airway conductance) over a 4 week long exposure to a β-agonist like salbutamol (Holgate, Baldwin et al. 1977). The tachyphylaxis to β-agonists has been attributed to desensitisation of the β2AR (Davis and Conolly 1980; Bruynzeel 1984; Bruynzeel, Meurs et al. 1985). Thus understanding β2AR desensitisation mechanisms would help in rationale design of drug combinations that would allow for longer action of β-agonists by inhibiting the agonist-specific dominant modes of β2AR desensitisation.

1.1.3. β2AR Desensitisation

β2AR desensitisation occurs in response to agonist-induced activation of the receptor. The major mechanisms by which desensitisation of β2AR signalling can occur are: (1) Phosphorylation of the receptor (Benovic, Kuhn et al. 1987; Kobilka, MacGregor et al. 1987; Bouvier, Hausdorff et al. 1988; Lohse, Lefkowitz et al. 1989; Roth, Campbell et al. 1991; Yuan, Friedman et al. 1994; Vaughan, Millman et al. 2006), (2) internalisation of uncoupled β2AR (Sher and Clementi 1985; Yu, Lefkowitz et al. 1993; Barak, Tiberi et al. 1994; Ferguson, Downey et al. 1996; January, Seibold et al. 1997; Conway, Minor et al. 1999; Seibold, Williams et al. 2000; Clark and Knoll 2002), and (3) phosphodiesterase activation and subsequent degradation of cAMP (Barber, Goka et al. 1992; Broadley 1999). The extent of activation of individual modules of desensitisation is dependent on the amount, duration, type of β-agonist and amount of β2AR (Whaley, Yuan et al. 1994; Tran, Friedman et al.

2004). Figure 1.2 describes these overall reaction modules in β2AR desensitisation.
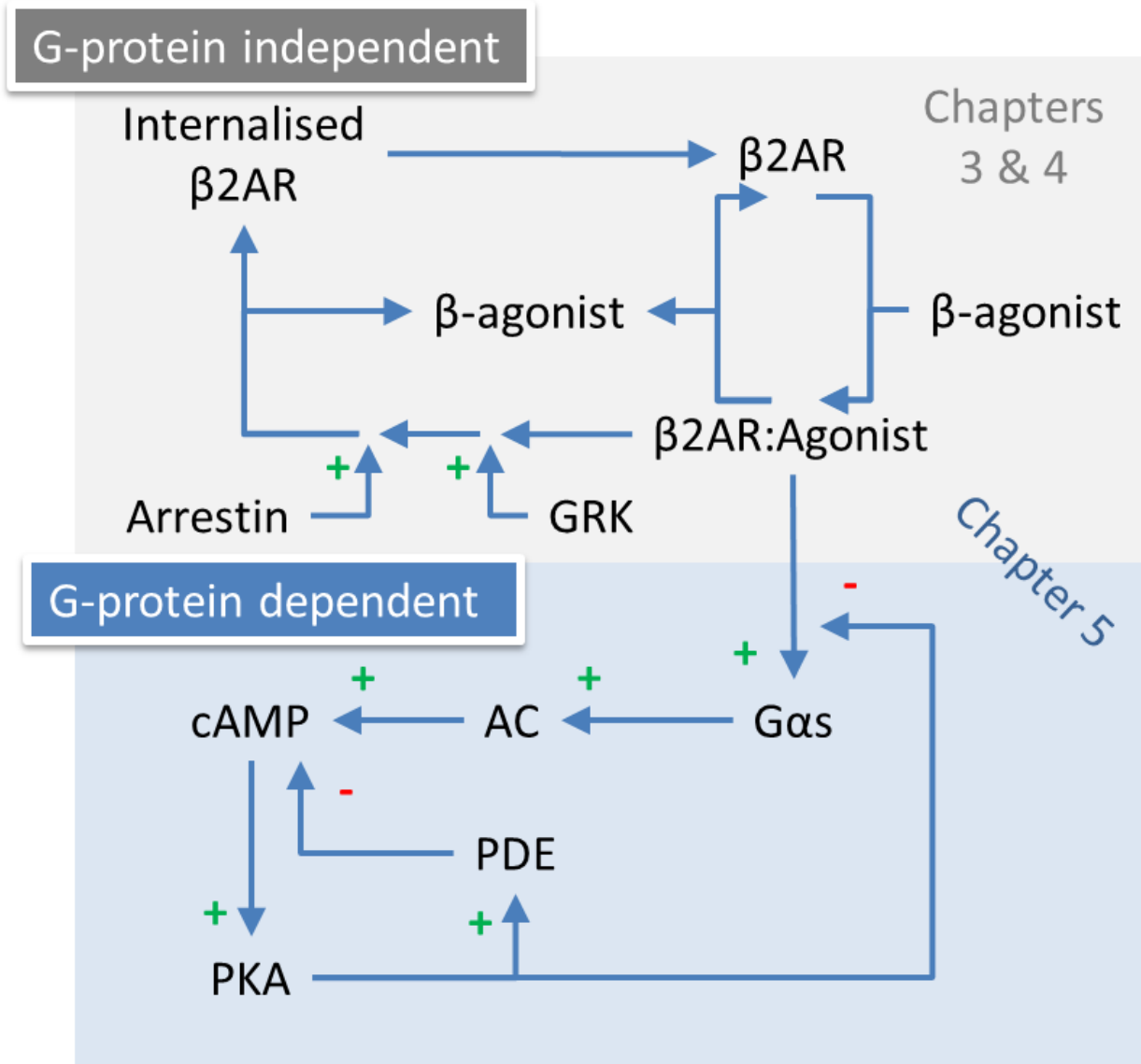
Figure 1.2 Modules of β2AR Regulation.

The reactions involved in β2AR regulation are classified into G-protein independent and dependent pathways. The '+' signs indicate a stimulatory effect of the modules along the direction of the arrow and a '-' sign indicates an inhibitory effect.

1.1.3.1. β2AR Phosphorylation

Kinase-mediated phosphorylation of the βAR is a major mode of receptor desensitisation (Stadel, Nambi et al. 1983; Hertel and Perkins 1984; Sibley, Benovic et al. 1987; Clark, Kunkel et al. 1988; Krupnick and Benovic 1998). At low concentrations of hormones or β-agonists there is a high potency, cAMP-dependent protein kinase A mediated, heterologous desensitisation of β2AR signalling (Benovic, Pike et al. 1985; Clark, Friedman et al. 1987; Clark, Kunkel et al. 1988; Lohse, Benovic et al. 1990; Tran, Friedman et al. 2004). In concurrence with this it was shown that mutation of putative PKA phosphorylation sites on β2AR led to marked reduction of desensitisation at low agonist concentrations (Hausdorff, Bouvier et al. 1989; Yuan, Friedman et al. 1994). Our group has shown that PKA activation leads to phosphorylation of at least S262 (Seibold, Williams et al. 2000). Mass spectrometric analysis (Trester-Zedlitz, Burlingame et al. 2005) of a small peptide containing the S262 site showed a stoichiometry of phosphorylation of one, which is in agreement with our results with PKA-mediated phosphorylation. Desensitisation of the receptor is achieved by causing a reduction in coupling efficiency of the receptor to Gs by from ~20% (GRK) to ~ 60% (PKA).

At high agonist concentrations there is a low potency, receptor occupancy driven, G-protein receptor kinase (GRK) mediated receptor phosphorylation (Benovic, Strasser et al. 1986; Clark, Kunkel et al. 1988; Palczewski 1997; Tran, Friedman et al. 2004). GRK activation leads to the phosphorylation of

at least three serine residues on the carboxyl tail of the receptor, viz. S355, S356, and S364 (Seibold, Williams et al. 2000). Our group has further characterised the S-355,356 sites by the use of phosphosite-specific antibody directed against pS-355,356 (Tran, Friedman et al. 2004). Mass spectrometric analysis of a peptide (residues 349-372) containing the three GRK sites showed that it was phosphorylated in HEK293 cells (Trester-Zedlitz, Burlingame et al. 2005). Stoichiometric analysis indicated that phosphorylation of S-355,356 was agonist-dependent, and S-364 was constitutively phosphorylated. Through siRNA studies it has been shown that GRK6 knockdown reduced S-355,356 phosphorylation by fivefold whereas GRK2 depletion increased isoproterenol-induced phosphorylation of these sites by 1.5 fold as detected by liquid chromatography−tandem mass spectrometry (Nobles, Xiao et al. 2011). In the same studies it has been suggested that GRK6-mediated phosphorylation of the β2AR is important for β-arrestin−dependent ERK1/2 activation, whereas GRK2 phosphorylation of the receptor may inhibit β2AR signalling to ERK1/2 on account of differences in reduction of ERK1/2 phosphorylation by either isoproterenol or carvedilol.

The GRK-mediated desensitisation of β2AR-mediated AC activation dominates only at higher agonist concentration due to the lack of significant amplification steps as compared to the PKA-mediated desensitisation at lower agonist concentrations. Our group has studied the effect of varying levels of β2AR expression on activation of adenylyl cyclase through Gαs

(Whaley, Yuan et al. 1994). We predicted the relationship between receptor number and EC_{50} of adenylyl cyclase activation. As the receptor density increased from 5 to 5000 fmol/mg of protein the EC_{50} for epinephrine activation of adenylyl cyclase decreased from 200 to 0.2 nM (Whaley, Yuan et al. 1994; Xin, Tran et al. 2008). The EC_{50}s on treatment with isoproterenol for the PKA and GRK site phosphorylations respectively are 30 pM and 200 nM in HEK 293 cells stably overexpressing the β2AR (Tran, Friedman et al. 2004). Thus there is a large separation of the two pathways in cells with high β2AR levels as a function of agonist concentration. This large separation of the EC_{50}s is not expected in HASMs where the receptor number is much lower and therefore the EC_{50}s will approach the Kds.

1.1.3.2. β2AR Internalisation

PKA or GRK phosphorylation of β2AR by itself is insufficient to produce complete desensitisation (Lohse, Benovic et al. 1990). A cofactor called arrestin is required to completely desensitise the β2AR post GRK-phosphorylation (Lohse, Benovic et al. 1990) since it completely uncouples the receptor from Gαs (Pan, Gurevich et al. 2003; Krasel, Bunemann et al. 2005). Arrestins bind directly to most GRK-phosphorylated GPCRs, forming a stoichiometric complex that is precluded from further G protein coupling. A polar core located in the hinge region between the two globular domains of the arrestin interacts with both non-phosphorylated and GRK-phosphorylated residues on the receptor tail (Hanson and Gurevich 2006). Receptor binding produces significant conformational changes in the

arrestin (Gurevich and Benovic 1993; Hirsch, Schubert et al. 1999; Vishnivetskiy, Paz et al. 1999; Vishnivetskiy, Schubert et al. 2000; Vishnivetskiy, Hirsch et al. 2002), whereas, conversely, arrestin binding stabilizes a receptor state with high agonist affinity, prompting some authors to characterise the receptor-arrestin complex as an alternative ternary complex analogous to the ternary complex of agonist-receptor-G protein in the absence of GTP (Gurevich, Pals-Rylaarsdam et al. 1997).

Both GRK phosphorylation and agonist-induced β2AR activation are a prerequisite to arrestin binding the receptor (Krasel, Bunemann et al. 2005). β-arrestin binding leads to the internalisation of the receptor via recruitment of clathrin and protein AP-2 (Koenig and Edwardson 1997). The internalised receptor either recycles back to the plasma membrane in a fully sensitised state (Yu, Lefkowitz et al. 1993), is targetted to lysosomes for degradation (Williams, Barber et al. 2000) or is a scaffold for signalling proteins like MAPK (Pierce, Maudsley et al. 2000; Huang, Sun et al. 2004; Xu, Baillie et al. 2008).

1.1.3.3. Phosphodiesterase Activity

The PDE superfamily is grouped through functional and homology classification into 11 subfamilies (Soderling and Beavo 2000). Inspite of being encoded by just 21 genes close to 200 plus distinct PDEs are reported on account of extensive alternative RNA splicing and multiple promoters (Bingham, Sudarsanam et al. 2006). PDEs across families are functionally

distinguished on account of distinct combination of pharmacological inhibitory profiles and unique enzymatic charactersistics with individual families showcasing distinct allosteric modifiers of enzyme activity. Individual PDEs also have distinct distribution at the tissue, cellular and subcellular level. The PDE4A-D subfamily is subject to considerable pharmacological scrutiny on account of its role in various disease states like respiratory disease (Conti, Richter et al. 2003; Houslay, Baillie et al. 2007). Increase in cAMP levels is the major stimulant of airway smooth muscle relaxation pathways in human airway smooth mucle (HASM). In these cells, the physiological regulation of cAMP degradation is primarily through PDE4D isoforms, with minor contributions from PDE3/4B isoforms (Billington, Joseph et al. 1999; Le Jeune, Shepherd et al. 2002). Consistent with the HASM cell culture experiments PDE4D is the major phosphodiesterase in murine tracheal extracts and PDE4D knockout mice show reduced airway smooth muscle contractility (Hansen, Jin et al. 2000; Mehats, Jin et al. 2003). In HASMs PDE4D5 seems most functionally relevant on account of its marked upregulation in response to elevated cAMP (Le Jeune, Shepherd et al. 2002; Hu, Nino et al. 2008). siRNA inhibition of PDE4D5 in HASMs causes a significant reduction in time required for cAMP-induced FRET to reach saturation in contrast to cells where PDE4D5 is uninhibited (Billington, Le Jeune et al. 2008). PDE4D5 can be recruited to the β2AR by a β-arrestin dependent mechanism. This allows for the possibility that localised quenching of cAMP might happen and it would be coupled with arrestin-

mediated desensitisation. Such a mechanism could be of significance in long-term regulation of the β2AR (Perry, Baillie et al. 2002; Bolger, McCahill et al. 2003).

Due to the importance of PDEs in regulating cAMP levels, PDE inhibitors like theophylline are used with glucocorticosteriods therapy as a second- or third-line treatment of asthma and COPD (Sullivan, Bekir et al. 1994; Weinberger and Hendeles 1996; Lim, Jatakanon et al. 2000; Rennard 2004; Spina 2008). Theophylline use is not favoured due to its narrow therapeutic index and its unwanted drug interactions with other drugs that lead to increase or decrease in serum concentrations of theophylline (Boswell-Smith, Cazzola et al. 2006). It also blocks adenosine stimulation causing many off-target effects. Thus careful monitoring of plasma levels of theophylline is required while prescribing. Newer generation of PDE inhibitors are isoform specific like PDE4-inhibitors roflumilast and cilomilast. These inhibitors show promise in improving lung function and reducing exacerbations of respiratory distress (Rabe 2011) but they still show off-target effects and longer term trials are needed to determine if these have an optimum place in COPD and asthma treatment (Cazzola, Picciolo et al. 2011; Chong, Poole et al. 2011).

1.1.4. G-Protein Independent Arrestin Signalling

A number of proteins bind arrestins and are recruited to agonist-occupied GPCRs, among them Src family tyrosine kinases (Luttrell, Ferguson et al. 1999; Barlic, Andrews et al. 2000; DeFea, Vaughn et al. 2000), members of the c-Jun N-terminal kinase 3 (JNK3) and ERK1/2 mitogen-activated protein (MAP) kinase cascades (DeFea, Zalevsky et al. 2000; McDonald, Chow et al. 2000; Luttrell, Roudabush et al. 2001), Mdm2, an E3 ubiquitin ligase (Shenoy, McDonald et al. 2001), the cAMP phosphodiesterases (PDE), PDE4D3/5 (Perry, Baillie et al. 2002), diacylglycerol kinase (Nelson, Perry et al. 2007), the inhibitor of nuclear factor (NF)κB, IκBα (Witherow, Garrison et al. 2004), the Ral-GDP dissociation stimulator (GDS), Ral-GDS (Bhattacharya, Anborgh et al. 2002), and the Ser/Thr protein phosphatase (PP)2A (Beaulieu, Sotnikova et al. 2005). It is via these interactions that arrestin binding to agonist-occupied GPCRs confers unique signalling properties, opening up a broad realm of previously unappreciated GPCR signal transduction.

Since arrestin binding completely uncouples G protein from the receptor, the transmission of G protein-dependent and arrestin-dependent signals should be mutually exclusive, at least at the individual receptor level. Comparison of the ERK1/2 activation time course resulting from G protein signalling and from the arrestin-dependent formation of an ERK1/2 activation complex on the angiotensin AT1A, lysophosphatidic acid (LPA), type I parathyroid hormone/PTH-related peptide (PTH1), and β2 adrenergic receptors demonstrate that the onset of arrestin-dependent ERK1/2 activation coincides

with the waning of G protein signalling and persists as receptors internalise (Ahn, Shenoy et al. 2004; Gesty-Palmer, El Shewy et al. 2005; Gesty-Palmer, Chen et al. 2006; Shenoy, Drake et al. 2006).

The arrestin-mediated and G-protein mediated signalling also tends to be spatially discrete. In the ERK1/2 cascade, it is clear that receptors that form stable complexes with arrestin, such as protease-activated receptor (PAR)-2, angiotensin AT1A, vasopressin V2, and neurokinin NK-1 receptors, activate ERK1/2 that accumulates in early endosomes along with the receptor (DeFea, Zalevsky et al. 2000; Luttrell, Roudabush et al. 2001; Tohgo, Pierce et al. 2002). Unlike ERK1/2 activated by heterotrimeric G protein-mediated pathways, signalsome-associated ERK1/2 does not translocate to the cell nucleus and fails to induce a transcriptional response or stimulate cell proliferation (DeFea, Zalevsky et al. 2000; Tohgo, Pierce et al. 2002). This contrasts with receptors, such as the β2 adrenergic and LPA receptors, which form transient complexes with arrestin that dissociate post internalisation (Oakley, Laporte et al. 2000; Wei, Ahn et al. 2004; Milano, Kim et al. 2006; Moore, Millman et al. 2007). Though, under physiologic conditions, arrestin-mediated signalling commences concurrent with G protein activation, it is clear that at least some arrestin-mediated signals do not require heterotrimeric G protein activity. Data obtained using receptor mutants uncoupled from G-proteins and arrestin pathway-selectiveligands have shown that arrestin-dependent activation of ERK1/2 by the angiotensin AT1A, β2 adrenergic, and

PTH1 receptors is G protein-independent (Azzi, Charest et al. 2003; Wei, Ahn et al. 2003; Gesty-Palmer, Chen et al. 2006; Shenoy, Drake et al. 2006).

Studies of mice lacking nonvisual arrestin isoforms suggest considerable functional redundancy among arrestin isoforms. Arrestin2- and arrestin3-null mice are grossly normal, with phenotypes that become apparent only upon treatment with pharmacological doses of GPCR agonists. Arrestin2-null mice exhibit exaggerated cardiac sensitivity to β adrenergic agonists (Conner, Mathier et al. 1997), whereas arrestin3-null mice demonstrate enhanced morphine-induced analgesia and attenuation of opiate tolerance (Bohn, Lefkowitz et al. 1999; Bohn, Lefkowitz et al. 2002). In each case, the phenotypes are consistent with impaired GPCR desensitisation rather than the loss of arrestin-mediated signalling.

1.1.5. Differences in Desensitisation of β2AR and Other GPCRs

Though β2AR is treated as a paradigm of GPCR desensitisation in textbooks there are differences in desensitisation mechanisms of other GPCRs. D2 is a dopaminergic GPCR. Locomotor hyperactivity induced by a D2 receptor agonist like apomorphine, is reduced in arrestin3 knockout mice (Beaulieu, Marion et al. 2008). Likewise, the dopamine transporter knockout mice exhibit hyperactivity on account of increased synaptic dopamine concentration. This is reduced when these knockout mice are crossbred with arrestin3 knockouts, a paradoxical result, since GPCR-mediated responses ought to be potentitated by the loss of arrestin-dependent desensitisation. Similarly opioid peptides

stimulate rapid internalisation of the μ opioid receptors while in contrast these receptors fail to internalise post-prolonged treatment with saturating concentrations of morphine, inspite of strong activation of receptor-mediated signalling via heterotrimeric G proteins (Keith, Murray et al. 1996). Morphine-activated opioid receptors escape arrestin-dependent regulation via uncoupling from heterotrimeric G proteins and Dyn-dependent endocytosis (Whistler and von Zastrow 1998). Over expression of β-arrestin though causes increased receptor internalisation and desensitisation. This suggests that under physiological conditions the role of arrestin in agonist-induced desensitisation could be different among GPCRs like D2 receptor, μ-opioid receptor and β2AR.

1.1.6. Biased Signalling

G protein-dependent and arrestin-dependent functions of many GPCRs can be dissociated pharmacologically by ligands that exhibit functional selectivity or "bias" favouring one pathway or the other (Kenakin 2002; Maudsley, Martin et al. 2005; Violin and Lefkowitz 2007; Gesty-Palmer and Luttrell 2008; Luttrell and Kenakin 2011). Conventional GPCR agonists and antagonists are believed to activate or inhibit all aspects of signalling equally, whereas "biased agonists" have the potential to change the signal output of a GPCR, thereby controlling not only the quantity but also the quality of efficacy. A number of ligands have been characterised that exhibit paradoxical reversal of efficacy (e.g., acting as antagonists or inverse agonists of G protein signalling but behaving as agonists with respect to arrestin recruitment and arrestin-dependent signalling). For example, Sar1-Ile4-Ile8, an angiotensin AT1A receptor antagonist, promotes

arrest-inducedreceptor sequestration in the absence of significant G protein activation (Holloway, Qian et al. 2002). Likewise, the PTH analog (D-Trp12,Tyr34)PTH(7–34) is an inverse agonist for PTH1 receptor-Gs coupling but promotes arrestin-dependent receptor internalisation (Gardella, Luck et al. 1996; Sneddon, Magyar et al. 2004). As a result, each is able to bring about ERK1/2 activation that is arrestin-dependent and under conditions in which G protein is not significantly activated (Gesty-Palmer, Chen et al. 2006). Likewise, (±)-1-[2,3-(dihydro-7-methyl-1H-inden-4-yl)oxy]-3-[(1-methylethyl)amino]-2-butanol (ICI118551), carvedilol and propranolol are β2AR ligands that show partial inverse agonism with respect to Gs activation, and partial agonism for the arrestin-mediated ERK1/2 activation (Azzi, Charest et al. 2003; Wisler, DeWire et al. 2007; Drake, Violin et al. 2008). Our group has shown that treatment of β2AR in HEK293 cells overexpressing receptor with saturating concentrations of salmeterol does not lead to significant internalisation (Moore, Millman et al. 2007). This phenomenon can be rescued by overexpression of arrestin. Through kinetic modeling we show that the most probable explanation for this is that salmeterol stabilizes a different β2AR state that in time shows equivalent GRK phosphorylation but has reduced affinity for arrestin, thereby reducing internalisation (Vayttaden, Friedman et al. 2010).

Studies have reported that the phospholipase C (PLC)-mediated inositol phosphate (IP) accumulation and phospholipase A_2(PLA$_2$)-mediated arachidonic acid (AA) release varies based on the identity of agonists stimulating the human serotonin$_{2A}$ (5-HT$_{2A}$) and 5-HT$_{2C}$ (Berg, Maayani et al.

1998; Kurrasch-Orbaugh, Watts et al. 2003). 2,5-dimethoxy-4-

methylphenylisopropylamine (DOM) and 2,5-Dimethoxyphenylisopropylamine

(2,5-DMA) are examples of structurally close ligands. They differ only in the

methyl group at C4. Inspite of these similarities in structure 2,5-DMA and DOM

are good examples of biased agonists. For PLC-IP accumulation in 5-HT$_{2C}$

receptor, both ligands are partial agonistsbut, DOM is a full agonist for PLA2-

AA release, and in contrast 2,5-DMA does not have a significant PLA2-AA

response. Taken together all these observations strongly suggest that the two-

state receptor activation model is too simplistic and one requires the invoking

of multiple active states of the GPCRs that are differentially stabilized by

various ligands.

1.2. Modelling β2AR Regulation

Given the background of β2AR regulation explained in previous sections it

becomes increasingly clear that though the main features of β2AR desensitisation

are GRK/PKA-mediated phosphorylation, arrestin recruitment and PDE activation,

understanding which of these components is the dominant signalling module in

clinically observed tachyphylaxis is not easily tractable by traditional experimental

methods alone. This complication is because of 1) extensive use of different model

systems for studying human β2AR desensitisation, wherein results from one model

do not easily translate into another model; 2) simultaneous activation of various

pathways, necessitating pharmacological or genetic manipulations to silence other

signalling pathways; 3) isoform-specific differences of various signalling

components in tissue distribution and signalling; and 4) G-protein independent

signalling. Thus it becomes necessary to first reduce all the complexities of β2AR signalling into a consensus mathematical model that is advised by experimental measurements of the system.

Reduction of the complexities of β2AR signalling into a consensus model might seem counterintuitive but such model reduction has been helpful in physical sciences. Borrowing an example from the physical sciences, light is modeled both as a wave and as a particle because no one model can fully explain all the observable properties of light. So reducing the complexity and modeling light as a wave or a particle allows us to understand how light behaves under some experimental conditions as a wave and in other conditions as a particle. Similarly in order to understand β2AR desensitisation I will reduce the complexities of β2AR signalling into three modules viz. 1) GRK/Arrestin-mediated β2AR desensitisation; 2) PKA-mediated β2AR desensitisation; and 3) PDE regulation. I will then test each module against a defined set of experimental readouts and see if a combined model can be created to explain β2AR desensitisation. In the process of model building we will understand better the different modules of β2AR desensitisation.

My overall goal is to establish quantitatively the relevance of the major pathways of desensitisation with endogenous β2AR receptor in cells of human airway origin. Towards that end the work plan was to use HEK293 cells stably overexpressing β2AR and obtain rates for key steps in GRK-, PKA- and PDE-mediated β2AR desensitisation. Using these rates I would then develop a comprehensive model for these pathways and once developed extend the model to HASMs where some of the experimental measures are difficult to come by. A well validated and

constrained model could then be used to understand the agonist specific differences in signalling that allow differences in length of action of LABAs vs. SABAs. This would help in teasing out agonist specific desensitisation pathways that are responsible for tachyphylaxis in a clinical scenario.

1.2.1. Other Models of β2AR

The collision coupling model is one of the first βAR models, it suggests that ligand activated receptors and G-proteins can collide and transiently couple to activate the G-proteins (Tolkovsky and Levitzki 1981). More recent β2AR models simulate downstream effects of isoproterenol-induced receptor activation and match experimentally measured whole cell (Violin, DiPilato et al. 2008) or near-membrane cAMP (Xin, Tran et al. 2008). Other βAR models are validated against more than one experimental readouts like isoproterenol induced -cAMP response, -PKA activation, -PLB phosphorylation in cardiomyocytes (Saucerman, Brunton et al. 2003) or - GRK phosphorylation/dephosphorylation, -receptor trafficking in HEK293s (Vayttaden, Friedman et al. 2010). Previous modelling work in the field has largely ignored the interplay between the PKA and GRK mediated β2AR desensitisation pathways. Our group in collaboration with Dr. Thomas Rich (University of South Alabama) examined the cAMP turnover profiles in HEK293 cells expressing only endogenous β2AR. Their ordinary differential equation (ODE) model described the importance of receptor levels, basal AC activity, receptor desensitisation, and regulation of PDE activity in controlling cAMP signals (Xin, Tran et al. 2008). This study did not model the GRK pathway in its

full complexity, and examined desensitisation only at high agonist concentrations at which the PKA component of β2AR desensitisation is assumed to be not significant. Another limitation of the model was that there was no correlation between receptor phosphorylation and receptor desensitisation.

Another modelling study (Violin, DiPilato et al. 2008) captured the cAMP profiles following β2AR activation as measured by using a fluorescent protein-tagged EPAC sensor (ICUE2). This model did not include the PKA-mediated β2AR desensitisation or the arrestin binding sequelae. The model used a Monte Carlo method for simulating the kinetics of the cAMP profiles. In a Monte Carlo method one uses a computer algorithm to randomly sample a mathematical space. Since the Monte Carlo method is a statistical sampling method, one of the caveats of this method is that if the modeller is not careful the parameters used in the model might not necessarily match experimentally determined values. For example, in this Monte Carlo model the rate constants for PKA site phosphorylation and dephosphorylation were 0.0021 and 0.1103 sec-1, values that are ~100 and 1000 fold greater respectively from our experimental values (Tran, Friedman et al. 2004; Tran, Friedman et al. 2007). One effect of artificially setting the PKA dephosphorylation rate very high is that the model will not be able to correctly capture the effects of PKA phosphorylation on the system. These differences might explain their conclusion that receptor inactivation by cAMP-dependent kinase is insignificant

which is at variance from what has been previously reported (Clark, Kunkel et al. 1988; Yuan, Friedman et al. 1994).

A major limitation of both these modelling studies was that cAMP profiles were the only experimentally defined constraints on the model. In Chapter 3 I describe my ODE model of β2AR desensitisation (Vayttaden, Friedman et al. 2010) that is constrained by six different types of experimental measurements viz. GRK phosphorylation, dephosphorylation, receptor internalisation, recycling, desensitisation and resensitisation. The model also describes the arrestin binding sequelae and the GRK pathway in its full complexity. The major conclusions of this modeling study will be discussed in Chapter 3.

1.2.2. Partial Agonist Models

Partial agonists are ligands that give sub-maximal receptor activation even at receptor saturation. For β2AR, isoproterenol (Isuprel®) and epinephrine (endogenous ligand) are examples of full agonists while salmeterol (Servent®) and albuterol (Ventolin®, Proventil®) are examples of partial agonists. Barring cyclopentylbutanephrine, the initial rate of GRK-mediated β2AR phosphorylation correlates with the coupling efficiency of partial agonists (January, Seibold et al. 1997; Tran, Friedman et al. 2004; Drake, Violin et al. 2008). Given the extensive clinical use of partial agonists especially as long acting β-agonists I have extended my model (Vayttaden, Friedman et al. 2010) described in Chapter 3 to model GRK-mediated β2AR phosphorylation in response to a wide panel of partial agonists (Figure 4.1). Salmeterol (Figure

1.3) is a weak β-agonist widely used as a complement to steroid therapy in the

treatment of asthma and COPD and available in the North American market as

Advair[TM] which is the combination of a steroid (fluticasone propionate) and

salmeterol (Spencer and Jarvis 1999; Markham and Jarvis 2000; Nelson 2001;

Cowie, Boulet et al. 2007; McKeage and Keam 2009). It is equi-efficacious to

strong β-agonists in reversing bronchoconstriction and improving clincial

outcomes on chronic use.
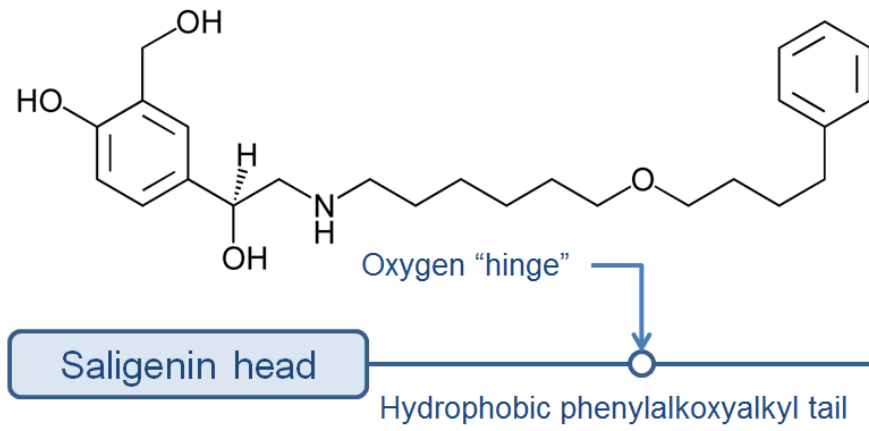
Figure 1.3 Structural Formula of Salmeterol.

Salmeterol has a salgenin head that binds the active site on the receptor and a hydrophobic tail.

Despite its clinical significance, salmeterol's mechanism of β2AR activation and regulation of downstream signalling in HASMs is not well understood. Following the publication of salmeterol multicenter asthma research trial results (Nelson, Weiss et al. 2006) Federal Drug Administration mandated a black-box warning for salmeterol even though a salmeterol/steroid combination therapy was not part of this meta-analysis. The text of the Advair black-box warning is as follows "*Long-acting β2-adrenergic agonists, such as salmeterol, one of the active ingredients in ADVAIR DISKUS, may increase the risk of asthma-related death. Therefore, when treating patients with asthma, physicians should only prescribe ADVAIR DISKUS for patients not adequately controlled on other asthma-controller medications (e.g., low- to medium-dose inhaled corticosteroids) or whose disease severity clearly warrants initiation of treatment with 2 maintenance therapies. Data from a large placebo-controlled US study that compared the safety of salmeterol (Serevent® Inhalation Aerosol) or placebo added to usual asthma therapy showed an increase in asthma-related deaths in patient receiving salmeterol (13 deaths out of 13,176 patients treated for 28 weeks on salmeterol versus 3 deaths out of 13,179 patients on placebo)*"

The 8-12 hour persistence of salmeterol is responsible for its clinical effectiveness (Beach, Young et al. 1992; Johnson, Butchers et al. 1993; Nials, Ball et al. 1994; Palmqvist, Persson et al. 1997). This is also the Achilles heel of mechanistic studies for salmeterol since it precludes washout experiments, and this too has contributed to many controversies and misconceptions in the field (Duringer, Grundstrom et al. 2009; Nino, Hu et al. 2009; Cooper, Kurten et al. 2011). A well

constrained and validated model of salmeterol action on β2AR could help in clarifying the mechanism of salmeterol action especially since it is possible to surmount difficulties of poor washout *in silico*. In Chapter 4 I discuss existing models of salmeterol action. Briefly they are the microkinetic and exosite model. The microkinetic model posits that lipophilicity of salmetereol leads to membrane insertion of salmeterol and due to its delayed release there is a pool of salmeterol around the receptor microenvironment (Anderson, Linden et al. 1994). The exosite model posits that salmeterol binds the receptor to an exosite in addition to the active site. This exosite binding is quasi-irreversible and allows for continued retention of salmeterol near the receptor (Jack 1991). I combined the exosite and microkinetic models with my validated model of GRK-mediated β2AR desensitisation discussed in Chapter 3.

1.2.3. Combined Models of PKA-/GRK-/PDE-Mediated β2AR Regulation

In order to identify the dominant β2AR desensitisation pathways under different therapeutic regimens it becomes necessary to create a unified model of PKA-/PDE-/GRK-/Arrestin-mediated regulation of β2AR signalling. In Chapter 5 I present very preliminary work towards this unified model. To create a consensus model I combined my model of the GRK/Arrestin modules (Vayttaden, Friedman et al. 2010) with that of the PKA/PDE modules that our group had published previously (Xin, Tran et al. 2008). The unified model thus created will be validated against experimental measurements of agonist-induced GRK-mediated β2AR-phosphorylation, PKA-mediated β2AR-

phosphorylation, β2AR-dephosphorylation, -trafficking, -desensitisation, -resensitisation and -cAMP profile.

1.3. Conclusion

The β2AR activates smooth muscle relaxation through both cAMP-dependent and independent pathways. In order to understand why clinical tachyphylaxis happens in response to β-agonists it becomes necessary to understand agonist specific activation of the various β2AR desensitisation pathways. These studies are difficult and extremely time consuming to perform in vivo or in vitro on account of multiple isoforms and cross-reactions in signalling pathways. Towards that end I have developed various computational models that explore different desensitisation pathways and the effects of different β-agonists.

One of the limitations of the work presented in this thesis is that it is geared towards understanding the effects of β-agonist mediated activation of β2AR in only airway smooth muscle. When a patient is treated for asthma more than one tissue type "sees" the β-agonist. β2AR is expressed in cells like mast cells, T cells etc. all which play a role in the inflammatory component of asthma (Sitkauskiene and Sakalauskas 2005; Anderson 2006; Deshpande and Penn 2006; Black, Oliver et al. 2009; Loza and Penn 2010). Additionally the patient on maintenance therapy for asthma is treated with a combination of steroid and β-agonist so ideally the effect of β-agonists should be studied in the background of the effects steroid treatment. Inspite of the above described limitations as a first pass the models described here could be used as tools for high throughput hypothesis testing of the β2AR

regulatory components allowing us to select specific promising experiments to follow through in vivo or in vitro.

Of most relevance to this thesis, the models described herein have resulted in some novel conclusions: (i) receptor dephosphorylation at the membrane and GRK-phosphorylated receptor recycling are required for proper β2AR kinetics (Chapter 3, Figure 3.9); (ii) discovery of latent memory in the β2AR signalling machinery (Chapter 3, Figures 3.11A, 3.12); (iii) realisation that receptor internalisation was not required for β2AR resensitisation (Chapter 3, Figure 3.12); (iv) salmeterol does not cause significant agonist-induced β2AR internalisation, probably by destabilising the salmeterol/β2AR/arrestin complex; (v) reduced stability of salmeterol/β2AR/arrestin complex might be the key property that explains long action of salmeterol (Chapter 4, Figure 4.10); and (vi) it follows from reduced arrestin binding to salmeterol/β2AR complex that salmeterol-induced β2AR desensitisation would be predominantly mediated by the PKA pathway (PKA-mediated β2AR phosphorylation and PDE activation). The preliminary work towards modelling the combined effect of PKA-/GRK-/PDE-mediated regulation of β2AR signalling is discussed in Chapter 5.

These models explain the basis of loss of efficacy during abuse of a rescue inhaler and the reason for long action of β-agonists used in maintenance therapy. The conclusions made herein reiterate the importance of modeling in studying β2AR regulation since many of the observations made through modeling would not have been easy to make solely by experiments.

2. Materials and Methods

2.1. Experimental Methods

Data used in this thesis comes predominantly from experiments performed using either HEK 293 cell lines with stable overexpression of β2AR at levels of 3–6 pmoles/mg membrane protein or HASMs that have β2AR at levels of ~ 0.03 pmoles/ mg membrane protein. Due to the low levels of β2AR in HASMs, receptor phosphorylation could not be detected with available phosphosite-specific antibodies. However, cAMP measurements could be performed in these cells. The stable overexpression of the WT β2AR comes in three "flavours" viz. a) an N-terminal FLAG (DYKDDDDK) epitope tag (Tran, Friedman et al. 2007); b) an HA (YPYDVPDYA) tag on the N-terminus (Morrison, Moore et al. 1996); and c) both an HA (N-terminus) and a 6His (C-terminus) – Hβ2ARH (January, Seibold et al. 1997; Seibold, January et al. 1998). These tags do not significantly perturb the desensitisation parameters discussed in Tables 3.1 or 5.1 as measured by adenylyl cyclase in cell-free membrane preparations (Morrison, Moore et al. 1996; January, Seibold et al. 1997; Seibold, January et al. 1998; Iyer, Tran et al. 2006; Vaughan, Millman et al. 2006; Tran, Friedman et al. 2007), therefore in the discussion I refer to these stably expressing cell lines as expressing WT β2AR. Occasionally we have used epinephrine instead of isoproterenol, and found no changes in the desensitisation parameters at similar levels of receptor occupancy (Tran, Friedman et al. 2004). The overexpression does affect dramatically the basal levels of cAMP (much enhanced) and the time course and turnover of cAMP. Practically we find that cAMP levels do not decrease in time, paradoxically it appears that the

phosphodiesterase activity (as well as PKA activity – personal note from Peter Fishman) is markedly increased to compensate for constitutive activity. This problem is not discussed in any of the work by our group and others in the use of overexpression lines. Therefore, to model and simulate cAMP turnover it is best to use cells expressing either low or endogenous levels of receptor. On the other hand it will be a test of the models to simulate the effect of a 100 fold increase in receptors on cAMP turnover in the face of much higher PDE activity.

An interesting further paradox is that our basal level of GRK site phosphorylation is almost undetectable (2-5% of the ISO stimulated levels, whereas the PKA site phosphorylation shows a marked basal level about 15-25% of the stimulated level.

2.1.1. Intact Cell Membrane Dephosphorylation

HEK 293 cells stably overexpressing the WT β2AR were grown to confluency in 6-well plates. They were treated with 1µM isoproterenol dissolved in ascorbate/thiourea, pH 7 at a final concentration of 0.1 mM ascorbate/1 mM thiourea (AT) at 37°C for 30 secs. Post 30 sec saturating agonist challenge, the medium was removed and replaced with medium containing 1.0 µM propranolol (an antagonist). 30 sec of treatment with a saturating concentration of a full agonist should lead to negligible (<0.5%) internalisation but close to 75% maximal GRK phosphorylation. To stop all reactions, the medium was aspirated, and the cells were rapidly washed with 1 ml of ice-cold HE buffer (20 mM HEPES and 1.0 mM EDTA, pH 7.7) and placed on ice. Cells were solubilised by addition of 200 µl of ice cold solubilisation buffer (20 mM HEPES,

pH 7.4, 150 mM NaCl, 0.9% dodecyl-β-maltoside, 20 mM tetrasodium

pyrophosphate, 10 mM NaF, 0.1 µM okadaic acid, 10 µg/ml each of

benzamidine, trypsin inhibitor, and leupeptin) to each well. The cells were

scraped into the solubilisation buffer, transferred to 1.5-ml microcentrifuge

tubes, and rocked for 30 min at 4°C. The solubilised extract was clarified by

centrifugation for 15 min at 15,000 rpm and 4°C. Post centrifugation, the

clarified supernatant of the cell extract was transferred to a new microcentrifuge

tube and treated with 150 units of PNGase F (2 hours, 37°C) to allow for

deglycosylation. Samples were then heated at 65°C for 15 min in SDS sample

buffer (2% sodium dodecyl sulphate, 10% glycerol, 100 mM Tris, pH 6.8,

bromphenol blue, and 10 mM dithiothreitol). 20 µL aliquots of samples were run

on 12% SDS-polyacrylamide gel electrophoresis and transferred to

nitrocellulose for immunoblotting. These nitrocellulose membranes were then

probed with phosphoserine-specific antibodies, anti-pS(355,356) for the GRK

sites on the β2AR. Post phosphoserine-specific antibody treatment the

membranes were washed twice and incubated with suitable dilution of goat anti-

rabbit IgG horseradish peroxidase (Bio-Rad, Hercules, CA) and detected by

SuperSignal reagent. In order to determine receptor levels the immunoblots

were stripped and reprobed with a β2AR-specific rabbit anti-C-tail antibody. The

blots were imaged using a camera system (GeneGnome; Syngene, Frederick,

MD) or visualised on film using SuperSignal (Piercenet, Rockford, IL), and

bands quantified using Syngene software. The signal from the anti-

pS(355,356)-specific antibodies were normalised to the corresponding signal

from anti-C-tail antibody. For averaging data across different dephosphorylation experiments, the results were calculated as a fraction of the control isoproterenol treatment followed by the means ± S.E.M.

2.2. Computational Methods

In this dissertation I have described 10 computational models of β2AR regulation. These have been developed using a suite of different simulators and mathematical solvers. The choice of simulators was motivated primarily by the extent of its use among collaborators to allow for ease of model sharing followed by the ease of model development. The choice of solvers was motivated by the ability to get an efficient mathematical solution. Efficiency is used loosely here to reflect the measure of the computational time invested in solving the system of equations to get a reproducible solution, the faster we get a solution the more efficient is the simulation. A reproducible solution won't be significantly affected by change in time steps of the simulation (c.f. Figure 2.1 for discussion of time steps) and it will be a positive solution since negative concentrations is a physical impossibility. So an attempt is made to use the largest time step at which a stable solution is attained since the simulation time also tends to increase with the decrease in the time step, and the simulated solution is usually better approximated to the actual curves at smaller time steps. The point is to fix the time such that the simulation agrees as closely as time permits with the experimental data.
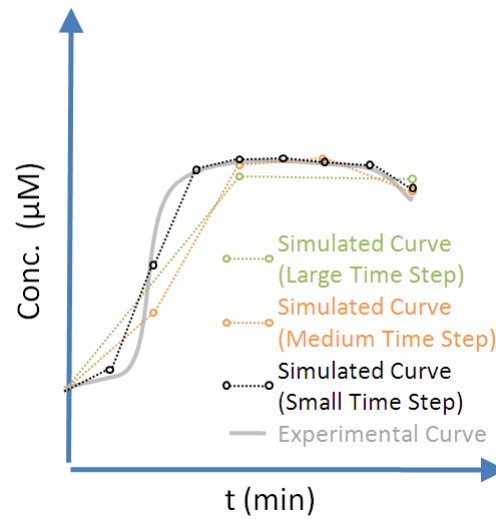
Figure 2.1 Effect of Choice of Time Step.

A mockup of an experimentally determined time course is shown in grey. The polygonal approximation of the curve is shown in different colours for the choice of various time steps – green (large), orange (medium) and black (small).

Table 2.1 A List of Models with the Simulator and Solver Used.

Model Numbers	Model Description	Simulator	Solver
1 – 6	GRK-mediated regulation of β2AR	MATLAB	Runge-Kutta 4th Order
		GENESIS/ Kinetikit	Euler
7 – 9	Salmeterol-induced GRK regulation of β2AR	COPASI	LSODE
		GENESIS/ Kinetikit	Euler
10	GRK/PKA/PDE-mediated regulation of β2AR signalling	COPASI	LSODE/ Hybrid LSODE/ Hybrid Runge Kutta (a variation of Runge-Kutta 4th Order)

2.2.1. Choice of Simulators

2.2.1.1. MATLAB

MATLAB® (MATrix LABoratory) is a proprietary numerical computing environment developed by MathWorks (Natick, MA). It can be used for matrix manipulations, data visualisation, algorithm development, data analysis, and numeric computation. I used MATLAB R2008 for developing the models described in Chapter 3 (models of GRK-mediated β2AR regulation) because of legacy issues since our group had previously implemented a model of PKA-/PDE-mediated β2AR regulation in MATLAB (Xin, Tran et al. 2008). Due to extensive toolboxes MATLAB allows one to perform numerical calculations and visualise results without the need for time consuming programming. And because MATLAB has been in use since 1984 in academic research and industry, a wide online community is available to help with potential problems. However, since MATLAB is an interpreted language, it can be slow and poor programming practices would compound the problem further. Modifying a pre-existing model and adding new modules or removing old modules of reactions/equations is usually not trivial. Also with MATLAB, users are subject to vendor lock-in making sharing and viable reuse of models limited to the MATLAB language.

2.2.1.2. GENESIS/Kinetikit

Kinetikit (Schutter 2001; Bhalla 2002; Vayttaden and Bhalla 2004) is a graphical simulation environment that extends the capabilities of GENESIS

(GEneral NEural SImulation System) (Touretzky 1989; Bower and Beeman 2007) to simulate large biochemical signalling pathways. Use of GENESIS/Kintekit does not require any product registration. I have used GENESIS/Kinetikit at the early stages of model development of all models described in this thesis dissertation. The biggest advantage for me was the ease of implementation of a variety of stimuli like paired pulses and agonist washouts post activation. Usability of GENESIS/Kinetikit requires experience to fully utilise the graphical user interface (GUI) and script language. Also Kinetikit is computationally reliable and efficient. The reason I didn't use GENESIS/Kinetikit extensively beyond the initial model development was because of the difficulty in portability of the models across different operating systems. For the use of all features of GENESIS/Kinetikit, one is dependent on the Linux environment and since our laboratory is predominantly Windows rich this limited portability of the models. Also since the GUI required familiarisation it wasn't easy for anybody other than the model author to follow the model development progress.

2.2.1.3.   COPASI

COPASI a graphical program that allows the simulation of biochemical processes (Hoops, Sahle et al. 2006). COPASI can be downloaded freely and in addition to deterministic and stochastic simulations of reaction networks, it allows for flux analysis. I used COPASI due to its ease of use and large suite of modeling analysis tools. The biggest advantage was the ability to use the sliders feature that allowed for real-time, interactive

parameter changes during simulations. This enhanced the model development experience with experimentalists in our group settings. COPASI is not without its quirks that do affect its usability. Unlike GENESIS/Kinetikit COPASI does not have a very good network diagram visualisation. While modelling very large networks, network diagram visualization might not be "pretty" but it still is a very important tool in being able to zoom in and find a reaction or associated parameters. In COPASI one is limited to navigating a long table of alphanumeric characters to locate a reaction or parameter of interest. While this mode of access is useful in data entry it is not always efficient in data retrieval since model development rarely proceeds in a linear fashion and there are additions and deletions of reactions/species leading to "lack of order" in tables. Another drawback with COPASI is that if the model uses assignments, rules and global quantities, certain type of solvers cannot be used efficiently leading to extended calculation times. For example, in my models there are many global quantities like total GRK-phosphorylated receptor which is assigned the value of sum total of all GRK-phosphorylated receptor species. The simulated global quantity of total GRK-phosphorylated receptor is useful in matching simulation results with experimental results of GRK phosphorylation. Also combining parameter estimation with a variety of stimuli like paired pulses and agonist washouts post activation is difficult.

2.2.2. Choice of Solvers

2.2.2.1. Euler

The Euler integration method (in GENESIS/Kinetikit) is an explicit method for numerical integration of ordinary differential equations (ODEs) when given its initial value. The advantage of this method is that it is computationally simple. The disadvantage is that to reduce error in estimations for stiff equations one will have to use very small timesteps making it computationally inefficient. All models (1-10) were initially implemented using GENESIS/Kinetikit 10 (Vayttaden and Bhalla 2004) and an Euler solver on a PC running Red Hat Linux (Red Hat Corp., Raleigh, NC).

2.2.2.2. LSODE

The LSODE (Livermore Solver for Ordinary Differential Equations) is an integration method for numerical integration of ODEs and can handle both stiff and non-stiff equations. It was written by Linda R. Petzold and Alan C. Hindmarsh and is the default method in COPASI to calculate timecourses. Models 7-9 (described in Chapter 4) and model 10 (described in Chapter 5) were implemented using COAPSI 4.6 and a Hybrid LSODE solver on a PC running Windows 7 (Microsoft Corp., Redmond, WA).

2.2.2.3. Runge-Kutta

The Runge-Kutta methods are a group of implicit and explicit iterative methods used in estimating solutions of ODEs. Different implementations of Runge-Kutta methods are available in MATLAB, GENESIS/Kinetikit and COPASI. Models 1-6 (described in Chapter 3) were implemented using MATLAB R2008 and a 4th order Runge-Kutta solver on a PC running Windows XP (Microsoft Corp., Redmond, WA) and model 10 (described in Chapter 5) was implemented using COAPSI 4.6 and a Hybrid Runge-Kutta solver on a PC running Windows 7 (Microsoft Corp., Redmond, WA).

2.2.3. Additional Model Details

The reactions for all models were written per the Law of Mass-Action (Guldberg 1864; Waage 1864; Waage and Guldberg 1864; Waage and Guldberg 2000 (Translation)) considering the system to exist in equilibrium. All analyses were done using Microsoft Office Excel 2003/2007 (Microsoft Corp., Redmond, WA) and plots were generated using GraphPad Prism 4/5 (GraphPad Software, Inc., La Jolla, CA).

2.2.4. Partial Agonist Simulations

2.2.4.1. Relative Efficacy

Partial agonist-mediated activation of β2AR was simulated in Model 1 with coupling efficacies of each agonist set relative to epinephrine (α) (c.f. Table 3.1, 4.1). The stated coupling efficacies/ efficiencies of various partial

42

agonists were from previous measurements in HEK 293s that stably overexpress WT β2AR (Tran, Friedman et al. 2004). The measurements of partial agonist-induced β2AR phosphorylation and internalisation were done at saturating agonist concentrations (Tran, Friedman et al. 2004; Moore, Millman et al. 2007). In simulations of partial agonists, concentrations were set equivalent to saturating epinephrine concentrations (10 µM) on account of the fact that efficacies/coupling efficiencies were set relative to epinephrine.

2.2.4.2. *Salmeterol Models*

In Model 1, differential coupling efficacies for salmeterol- vs. epinephrine-induced β2AR activation was considered for salmeterol simulations. In Models 8-10 in addition to differential coupling efficacies, simulations for salmeterol mediated β2AR activation also invoked membrane accumulation of salmeterol in the microkinetic model (Model 7), or a salmeterol-binding exosite (Model 8), or both exosite and microkinetics (Model 9). The models were written using previously described mathematical formalism for salmeterol and competing agonist binding to β2AR (Szczuka, Wennerberg et al. 2009) and post agonist-induced GRK-mediated β2AR regulation (Vayttaden, Friedman et al. 2010).

2.2.5. Simulation of Receptor Number Variation and Perturbations of Rate Constants.

In order to account for experiments such as overexpression or knockdowns of GRKs, phosphatases or arrestins, simulations of Models1-6 were performed by 2 to 50 fold variations of the relevant rate constants. In Model 7 the 100 fold overexpression of β2AR in HEK293s as compared to HASMs is accounted for by arbitrarily changing receptor levels from 100 µM (stable overexpressions) to 1µM (HASMs). The concentrations of receptor can also be estimated by calculations for an "ideal" HEK293 cell approximated to a sphere as given below.

Equation 2.1

Volume of an ideal HEK293 cell = 4/3 π R^3 ~ 500 fL (when R = 5000 nm)

Equation 2.2

Volume of plasma membrane in an ideal HEK293 cell = 4/3 π (R^3 - r^3) ~ 3 fL (when R = 5000 nm and r = 4990 nm, assuming a membrane thickness of 10 nm)

The total protein yield from a 10 cm dish ~ 1 mg and β2AR concentration ~ 3 pm/mg total protein. The approximate cell count in a confluent 10 cm dish is ~ 2 X 10^6 cells. This leads to an approximation of β2AR concentration to 3.0×10^{-6} mole/L in a whole cell or 5.0×10^{-4} mole/L in the membrane. This approximates to a receptor number of 1 X 10^5/ cell.

2.2.6. Sensitivity Analysis of Desensitisation and Resensitisation.

A univariate sensitivity analysis was carried out for Model 1 to test the effect of variation in parameter values on the simulation results of desensitisation and resensitisation. Barring the ligand binding and unbinding rates (which were left unperturbed), all other rates were individually varied 2-, 5-, 10-, 20-fold around the default rates (Table 3.1).

3. GRK-Mediated β2AR Regulation

This chapter is adapted from "Quantitative Modeling of GRK-Mediated β2AR Regulation." Vayttaden SJ, Friedman J, Tran TM, Rich TC, Dessauer CW, Clark RB (2010) PLoS Comput Biol 6(1): e1000647. doi:10.1371/journal.pcbi.1000647

I have modelled the GRK/Arrestin module of the β2AR regulation as it pertains to experimental measures of agonist-induced GRK-mediated β2AR-phosphorylation, β2AR-dephosphorylation, -trafficking, -desensitisation and -resensitisation (Figure 3.1). Our group has previously shown that stable overexpressions of the WT β2AR in HEK 293 cells were suited for examining many aspects of the β2AR regulation process. Most importantly, the duration and amplitude of β2AR desensitisation in these cells is comparable with the endogenous receptor (Clark and Knoll 2002). In the stable overexpression system, the EC_{50} of PKA-mediated β2AR phosphorylation is ~ 1000-fold lower than the EC_{50} for GRK-phosphorylation of the β2AR. This allows us to differentiate the GRK- and PKA-mediated β2AR desensitisation into separate modules. We have previously shown that at high agonist concentrations GRK accounts for the majority of β2AR desensitisation (Seibold, Williams et al. 2000). Table 3.1 lists the parameters used to model and simulate the consensus GRK pathway in response to various agonists at different concentrations and durations. The data simulated were from 90+ independent experiments on our stable overexpressions of human β2AR in HEK 293 cells. Using a unique model to simulate the wide dataset provided good modelling constraints. This ensured that the model applicability extended over a wide repertoire of agonist-induced β2AR response.
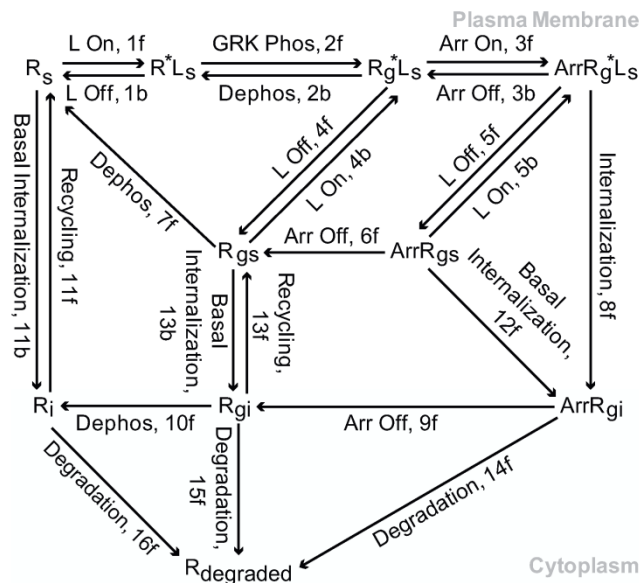
Figure 3.1 Reaction Diagram of the GRK-Mediated β2AR Regulation.

L is ligand; R^* is active state of β2AR; R_s and R_i are surface/plasma membrane and internalised β2AR; R_g is GRK-phosphorylated β2AR; Arr is arrestin. This reaction diagram describes the default model for simulations using the rate constants as described in Table 3.1.

Figure and Figure Legend Source: http://dx.doi.org/10.1371/journal.pcbi.1000647.g001

"Quantitative Modeling of GRK-Mediated β2AR Regulation." Vayttaden SJ, Friedman J, Tran TM, Rich TC, Dessauer CW, Clark RB (2010) PLoS Comput Biol 6(1): e1000647.

doi:10.1371/journal.pcbi.1000647

Table 3.1 Parameters for GRK-Mediated β2AR Regulation Model

Reaction Name	Parameter (/min)	Reference/Rationale
Ligand (Agonist) On	$k_{1f} = k_{4b} = k_{5b} = 500$	Rates used to achieve rapid ligand binding so that it is not rate limiting.[A]
Ligand (Agonist) Off	$k_{1b} = k_{4f} = k_{5f} = 4$	
Ligand (Agonist) On (in the presence of an antagonist)	$k_{1f} = k_{4b} = k_{5b} = 0.005$	Antagonist is assumed to behave as a competitive inhibitor (Prichard and Tomlinson 1986) so the agonist binding rates are greatly reduced.
Ligand (Agonist) Off (in the presence of an antagonist)	$k_{1b} = k_{4f} = k_{5f} = 4$	Agonist off-rates are unaffected in the presence of an antagonist that behaves like a competitive inhibitor
GRK Phosphorylation	$k_{2f} = \alpha[R*]1.4$	Initial rate of GRK phosphorylation on treatment with 10 µM epinephrine = 0.7-1.4 /min (Tran, Friedman et al. 2004).[B]
GRK Dephosphorylation	$k_{2b} = k_{7f} = k_{10f} = 0.036$	Phosphorylated receptor $t_{1/2}$ = 18 min (Tran, Friedman et al. 2007).
Arrestin On (to an agonist-bound receptor)	$k_{3f} = 27.0$	Rate of arrestin binding = 26.6 ± 5.9 /min (Krasel, Bunemann et al. 2005)
Arrestin Off (from an agonist-bound receptor)	$k_{3b} = 4.0$	Rate of arrestin dissociation assumed to match measured K_d.
Internalisation	$k_{8f} = 0.22$	k_f = 0.22 /min (Tran, Friedman et al. 2004).
Basal Internalisation	$k_{11b} = k_{12f} = k_{13b} = 0.0085$	Rates used to match negligible basal internalisation (Morrison, Moore et al. 1996).
Arrestin Off (from an agonist-free receptor)	$k_{6f} = k_{9f} = 11.0$	Rate of arrestin dissociation = 10.86 ± 1.2 /min (Krasel, Bunemann et al. 2005).
Receptor Degradation	$k_{14f} = k_{15f} = k_{16f} = 0.004$	$t_{1/2}$ ~ 3–4 hours (Liang, Hoang et al. 2008).
Receptor Recycling	$k_{11f} = k_{13f} = 0.09$	k_f = 0.09 /min (Tran, Friedman et al. 2004).

[A]Off-rates for isoproterenol ≥ 4 /min (Mueller, Motulsky et al. 1988), epinephrine > 100 /min (Krasel, Bunemann et al. 2005). For a K_d of 450 nM (epinephrine) and 283 nM (isoproterenol) the calculated on-rates are very fast. Slowing down the forward-rates to 500 /min does not affect the downstream events being simulated since they happen at a slower time scale. The

ligand off-rate is not set at lower than 4 /min in order to avoid making it rate limiting for arrestin dissociation.

[B]α = Coupling efficiency relative to epinephrine; Isoproterenol is assumed to have the same coupling efficiency as epinephrine since they are both full agonists. The relative coupling efficiencies for partial agonists are as follows, Epinephrine = Isoproterenol = 1, Fenoterol = 0.66, Formoterol = 0.63, Terbutaline = 0.33, Zinterol = 0.33, Albuterol = 0.25, Salmeterol = 0.13, Dobutamine = 0.04 and Ephedrine = 0.03. $[R^*]$ = ($[R_{total}]$ [Agonist]/([Agonist]+($K_{d\ agonist}$))); $[R_{total}]$ = 1; $K_{d\ epinephrine}$ = 450 nM; $K_{d\ isoproterenol}$ = 283 nM. Simulated phosphorylation rate = α $[R^*]$1.4 (for epinephrine); = α $[R^*]$0.7 (for isoproterenol).

Model 1: All rates are set as described above, for the default model.

Model 2: k_{2b} = k_{7f} = 0 /min since this model disallows dephosphorylation at the plasma membrane.

Model 3: k_{13f} = 0 /min since this model disallows recycling of phosphorylated receptor.

Model 4: k_{10f} = 0 /min since this model disallows dephosphorylation of the internalised receptor.

Model 5: k_{10f} = k_{13f} = 0 /min since this model does not allow neither dephosphorylation of the internalised receptor nor recycling of phosphorylated receptor.

Model 6: k_{2b} = k_{7f} = k_{13f} = 0 /min since this model does not allow neither dephosphorylation of the receptor at the plasma membrane nor recycling of phosphorylated receptor.

Table Source: http://dx.doi.org/10.1371/journal.pcbi.1000647.t001

"Quantitative Modeling of GRK-Mediated β2AR Regulation." Vayttaden SJ, Friedman J, Tran

TM, Rich TC, Dessauer CW, Clark RB (2010) PLoS Comput Biol 6(1): e1000647.

doi:10.1371/journal.pcbi.1000647

3.1. Assumptions

3.1.1. Two State Model

Since all parameters described in Table 3.1 were obtained using full agonists for the β2AR (epinephrine or isoproterenol), I assumed a simplified two state model for β2AR activation. Here the plasma membrane bound inactive β2AR is denoted by R_s and R^*L_s denotes the agonist-induced active β2AR. I also assumed ligand-induced β2AR activation since basal GRK Phosphorylation of WT β2AR is negligible (Tran, Friedman et al. 2004; Vaughan, Millman et al. 2006; Tran, Friedman et al. 2007; Drake, Violin et al. 2008).

3.1.2. Ligand Binding

The off-rate for isoproterenol from the β2AR is ≥4 /min (Mueller, Motulsky et al. 1988) and for epinephrine >100 /min (Krasel, Bunemann et al. 2005). To achieve the K_ds for isopreoterenol (283 nM) and epinephrine (450 nM), the on-rates have to be very fast. These fast rates were slowed down to 500 /min for two reasons; (i) even at these reduced speeds ligand binding was about 18 fold faster than the next fastest reaction so it did not affect the time course of the downstream events being modelled; and (ii) at these reduced speeds very small step sizes were not required to solve the differential equations using the Runge-Kutta solver (ODE23s) in MATLAB R2008 (MathWorks, Natick, MA).

3.1.3. Ligand Dissociation

I assumed that the unbinding rates for agonist from β2AR were uninfluenced by its arrestin binding or GRK phosphorylation status (Reactions 1b, 4f, 5f in Figure 3.1). This is a simplification of the kinetics since arrestin binding stabilizes a high-agonist affinity state of the receptor, prompting some authors to characterise the receptor-arrestin complex as an alternative ternary complex analogous to the ternary complex existing between agonist-receptor-G protein in the absence of GTP (Gurevich, Pals-Rylaarsdam et al. 1997). This simplification should not significantly affect the steady-state simulations of receptor phosphorylation, internalisation, desensitisation since the experimental measurements the simulations are constrained with are made under continuous presence of high agonist. The effect of assuming equivalent ligand dissociation rates for naïve, GRK-phosphorylated or arrestin bound receptor is that ligand dissociation rates from arrestin bound-receptor (Reaction 5f in Figure 3.1) end up being faster than normal leading to more rapid initial resensitisation post agonist removal. Since we did not have rates of ligand dissociation from arrestin bound receptor the model provided us a means to vary the ligand dissociation rate for arrestin bound species and compare the simulated results to the experimentally measured receptor resensitisation curve where the effects of this reaction would be most dominant. Through our simulations we showed that a ten-fold lower dissociation rate of ligand from arrestin-bound β2AR (Reaction 5f in Figure 3.1) is required to match the initial resensitisation rates correctly (Figure 3.3B).

3.1.4. Receptor Activity

In the model I assumed that the GRK phosphorylated β2AR (R_{gs}, $R_g^*L_s$ in Figure 3.1) has reduced activity (0.7) compared to naïve β2AR (Benovic, Kuhn et al. 1987; Lohse, Andexinger et al. 1992; Tran, Friedman et al. 2007). This is a simplification since the receptor can exist in any conformation in a wide parameter space and each of the conformations would have its own activity. The effect of this simplification of assigning the same activities for all "flavours" of GRK-phosphorylated receptor is that the receptor activity profile would be dependent on both time and concentration of agonists, so a one-size-fits-all model would not easily match all data points. Thus the mismatches in simulated receptor desensitisation and experimentally measured desensitisation (Figure 3.3A) could in part be because of this simplification. I also assumed that arrestin binding or internalisation completely uncouples the receptors therefore those species have no activity.

3.1.5. GRK-Phosphorylation Kinetics

I assumed that ligand activation of β2AR results in only a single event of GRK phosphorylation where both serines 355 and 356 are simultaneously phosphorylated. The anti-phosphosite antibody used in our β2AR phosphorylation studies detects only dual phosphorylation of serines 355, 356. Use of our antibody for studying GRK-mediated β2AR phosphorylation kinetics has been validated by various groups (Tran, Friedman et al. 2004; Shenoy, Drake et al. 2006; Violin, Ren et al. 2006; Pontier, Percherancier et al. 2008;

Woo, Wang et al. 2009). The assumption of a single phosphorylation event and equating Ser355,356 phosphorylation with "the" GRK phosphorylation event is a simplification since we do know that in our cells the phosphorylation of Ser364 too is associated with GRK (Seibold, Williams et al. 2000). Also serine to alanine substitution of serines 355, 356, and 364 eliminated receptor-level desensitisation in the PKA- background (S261, 262A and S345, 346A) and caused ~ 90% reduction in phosphorylation as assessed by ^{32}P-prelabeling. So there is at least a 10% receptor phosphorylation that cannot be attributed to the currently identified GRK phosphorylation sites. Inspite of these limitations the decision to assume a single event of GRK phosphorylation where both serines 355 and 356 are simultaneously phosphorylated is justified because 1) there are no experimental readouts of individual phosphorylation sites available; 2) the dual phosphorylation of S365, 366 correlates well with both a dose response and time course of agonist treatment. The disadvantage of this assumption is that it is no longer possible to project multi-phosphorylation states of the receptor that could play a role in receptor sorting post-internalisation selecting for recycling vs. receptor degradation. Also assuming a single phosphorylation event prevents assigning multiple phosphorylation site specific activities to the receptor, this could in turn affect the quality of simulation fits.

In my models 1-6 the rate of GRK-mediated β2AR phosphorylation is dependent on the fraction of agonist-bound β2AR denoted by [R*], and coupling efficiency of the ligand denoted by α. We've measured epinephrine induced GRK-mediated β2AR phosphorylation to range from 0.7–1.4/min (Tran,

Friedman et al. 2004). I assume that isoproterenol induced β2AR

phosphorylation rates will be in the same range since epinephrine and

isoproterenol have comparable efficacies.

We have previously shown that both the plasma membrane and endosomal

fraction of β2AR can undergo dephosphorylation (Iyer, Tran et al. 2006; Tran,

Friedman et al. 2007). Therefore I allow both plasma membrane and cytosolic

dephosphorylation of β2AR in my model (c.f. Footnote of Table 3.1).

3.1.6. Arrestin Kinetics

The arrestin on/off rates were obtained from experiments on fluorescently

tagged proteins (Krasel, Bunemann et al. 2005). I assumed that these

fluorescent tags did not affect the measured kinetics. The arrestin off-rate from

a ligand bound β2AR complex (Reaction 3b in Figure 3.1) was estimated to be

~4.0/min from previous measurements of the K_d (Gurevich, Dion et al. 1995).

3.1.7. Post-Internalisation Events

Consistent with the rapid on/off-rates and high K_ds of epinephrine or

isoproterenol (Mueller, Motulsky et al. 1988; Devanathan, Yao et al. 2004) I

assumed ligand dissociation post β2AR internalisation to be very rapid. We

have previously shown negligible rates of basal β2AR internalisation (Morrison,

Moore et al. 1996). Since both basal and agonist induced β2AR internalisation

rates are slower than agonist dissociation I have collapsed β2AR internalisation

and post-internalisation agonist dissociation into a single step. This assumption

limits the usefulness of the model in simulating post-internalisation events on

treating with certain partial agonists like Salmeterol which don't easily dissociate from the receptor (Jack 1991; Rong, Arbabian et al. 1999) and are postulated to have low affinity for arrestin (Moore, Millman et al. 2007; Vayttaden, Friedman et al. 2010).

In the GRK-mediated β2AR regulation model I allow arrestin-free internalised β2AR to recycle independent of its phosphorylation status (Tran, Friedman et al. 2007). Currently the precise mechanisms and pathways of β2AR downregulation are unclear even though we have shown it to be biphasic (Williams, Barber et al. 2000). Thus to simplify downregulation reactions in the model I assume that all internalised β2AR species can undergo downregulation ($t_{1/2}$ = 3–4 hours) (Morrison, Moore et al. 1996; Williams, Barber et al. 2000; Liang, Hoang et al. 2008).

3.1.8. Pseudo-First Order Kinetics

In HEK293s GRK2/5/6 levels exceeds even overexpressed β2AR levels by approximately 100 fold (Tran, Jorgensen et al. 2007). We have also established that the level of desensitisation in both HEK 293 cells with endogenous (30 fmol/mg) or overexpressed β2AR (3000 fmol/mg) is comparable. Arrestin levels therefore should be sufficiently high to allow complete desensitisation even on 100 fold overexpression of β2AR. Others (Menard, Ferguson et al. 1997) have shown that in comparison to four cell lines HEK 293 cells have relatively the the highest levels of arrestin and GRK. In the light of the obvious excess of GRKs and arrestin over β2AR I represent the second order reactions of GRK-

mediated β2AR phosphorylation and arrestin binding to the β2AR as pseudo-first order reactions. These assumptions force us to use variation in rates of arrestin binding or GRK-phosphorylation as a proxy to the effects of variation in levels of arrestin and GRK.

3.2. Model Validation

My mathematical model of GRK-mediated β2AR regulation was validated against six types of biochemical measurements (~ 90+ distinct experiments) in HEK 293 cells stably overexpressing the WT β2AR across a range of agonist concentrations (Figures 3.2, 3.3, 4.1). The model validation results are discussed below.

3.2.1. GRK Phosphorylation

 My model captured the main temporal features of GRK-mediated β2AR phosphorylation across a wide range of epinephrine concentrations wherein the stimulation was from 0–30 min (Figure 2.2A) and in response to a variety of partial agonists (Figure 4.1). GRK-mediated β2AR phosphorylation was measured in whole cell extracts as described here.

GRK phosphorylations of the β2AR at residues Serine (355, 366) were determined using anti-phosphosite-specific antibodies (Santa Cruz Biotechnology, Inc., Santa Cruz, CA) (Tran, Friedman et al. 2004). HEK293s stably overexpressing WT β2AR were incubated with isoproterenol (Sigma, St. Louis, MO), through different treatment times. Post-treatment the whole cell protein was extracted with a solubilisation buffer and then incubated with Peptide N-glycosidase F (New England Biolabs, Ipswich, MA) to remove

glycosyl residues. This was followed by a treatment with SDS sample buffer prior to running on polyacrylamide gel electrophoresis. Following the gel transfer, the levels of GRK site phosphorylation were determined by western blots. First, the phosphorylation data was normalised to β2AR levels and then to allow inter-experimental comparison it was normalised to the maximum phosphorylation with saturating concentrations of epinephrine.

GRK-mediated β2AR phosphorylation was simulated by selecting dosage and duration of ligand treatment corresponding to the experimental measurements. The sum total of Rgs, Rg*Ls, ArrRgs, ArrRg*Ls, ArrRgi and Rgi (Figure 3.1) was plotted as a percentage of total β2AR against the experimentally measured GRK phosphorylated β2AR (Figure 3.2A).
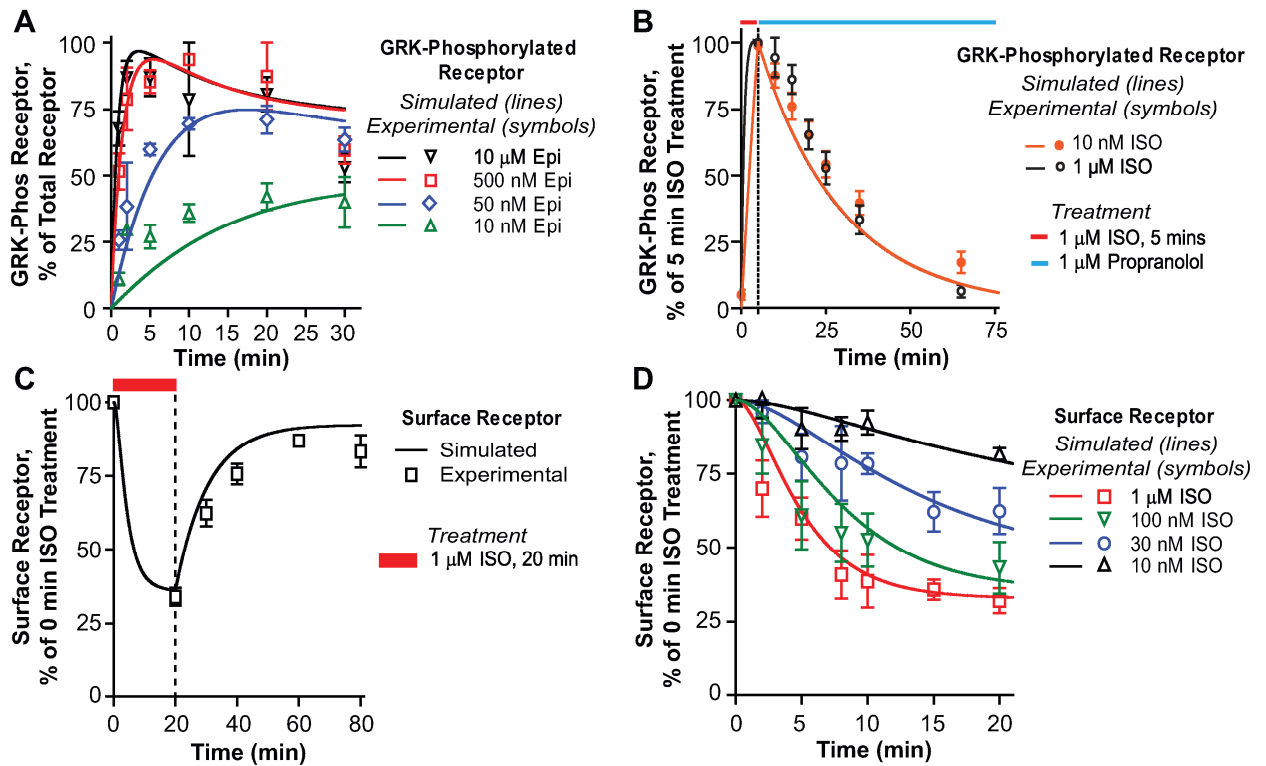
Figure 3.2. Comparisons of Experimental Results with Simulations of the Model.

Panels A–D: Comparisons of simulations (continuous lines) of the model shown in Figure 2.1, with experimental data obtained in HEK 293 cells stably overexpressing FLAG WT β2AR (discrete data points). **(A)** Time course of GRK phosphorylation of the receptor on treatment with different concentrations of epinephrine (Tran, Friedman et al. 2004). **(B)** Dephosphorylation of the GRK phosphorylated site on the receptor after 5 min treatment with either 1.0 µM or 10 nM ISO (red bar) followed by addition of propranolol (blue bar) and measure of loss of GRK site phosphorylation. Phosphorylated receptor is expressed as a percent of phosphorylation achieved at the end of 5 min treatment with either agonist concentration (Tran, Friedman et al. 2007). **(C)** Recycling of the receptor after 20 min treatment with 1µM isoproterenol followed by rapid washout of agonist (Morrison, Moore et al. 1996). **(D)** Internalisation of β2AR on treatment with various concentrations of isoproterenol as indicated. Surface receptor is measured by the loss of [³H]CGP-12177 (Tran, Friedman et al. 2007).

Figure and Figure Legend Source: http://dx.doi.org/10.1371/journal.pcbi.1000647.g002

3.2.2. Dephosphorylation

Dephosphorylation of the GRK phosphorylated β2AR was simulated across a 100 fold agonist concentration range as shown in Figure 3.2B. Dephosphorylation of the GRK-phosphorylated WT β2AR was measured in whole cell extract as described below.

In dephosphorylation experiments HEK293s stably overexpressing WT β2AR were treated for 5 min with either 1.0 μM or 10 nM isoproterenol. Post agonist treatment the cells were washed and incubated with medium containing 0.1 μM propranolol (Sigma, St. Louis, MO) (Tran, Friedman et al. 2004). The loss of GRK site phosphorylations at Serine (355, 366) was then assayed using western blots as discussed in Section 3.2.1. In the dephosphorylation experiments, phosphorylation at 5 min with different agonist concentrations was normalised as maximum phosphorylation foreach concentration.

The dephosphorylation simulations had two parts - the first part dealt with ligand-induced GRK-mediated β2AR phosphorylation, and the second part dealt with the antagonist treatment allowing for β2AR dephosphorylation. Concentrations of all species of β2AR for the second part of the simulation were initialised to the terminal state from the first simulation. During the second phase of the simulations the ligand on rates were reduced 100,000 fold (to mimic competitive binding with an antagonist). On completion of the simulations, the sum total of Rgs, Rg*Ls, ArrRgs, ArrRg*Ls, ArrRgi and Rgi

(Figure 3.1) was plotted as a percentage of total β2AR against the experimentally measured GRK phosphorylated β2AR (Figure 3.2B).

3.2.3. Recycling

β2AR recycling was measured by [³H]CGP-12177 binding, post a 20 min isoproterenol treatment followed by a wash as described here. HEK 293s stably overexpressing WT βAR were treated with 1 µM agonist (isoproternol) through 20 min to maximise internalisation. Post ligand treatment, the cells were washed to remove ligand and incubated for the times indicated at 37°C to allow recycling. Surface β2AR levels were assayed using [³H]CGP-12177 binding as described in the previous section (Seibold, Williams et al. 2000). The measure of β2AR at the surface at time 0 was normalised as 100% surface βAR.

Recycling was simulated similar to dephosphorylation as described in 3.2.2 since both experiments involved two perturbations during the course of an experiment. On completion of the β2AR recycling simulations the sum total of Rs, R*Ls, Rgs, Rg*Ls, ArrRgs and ArrRg*Ls (Figure 3.1) was plotted against the experimentally measured surface β2AR with the surface receptor at time zero normalised to 100% (Figure 3.2C).

3.2.4. Internalisation

HEK 293s stably overexpressing WT βAR were treated with varying agonist (isoproterenol) concentrations through different treatment times. Post ligand treatment and washing, receptor internalisation was measured in intact cells using [³H]CGP-12177 (20 nM) binding (Tran, Friedman et al. 2007). [³H]CGP-

12177 is a hydrophilic antagonist that binds only surface (plasma membrane) βAR at 0–4°C. The binding assay is conducted ±1μM alprenolol (Sigma, St. Louis, MO), a β2AR antagonist used to determine non-specific binding of [^{3}H]CGP-12177. The measure of surface β2AR at time 0 was normalised as 100% surface β2AR for different agonist concentrations.

On completion of the internalisation simulations the sum total of Rs, R*Ls, Rgs, Rg*Ls, ArrRgs and ArrRg*Ls (Figure 3.1) was plotted against the experimentally measured surface β2AR with the surface receptor at time zero normalised to 100% (Figure 3.2D).

3.2.5. Desensitisation

The β2AR desensitisation measurements (Figure 3.3A) were made in HEK 293 cells that either stably overexpressed WT β2AR or a β2AR lacking the two PKA consensus sites (S261, 262A and S345, 346A termed PKA-). PKA- was used to eliminate the effects of PKA-mediated β2AR desensitisation (Seibold, Williams et al. 2000). Desensitisation of β2AR stimulation of AC was performed as described below.

HEK 293s that stably overexpressed either WT βAR or a β2AR lacking the two PKA consensus sites (S261, 262A and S345, 346A) were treated with various concentrations of agonist (isoproterenol). Post washout of ligand, membrane fractions were separated using sucrose step gradients. Desensitisation was measured as the increase in EC_{50} for isoproterenol stimulation of AC relative to controls and the results were calculated as fraction activity remaining (Tran,

Friedman et al. 2007). Through our previous studies we have shown that there is a 35% decrease in V_{max} from downstream effects, most likely on AC (Whaley, Yuan et al. 1994; Seibold, Williams et al. 2000). So in the model of receptor-level GRK-mediated desensitisation described here we ignore these V_{max} changes. The model described in Chapter 5 does address downstream effects due to PDE activity but even this model ignores V_{max} effects due to postranscriptional modifications of AC.

On completion of the simulation run, activity was calculated as the weighted sum of Rs, R*Ls, Rg*Ls and Rgs normalised to initial receptor activity. The weighting of the active β2AR species was decided as discussed above in 3.1.4. Simulated β2AR activity was plotted against the experimentally measured active β2AR (Figure 3.3A). Since the model lacked PKA-mediated β2AR regulation it underestimated early (first two minutes) desensitisation post-ligand treatment for the WTβ2AR, but there was significant concurrence with experimental data over longer treatment times.
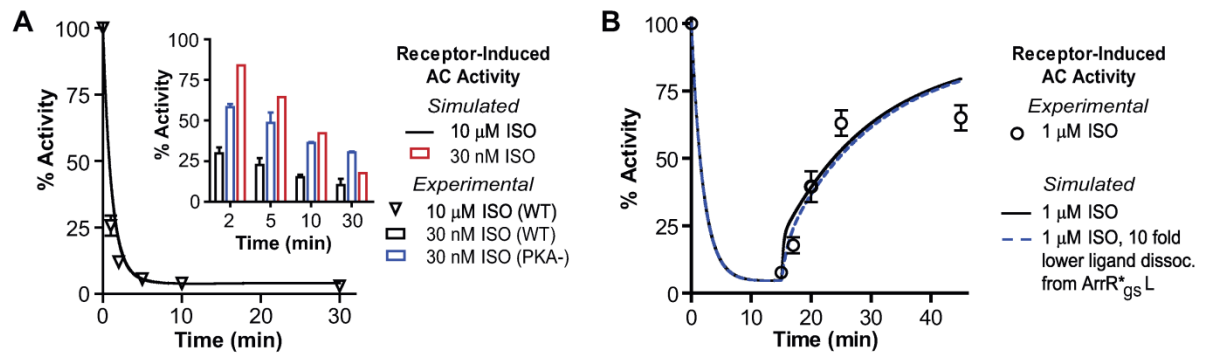
Figure 3.3. Validation of the Model with Two Sets of Experimental Results.

Validation of the simulations (continuous lines) of the model shown in Figure 3.1, with experimental data obtained in HEK 293 cells stably overexpressing the FLAG WT β2AR (discrete data points). **(A)** Desensitisation of β2AR stimulation of adenylyl cyclase after treatment with 10 μM isoproterenol. Inset shows β2AR desensitisation on stimulation with 30 nM isoproterenol. Red – simulated results; Black – WT cells; Blue - cells stably overexpressing β2AR lacking PKA phosphorylation sites (PKA-). At lower concentrations the model matches PKA- desensitisation more closely since it does not include PKA-mediated β2AR desensitisation. **(B)** Resensitisation of the β2AR stimulation of adenylyl cyclase. WT β2AR were stimulated with 1μM isoproterenol for 15 min, followed by addition of metoprolol as described in 3.2.6. Dotted line shows simulated % activity of the β2AR when ligand dissociation from arrestin-bound receptor complex is reduced by ten-fold.

Figure and Figure Legend Source: http://dx.doi.org/10.1371/journal.pcbi.1000647.g003

"Quantitative Modeling of GRK-Mediated β2AR Regulation." Vayttaden SJ, Friedman J, Tran TM, Rich TC, Dessauer CW, Clark RB (2010) PLoS Comput Biol 6(1): e1000647. doi:10.1371/journal.pcbi.1000647

3.2.6. Resensitisation

The β2AR resensitisation experiments (Figure 3.3B) were done in HEK 293 cells that stably overexpressed WT β2AR as described here.

In order to measure resensitisation of WT β2AR, propranolol could not be used for the blockade of isoproterenol stimulation as described for desensitisation in Section 3.2.5, because its rate of dissociation from the receptor was too slow to allow for resensitisation time course measurements. To avoid this handicap we used a low affinity antagonist of the βARs like 100 μM metoprolol (240 nM K_d) (Sigma, St. Louis, MO) (Tran, Friedman et al. 2007). Post different resensitisation times cells were washed free of metoprolol, and membranes were prepared and assayed for isoproterenol stimulation of AC (Tran, Friedman et al. 2007). The measure of membrane AC activity at time 0 is normalised as maximum activity in desensitisation and resensitisation experiments.

β2AR resensitisation was simulated in two parts, as described previously for dephosphorylation (3.2.2) and recycling (3.2.3). At the end of the simulation run, activity was calculated as the weighted sum of Rs, R*Ls, Rg*Ls and Rgs normalised to the initial receptor activity. The weighting of the active β2AR species was decided as discussed above in 3.1.4. As an artefact of the rates (Reaction 5f, Figure 3.1) used in the default model (Table 3.1, Model 1) there is initially a rapid increase in resensitisation. This artefactual spike can be removed on lowering the rate of agonist dissociation from an arrestin-bound

β2AR complex (Reaction 5f, Figure 3.1) by ten-fold which is in line with the

increased apparent stability of this complex (Gurevich, Dion et al. 1995).
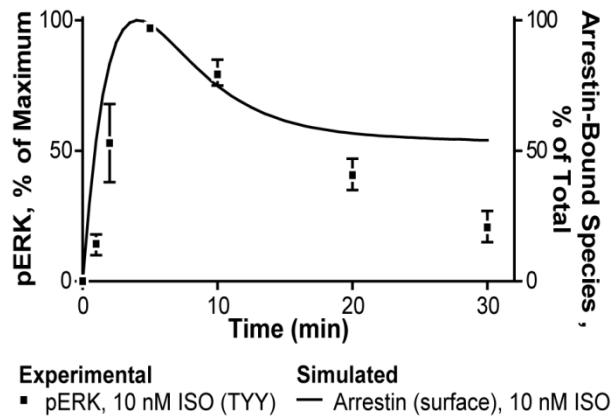
Figure 3.4. Correlation of Simulated Surface Arrestin with G Protein Independent ERK Activation.

pERK data (Shenoy, Drake et al. 2006) matches initial accumulation of simulated surface arrestin (Arrs + ArrRg*Ls; Figure 2.1). The discrepancy in latter time points might be due to activation of ERK phosphatases which is not explicitly modelled. TYY mutants are uncoupled from G protein so the ERK phosphorylation seen is independent of G protein activation.

3.2.7. Arrestin-Dependent ERK Activation

There have been a number of experiments demonstrating G protein-independent signalling that appears to depend on arrestin scaffolding of MAPK cascades (Pierce, Luttrell et al. 2001; Song, Coffa et al. 2009). Since I did not use any arrestin signalling data to create the model, the ability to match arrestin-mediated ERK signalling data would be an independent validation of my model. I have compared the simulated time course of surface arrestin species viz. sum total of Arrs and ArrRg*Ls (Figure 3.1) with recent data (Shenoy, Drake et al. 2006) showing the G protein independent activation of ERK (Figure 3.4). For the early times of agonist stimulation there is good correlation of simulated surface arrestin with G protein independent ERK activation. The discrepancy in latter time points might be due to activation of ERK phosphatases which is not explicitly modelled.

3.2.8. Sensitivity Analyses

I subjected the model to a univariate sensitivity analyses by varying individual rates over a twenty-fold range and studying its effects on the simulated β2AR desensitisation and resensitisation under conditions described in 3.2.5 and 3.2.6. The motivation to run sensitivity analyses on desensitisation and resensitisation were, 1) these were functional readouts of the signalling pathway; 2) these were experiments that validated the behaviour of the insilico β2AR signalling pathway; and 3) test for the robustness of the model by

checking for the dependence of modeled behavior on choice of reaction parameters.

The simulations were carried out as described in Methods 2.2.6 and the results plotted as the difference from the average experimental value at each time point.

In the simulated β2AR desensitisation experiments the model was significantly sensitive to perturbations of only three rates (Figure 3.5). Decreasing GRK-mediated β2AR phosphorylation (k_{2f}, Table 3.1) reduced the desensitisation at earlier time points. Reduction of arrestin affinity for the β2AR-agonist complex (k_{3f}, k_{3b}, Table 3.1) decreased desensitisation at later time points. These observations were consistent with the model design.

The interpretation of the sensitivity analysis for β2AR resensitisation (Figure 3.6) is not straightforward because I'd to first desensitise the system. The pre-desensitisation affected the initial simulated values of resensitisation. Reducing $ArrR_g^*L_s$ internalisation (k_{8f}, Table 3.1) decreased β2AR desensitisation at 15 min (see conditions in Figure 3.3B) leading to a higher baseline at the start of resensitisation causing an overestimate of initial resensitisation. Perturbing internalisation rates did not have any additional effects on latter time points of resensitisation. Increasing β2AR recycling (k_{11f}, k_{13f}, Table 3.1) reduced the internalised pool of β2AR and caused an overestimation of β2AR resensitisation. As a quality control measure the sensitivity analyses did not

reveal any unexpected surprises in the model behavior and it was robust over a

wide range of perturbations.
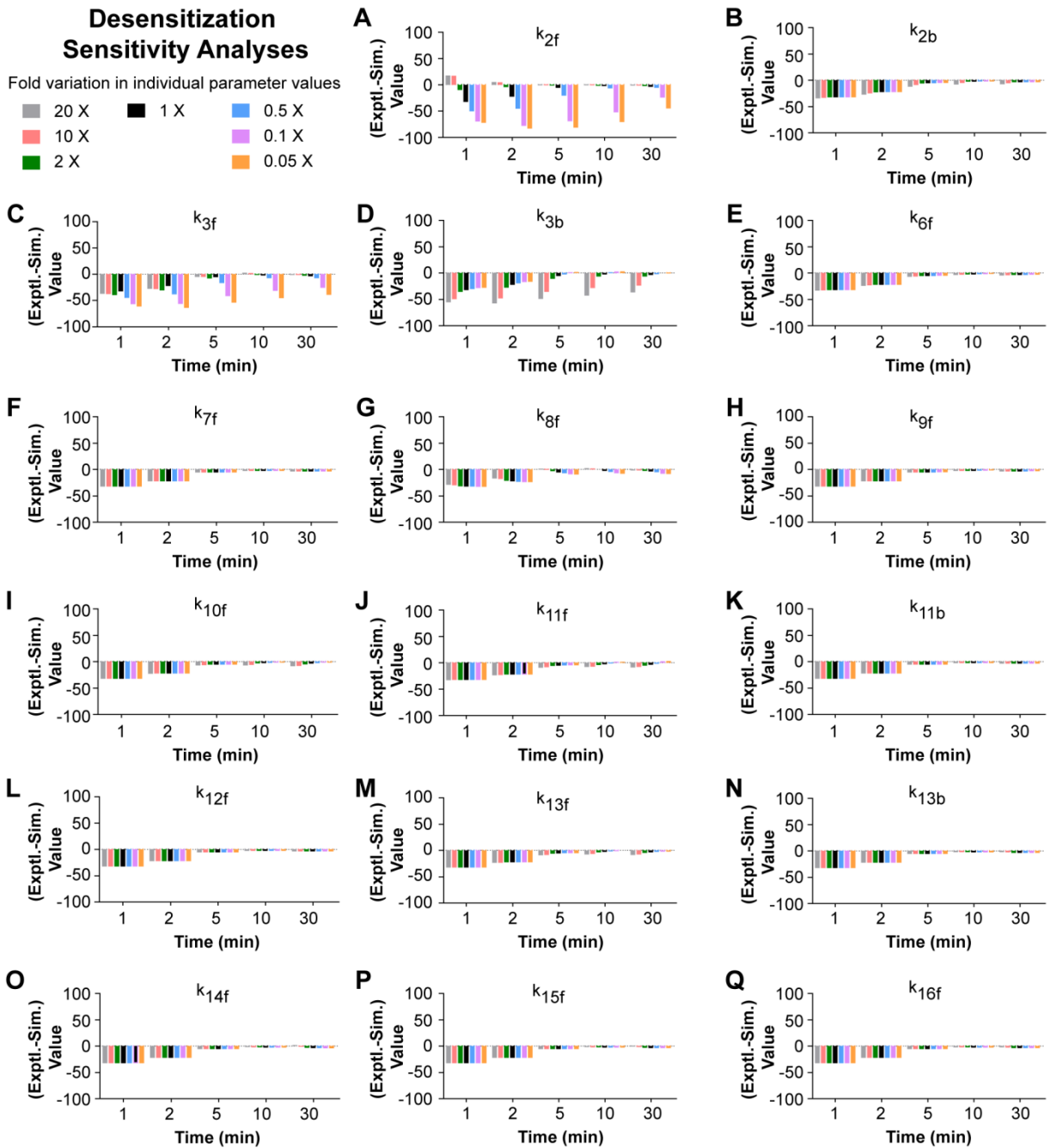
Figure 3.5. Univariate Sensitivity Analyses of the Model for Desensitisation.

Panels A–Q: Simulated isoproterenol (10 µM) induced β2AR desensitisation over a twenty-fold variation of individual rates. Negative values indicate a simulated measurement higher than experimental measure.

Figure and Figure Legend Source:

http://dx.doi.org/10.1371/journal.pcbi.1000647#pcbi.1000647.s002

"Quantitative Modeling of GRK-Mediated β2AR Regulation." Vayttaden SJ, Friedman J, Tran TM, Rich TC, Dessauer CW, Clark RB (2010) PLoS Comput Biol 6(1): e1000647. doi:10.1371/journal.pcbi.1000647

Figure 3.6. Univariate Sensitivity Analyses of the Model for Resensitisation.

Panels A–Q: Simulated β2AR resensitisation post 15 min isoproterenol (1 µM) treatment over a twenty-fold variation of individual rates. Negative values indicate a simulated measurement higher than experimental measure.

Figure and Figure Legend Source:

http://dx.doi.org/10.1371/journal.pcbi.1000647#pcbi.1000647.s003

"Quantitative Modeling of GRK-Mediated β2AR Regulation." Vayttaden SJ, Friedman J, Tran TM, Rich TC, Dessauer CW, Clark RB (2010) PLoS Comput Biol 6(1): e1000647. doi:10.1371/journal.pcbi.1000647

3.3. Model Description

The ordinary differential equations for the GRK-mediated β2AR regulation based on the Laws of Mass Action are given below.

Equation 3.1

$$d[R_s]dt = -(k_{1f} + k_{11b})(R_s) + (k_{1b})(R^*L_s) + (k_{11f})(R_i)$$

Equation 3.2

$$d[R^*L_s]dt = -(k_{1b} + k_{2f})(R^*L_s) + (k_{1f})(R_s) + (k_{2b})(R_g^*L_s)$$

Equation 3.3

$$d[R_g^*L_s]dt = -(k_{2b} + k_{3f} + k_{4f})(R_g^*L_s) + (k_{2f})(R^*L_s) + (k_{3b})(ArrR_g^*L_s) + (k_{4b})(R_{gs})$$

Equation 3.4

$$d[ArrR_g^*L_s]dt = -(k_{3b} + k_{5f} + k_{8f})(ArrR_g^*L_s) + (k_{3f})(R_g^*L_s) + (k_{5b})(ArrR_{gs})$$

Equation 3.5

$$d[ArrR_{gs}]dt = -(k_{5b} + k_{6f} + k_{12f})(ArrR_{gs}) + (k_{5f})(ArrR_g^*L_s)$$

Equation 3.6

$$d[R_{gs}]dt = -(k_{4b} + k_{7f} + k_{13b})(R_{gs}) + (k_{4f})(R_g^*L_s) + (k_{13f})(R_{gi}) +$$

$$(k_{6f})(ArrR_{gs})$$

Equation 3.7

$$d[\text{ArrR}_{gi}]dt = -(k_{9f} + k_{14f})(\text{ArrR}_{gi}) + (k_{8f})(\text{ArrR}_g^*L_s) + (k_{12f})(\text{ArrR}_{gs})$$

Equation 3.8

$$d[\text{R}_{gi}]dt = -(k_{10f} + k_{13f} + k_{15f})(\text{R}_{gi}) + (k_{9f})(\text{ArrR}_{gi}) + (k_{13b})(\text{R}_{gs})$$

Equation 3.9

$$d[\text{R}_i]dt = -(k_{11f} + k_{16f})(\text{R}_i) + (k_{11b})(\text{R}_s) + (k_{10f})(\text{R}_{gi})$$

Equation 3.10

$$d[\text{R}_{\text{degraded}}]dt = (k_{14f})(\text{ArrR}_{gi}) + (k_{15f})(\text{R}_{gi}) + (k_{16f})(\text{R}_i)$$

In the equations 3.1-3.10 kxf and kxb denote the forward and backward rates for the reaction number denoted by x. Rs = β2AR on the plasma membrane; R*Ls = Agonist bound β2AR on the plasma membrane; Rg*Ls = Agonist bound, GRK phosphorylated β2AR on the plasma membrane; ArrRg*Ls= Agonist and arrestin bound, GRK phosphorylated β2AR on the plasma membrane; ArrRgs = Arrestin bound, GRK phosphorylated β2AR on the plasma membrane; ArrRgi = Arrestin bound, GRK phosphorylated β2AR in the internalised compartments; Rgi = GRK phosphorylated β2AR in the internalised compartments; Ri = β2AR in the internalised compartments; Rdegraded = Degraded β2AR in the cytoplasm.

3.4. Model Results and Discussions

GRK and arrestin isoforms have been frequently targeted for overexpression or knockdown in different cells types (Ahn, Nelson et al. 2003; Penela, Ribas et al. 2003; Reiter and Lefkowitz 2006; Violin, Ren et al. 2006; Luo, Busillo et al. 2008). These proteins also differ in their overall expression levels and localisation (Zhang, Barak et al. 1997; Komori, Cain et al. 1998). They also undergo post-translational modifications which might affect its activity (Lin, Krueger et al. 1997; Lin, Chen et al. 2002; Penela, Ribas et al. 2003; Shenoy, Drake et al. 2006). Given that there is wide variability in the activity or level of these β2AR regulatory proteins in different cell types I was interested in the effect of this variability on the modelling results. I varied GRK-mediated β2AR phosphorylation and arrestin β2AR binding rates over a hundred-fold range around rates mentioned in Table 3.1 and plotted its effects on β2AR phosphorylation, desensitisation and internalisation over a 0–30 min time course.
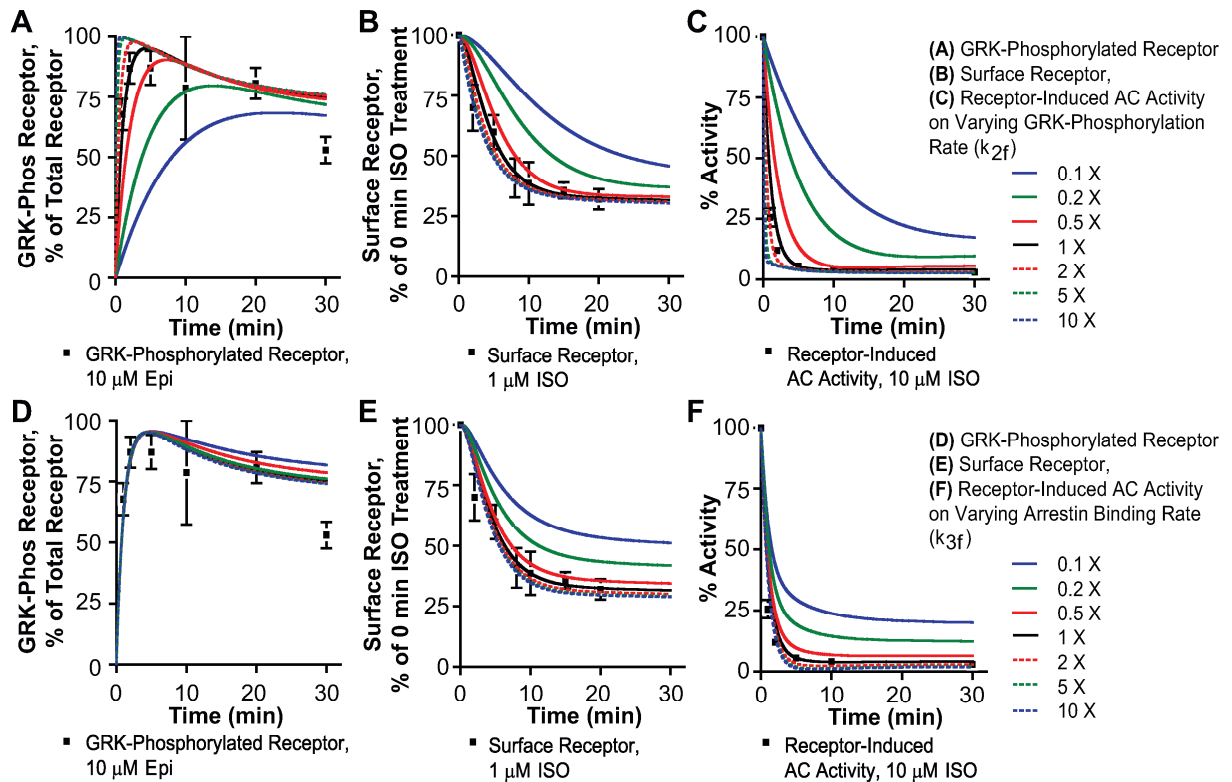
Figure 3.7 Simulated Effects of Varying Rates of GRK Phosphorylation and Arrestin Binding.

Panels A–C: Simulated effects of hundred-fold variation in GRK phosphorylation rates on **(A)** phosphorylation, **(B)** internalisation and **(C)** desensitisation. **D–E:** Simulated effects of hundred-fold variation in arrestin binding rates on **(D)** phosphorylation, **(E)** internalisation and **(F)** desensitisation. Experimental data as given in Figure 3.2A, C, and Figure 3.3A.

Figure and Figure Legend Source: http://dx.doi.org/10.1371/journal.pcbi.1000647.g004

"Quantitative Modeling of GRK-Mediated β2AR Regulation." Vayttaden SJ, Friedman J, Tran TM, Rich TC, Dessauer CW, Clark RB (2010) PLoS Comput Biol 6(1): e1000647. doi:10.1371/journal.pcbi.1000647

3.4.1. Variation in GRK-Mediated β2AR Phosphorylation Rates

Steady states of GRK phosphorylated β2AR were unaffected over hundred-fold variation in GRK phosphorylation rates (Figure 3.7 A-C) on treatment with saturating concentration (10 µM) of epinephrine. Initial GRK phosphorylation was significantly affected only by a decrease in the phosphorylation rates (Figure 3.7A). Since β2AR phosphorylation measurements in most GRK overexpression and knockdown studies are performed with saturating agonist concentrations at steady state, my model suggests that this would increase the risk of false negative results. A more exacting measure for the effects of GRK overexpression and knockdown experiments would be an estimate of the initial rates of GRK-mediated receptor phosphorylation at sub-saturating ligand concentrations. To test this assertion I simulated the effects of hundred-fold variations in rates of GRK-mediated β2AR phosphorylation following treatment with 50 nm epinephrine. Figure 3.8 clearly shows that effects of variations in GRK-mediated β2AR phosphorylation are more pronounced at subsaturating ligand concentrations.

Since GRK phosphorylation of the β2AR is a pre-requisite for agonist-induced arrestin binding (Krasel, Bunemann et al. 2005) and internalisation, only perturbations that markedly affected GRK phosphorylation affected internalisation. Therefore only lowering the GRK-mediated β2AR phosphorylation rates had any marked effect on the initial rates of internalisation, with little effect on the maximum internalisation (Figure 3.7B). The effects on desensitisation were similar to phosphorylation albeit they were

phase shifted on account of these being sequential events (Figure 3.7C).

Therefore effects of variations in GRK-mediated β2AR phosphorylation on both

internalisation and desensitisation are best studied at early time points with

subsaturating ligand concentrations.
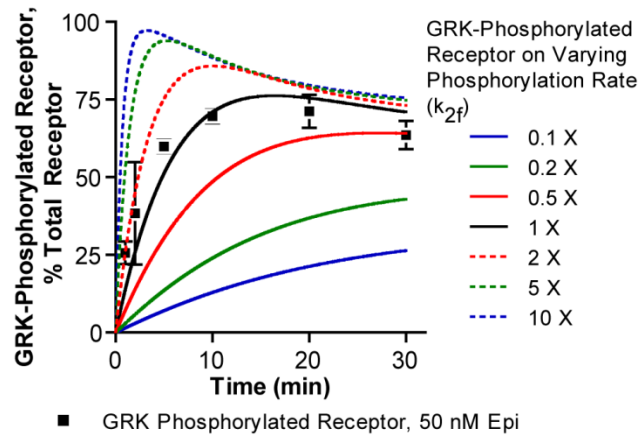
Figure 3.8 Simulated Effects of Varying Rates of GRK Phosphorylation.

Effect of variations in GRK levels or activity on phosphorylation at subsaturating concentration of epinephrine (50 nM) is simulated by ten-fold up or down variations in GRK phosphorylation rates.

Figure and Figure Legend Source:

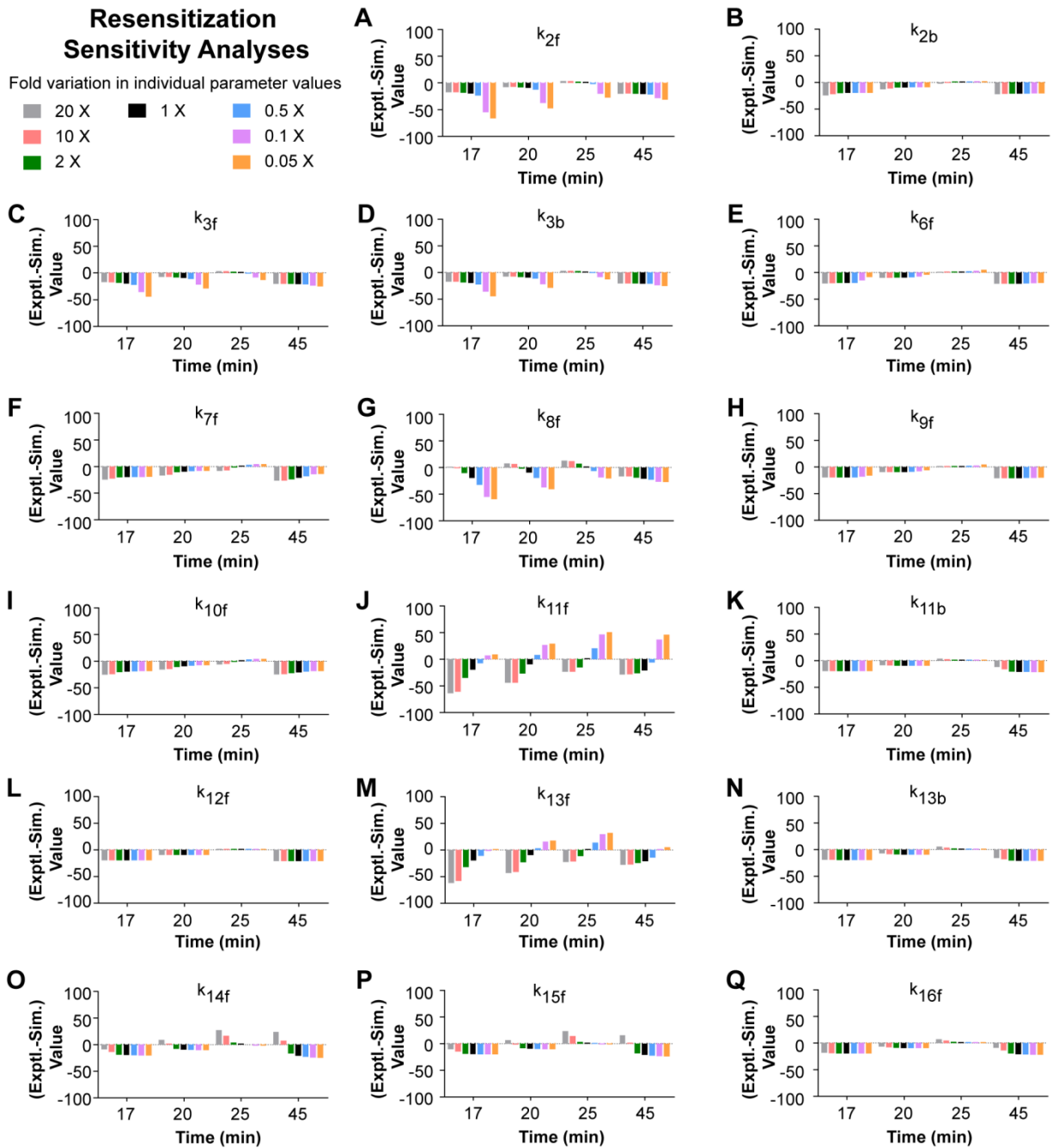http://dx.doi.org/10.1371/journal.pcbi.1000647 #pcbi.1000647.s004

"Quantitative Modeling of GRK-Mediated β2AR Regulation." Vayttaden SJ, Friedman J, Tran TM, Rich TC, Dessauer CW, Clark RB (2010) PLoS Comput Biol 6(1): e1000647. doi:10.1371/journal.pcbi.1000647

3.4.2. Variation in Arrestin β2AR Binding Rates

I varied the rates of arrestin binding β2AR over a hundred-fold range and studied the effect it had on GRK-mediated β2AR phosphorylation, internalisation and desensitisation (Figure 3.7D-F). Perturbing arrestin binding rates did not have significant effects on the initial maxima of GRK-mediated β2AR phosphorylation (Figure 3.7D). This was expected and served as a good sensitivity analyses since arrestin binding occurs only subsequent to GRK-mediated β2AR phosphorylation. Reducing arrestin binding rates (Figure 3.7E) decreased internalisation by approximately 40% within 5-10 minutes post agonist treatment, whereas increasing these rates did not significantly increase the maximum internalisation at 30 minutes. The effect of variations in arrestin binding rates on β2AR desensitisation was similar to that of internalisation in that only a reduction in arrestin binding rates decreased desensitisation.

3.4.3. Effects of β2AR Trafficking and the Cellular Location of Dephosphorylation

The possibility of cell surface dephosphorylation of the GRK phosphorylated β2AR and the recycling of the phosphorylated β2AR has been a contentious issue (Yu, Lefkowitz et al. 1993; Pippig, Andexinger et al. 1995; Krueger, Daaka et al. 1997; Iyer, Tran et al. 2006; Kelly 2006). Our group has shown that 1) blocking internalisation does not prevent β2AR dephosphorylation (Iyer, Tran et al. 2006), and 2) that β2AR dephosphorylation can occur even at undetectable levels of internalisation (Tran, Friedman et al. 2007). I have determined GRK

site β2AR dephosphorylation rates at the membrane to be ~0.04/min per method described in 2.1.1.

Other GPCRs such as f TRH receptors (Jones and Hinkle 2005) and D1 dopamine receptors (Gardner, Liu et al. 2001) also undergo dephosphorylation at the plasma membrane. To investigate the effects of membrane dephosphorylation and phosphorylated receptor recycling I created six different models (Figure 3.9A-F) that vary different reactions as described in the footnote of Table 3.1. For ease of visualisation of the cellular distribution of the GRK phosphorylated β2AR, I plotted the total (black), the cytosolic (blue), and the surface (red) GRK phosphorylated β2AR.
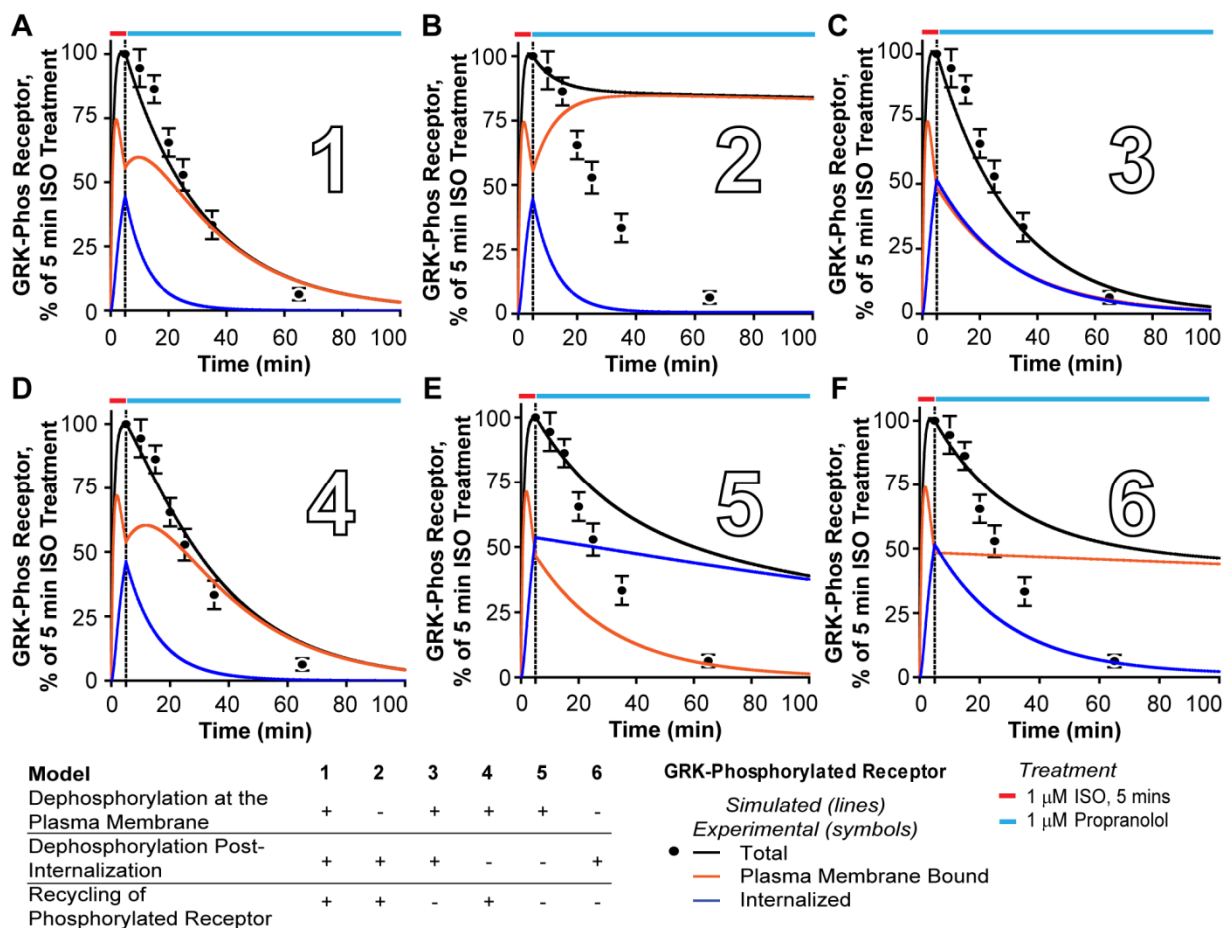
Figure 3.9 Simulated Effects of Phosphatase Location and Recycling of Phosphorylated β2AR on Receptor Dephosphorylation.

HEK 293 cells stably overexpressing WT β2AR were treated for 5 min with 1 µM ISO (red bar) followed by washout and addition of 1 µM propranolol (blue bar). Experimental data (Tran, Friedman et al. 2007) are shown as discrete points with standard errors and the simulations are shown as continuous lines. The black lines are the total phosphorylated receptor, red indicates the phosphorylated receptor on the plasma membrane and blue indicate internalised levels of phosphorylated β2AR. **(A)** Model 1 allows for dephosphorylation of both the internalised and plasma membrane bound receptor along with recycling of phosphorylated and dephosphorylated receptor. **(B)** Model 2 disallows plasma membrane dephosphorylation but

allows both dephosphorylation of the internalised receptor and recycling of phosphorylated receptor. **(C)** Model 3 allows for dephosphorylation of both the internalised and plasma membrane bound receptor but limits recycling to only dephosphorylated receptor. **(D)** Model 4 allows for dephosphorylation only at the plasma membrane and also allows recycling of phosphorylated receptor. **(E)** Model 5 allows for dephosphorylation only at the plasma membrane and disallows recycling of phosphorylated receptor. **(F)** Model 6 allows for dephosphorylation only after internalisation and prevents recycling of phosphorylated receptor.

Model 1: All rates are set as described in Table 3.1, for the default model.

Model 2: $k_{2b} = k_{7f} = 0$ /min since this model disallows dephosphorylation at the plasma membrane.

Model 3: $k_{13f} = 0$ /min since this model disallows recycling of phosphorylated receptor.

Model 4: $k_{10f} = 0$ /min since this model disallows dephosphorylation of the internalised receptor.

Model 5: $k_{10f} = k_{13f} = 0$ /min since this model does not allow neither dephosphorylation of the internalised receptor nor recycling of phosphorylated receptor.

Model 6: $k_{2b} = k_{7f} = k_{13f} = 0$ /min since this model does not allow neither dephosphorylation of the receptor at the plasma membrane nor recycling of phosphorylated receptor.

Figure and Figure Legend Source adapted from:

http://dx.doi.org/10.1371/journal.pcbi.1000647.g005

"Quantitative Modeling of GRK-Mediated β2AR Regulation." Vayttaden SJ, Friedman J, Tran TM, Rich TC, Dessauer CW, Clark RB (2010) PLoS Comput Biol 6(1): e1000647. doi:10.1371/journal.pcbi.1000647

In Figure 3.9A I modelled our default reaction topology that allowed for both receptor dephosphorylation at the cell surface and phosphorylated receptor recycling. I contrasted this with Figure 3.9F where I modelled a reaction topology that did not allow for both plasma membrane dephosphorylation and recycling of phosphorylated receptor. This was in keeping with the prevalent view around early 2000s (Krupnick and Benovic 1998; Billington and Penn 2003). I showed that under these conditions the system failed to achieve more than 50% β2AR dephosphorylation which was discordant with our experimental measurements (Tran, Friedman et al. 2007). Increasing the cytosolic dephosphorylation rate did not help in rescuing the simulated dephosphorylation curves. Thus through modeling I was able to show that the prevalent model of early 2000s was not able to explain dephosphorylation measurements done in our lab.

Since there were two reactions being contested viz. receptor dephosphorylation at the plasma membrane and phosphorylated receptor recycling, I decided to explore the effects of disallowing one of each reaction and cytosolic dephosphorylation in the remaining models to ensure that a random variation of these reaction topologies wouldn't match our experimental data (Figure3.9B-E). Of the models tested Figure 3.9C and D showed that two models matched the measured dephosphorylation kinetics in addition to my default model. This therefore required additional testing of the two models to see if they matched other experimental measurements of our β2AR over expression system.

Preventing recycling of GRK phosphorylated β2AR did not skew the simulated

rate of β2AR dephosphorylation (Figure 3.9C). I subjected Model 3 to further

tests (Figure 3.10A-E) against other experimental measurements and showed

that in the absence of GRK phosphorylated β2AR recycling, the model did not

match the experimental measurements of internalisation (Figure 3.10B),

recycling (Figure 3.10C) and resensitisation (Figure 3.10E). In the light of these

observations it was clear that Model 3 could not represent the topology of

reactions for β2AR in our over expression HEK293s.
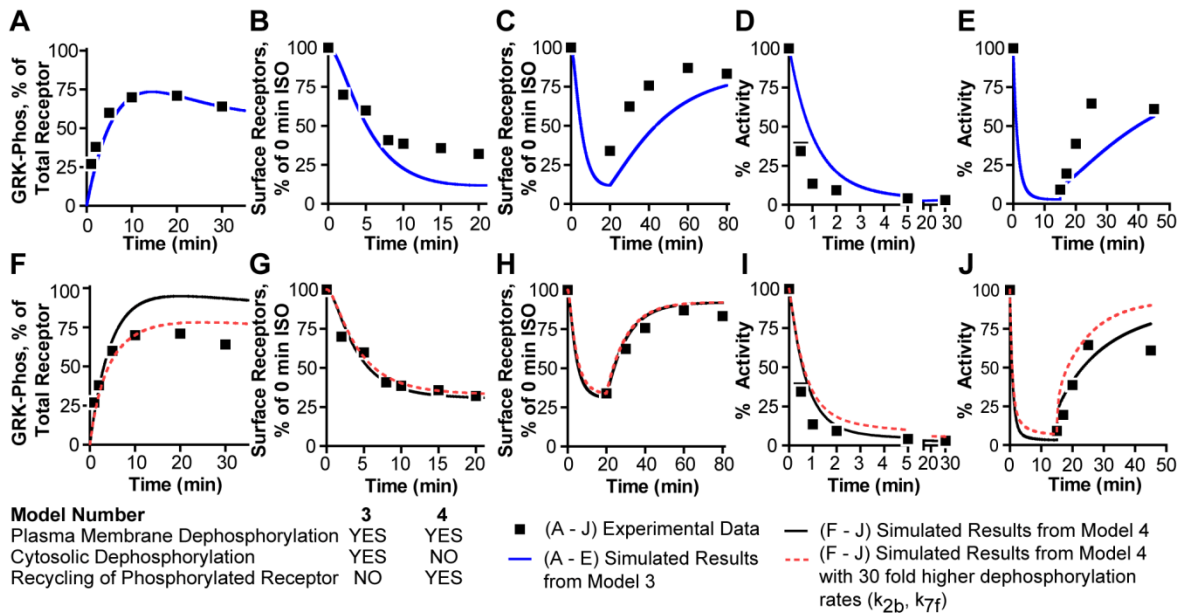
Figure 3.10 Comparisons of Five Experimental Results with Simulations of Model 3 and 4.

Through panels A–E I test alternate models 3 and 4 to see how well they match other experimental readouts of the β2AR signalling system besides dephosphorylation (c.f. Figure 3.9C, D). Comparisons of simulations (continuous lines) of model 3 (A–E) and model 4 (F–J), with experimental data obtained in HEK 293 cells stably expressing the WT β2AR (discrete data points). **(A, F)** Time course of GRK phosphorylation of the receptor on treatment with 50 nM isoproterenol (Tran, Friedman et al. 2004). **(B, G)** Internalisation of the β2AR on treatment with 1 μM isoproterenol. Surface receptor is measured by the loss of [^{3}H]CGP-12177. **(C, H)** Recycling of the receptor after 20 min treatment with 1μM isoproterenol followed by rapid washout of agonist (Morrison, Moore et al. 1996). **(D, I)** Desensitisation of β2AR stimulation of adenylyl cyclase post treatment with 10 μM isoproterenol. **(E, J)** Resensitisation of the β2AR stimulation of adenylyl cyclase. WT β2AR were stimulated with 1μM isoproterenol for 15 min, followed by addition of metoprolol as described in 3.2.6.

Figure and Figure Legend Source:

http://dx.doi.org/10.1371/journal.pcbi.1000647#pcbi.1000647.s005

"Quantitative Modeling of GRK-Mediated β2AR Regulation." Vayttaden SJ, Friedman J, Tran TM, Rich TC, Dessauer CW, Clark RB (2010) PLoS Comput Biol 6(1): e1000647. doi:10.1371/journal.pcbi.1000647

There was a good match between the measured and simulated dephosphorylation rates in Figure 3.9D where I had allowed recycling of the GRK phosphorylated β2AR and dephosphorylation only at the plasma membrane. I subjected Model 4 to further tests in Figure 3.10F-J. I showed that in the absence of cytoplasmic β2AR dephosphorylation, a 30 fold higher plasma membrane dephosphorylation rate is required to match the experimentally measured phosphorylation kinetics (Figure 3.10F). Absence of cytosolic β2AR dephosphorylation is at odds with experimental observations of the β2AR (Sibley, Strasser et al. 1986; Pippig, Andexinger et al. 1995; Tran, Friedman et al. 2007). In the light of these observations it was clear that Model 4 could not represent the topology of reactions for β2AR in our over expression HEK293s. This model cannot be summarily rejected for other GPCRs though where significant cytosolic dephosphorylation might not occur under physiological conditions.

I allowed for solely plasma membrane dephosphorylation and prevented phosphorylated receptor recycling in Model 5 (Figure 3.9E). Under these conditions the dephosphorylation rates were significantly reduced. Thus of the six models designed, only one model viz. model 1 (Figure 3.1, Table 3.1, Figure 3.9A) accounted for six different types of experimental measurements (Figures 3.2, 3.3). This model was functionally unique and random variation in topologies of dephosphorylation and recycling reactions could not recapitulate all experimental measurements of our β2AR over expression system in HEK293s.

3.4.4. Frequency Coding

Most of the studies discussed until now were performed in the presence of saturating agonist concentrations for long durations. Such a prolonged exposure rarely occurs under normal physiological conditions without pharmacological intervention. Rather based on the target tissue the β2AR "sees" different frequencies and amplitudes of stimuli. Synaptic β2AR "sees" high norepinephrine concentrations in a pulsatile fashion (Trendelenburg, Gaiser et al. 1999; Stjarne 2000) due to the small synaptic volumes, rapid removal and reuptake of norepinephrine. In contrast to the synaptic stimuli, the bloodstream concentrations of agonist post epinephrine secretion from the adrenal gland are much lower but for relatively longer periods.
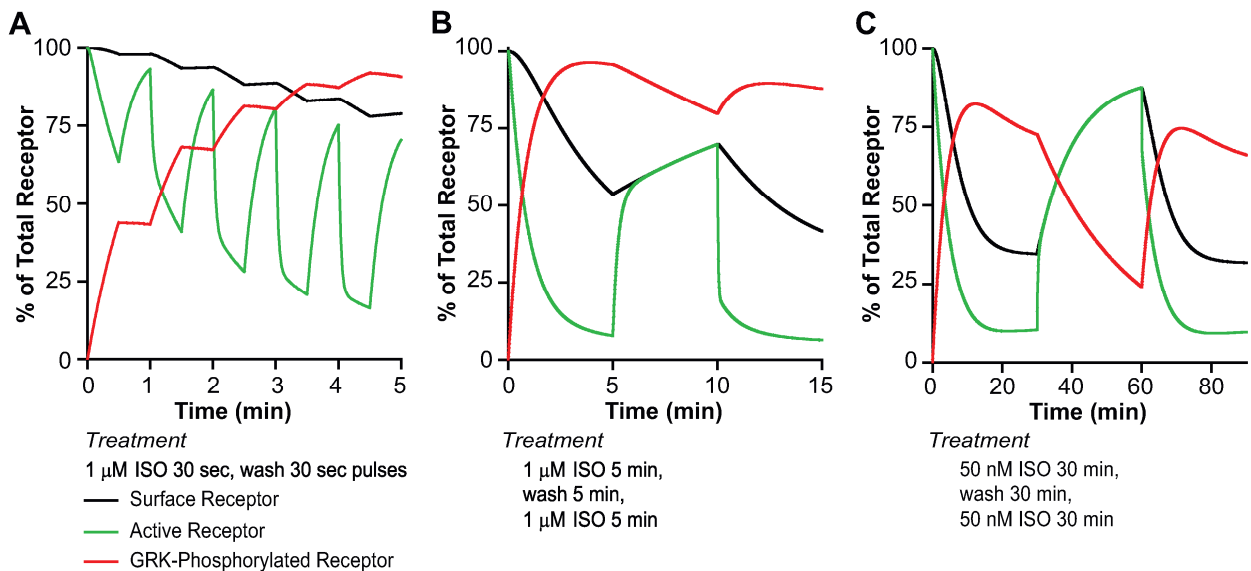
Figure 3.11 Simulations of the Effects of Frequency Modulation.

In these panels I describe the effect of varying the frequency of stimulation on surface (black), phosphorylated (red) and active (green) receptor species. **(A)** Rapid stimulation with a train of 1 µM isoproterenol pulses for 0.5 min followed by a 0.5 min washout. Note that this achieves more than 80% desensitisation with only 20% internalisation. **(B)** This panels shows the results of a 5 min stimulation with 1.0 µM isoproterenol and a 5 min washout. **(C)** Simulation of 30 min stimulation with 50 nM isoproterenol followed by washout of 30 min. This panel shows that even with low β2AR occupancy (15%) the prolonged stimulation time gives substantial desensitisation.

Figure and Figure Legend Source: http://dx.doi.org/10.1371/journal.pcbi.1000647.g006

"Quantitative Modeling of GRK-Mediated β2AR Regulation." Vayttaden SJ, Friedman J, Tran TM, Rich TC, Dessauer CW, Clark RB (2010) PLoS Comput Biol 6(1): e1000647. doi:10.1371/journal.pcbi.1000647

I explored the effects of varying frequencies of agonist stimulation on my model. The first scenario shown here is that of stimuli at ~ 0.0167 Hz which is equivalent to 30 s bursts of agonist followed by 30 s washouts. I assumed that the washouts were perfect and allowed for instantaneous agonist dissociation from the receptor (Figure 3.11A). Under this stimulation pattern almost 100% GRK phosphorylation (red – GRK phosphorylated β2AR) is achieved with only 20% internalisation (black – surface β2AR) but about 80% desensitisation (green – active β2AR). Post agonist washout, resensitisation was rapid due to fastdissociation of arrestin from the receptor. In spite of this near complete recovery, during subsequent pulsatile activation of the β2AR, the signalling machinery "remembers" previous agonist exposure and desensitises much more strongly on subsequent exposures. This memory of prior stimuli can be attributed to the accumulation of the GRK phosphorylated β2AR due to slower dephosphorylation.

In Figure 3.11B I stimulate the system with a continuous 5 min long delivery of 1µM isoproterenol followed by a 5 min wash and subsequent restimulation for 5 min. Under this stimulus profile close to 95% β2AR is desensitised with ~ 50% β2AR internalised. In Figure 3.11C I tested the response of the β2AR system on prolonged exposure to sub-saturating levels of agonist. I simulated the response to 30 min delivery of 50 nM isoproterenol followed by 30 min wash and restimulation. Under longer periods of ligand treatment (Figure 3.11B, C) the resensitisation was biphasic (c.f Figure 3.3B). The rapid phase of resensitisation is dependent upon arrestin dissociation from the receptor while

the slower phase is dependent upon receptor recycling and dephosphorylation (Tran, Friedman et al. 2007).

The phenomenon of latent memory that I described in Figure 3.11A was only observed at higher frequencies of agonist stimulation. For longer periods of stimulation (Figure 3.11C), as might be seen during treatment with a strong, stable agonist in diseases such as asthma, receptor recycling would play a significant role in resensitisation.

3.4.5. Latent Memory

Having previously shown in Figure 3.11A that the β2AR signalling machinery could "remember" previous stimuli I wanted to explore the effects of variation in inter-pulse duration (time between paired pulse stimulation), β2AR dephosphorylation and arrestin dissociation on this latent memory. I simulated a paired pulse pattern of β2AR activation with 1μM isoproterenol (Figure 3.12A). Even on rapid, near complete β2AR resensitisation, the system remembered previous stimuli and showed stronger desensitisation in response to subsequent stimuli ("active" β2AR- green lines, Figure 3.12A). The latent memory can be attributed to stockpiling of GRK phosphorylated β2AR on the surface (red). Pre-phosphorylation of the β2AR primes the system for faster arrestin binding to surface receptor (blue) on subsequent agonist activation, leading to increased desensitisation. Increasing the inter-pulse duration weakened the memory (Figure 3.12B), since it allowed the slow rate of dephosphorylation to catch up. The memory survived beyond 30 min post first

stimulus. An extreme 50 fold increase in dephosphorylation rates was required

to erode the memory of the previous stimuli (Figure 3.12C).
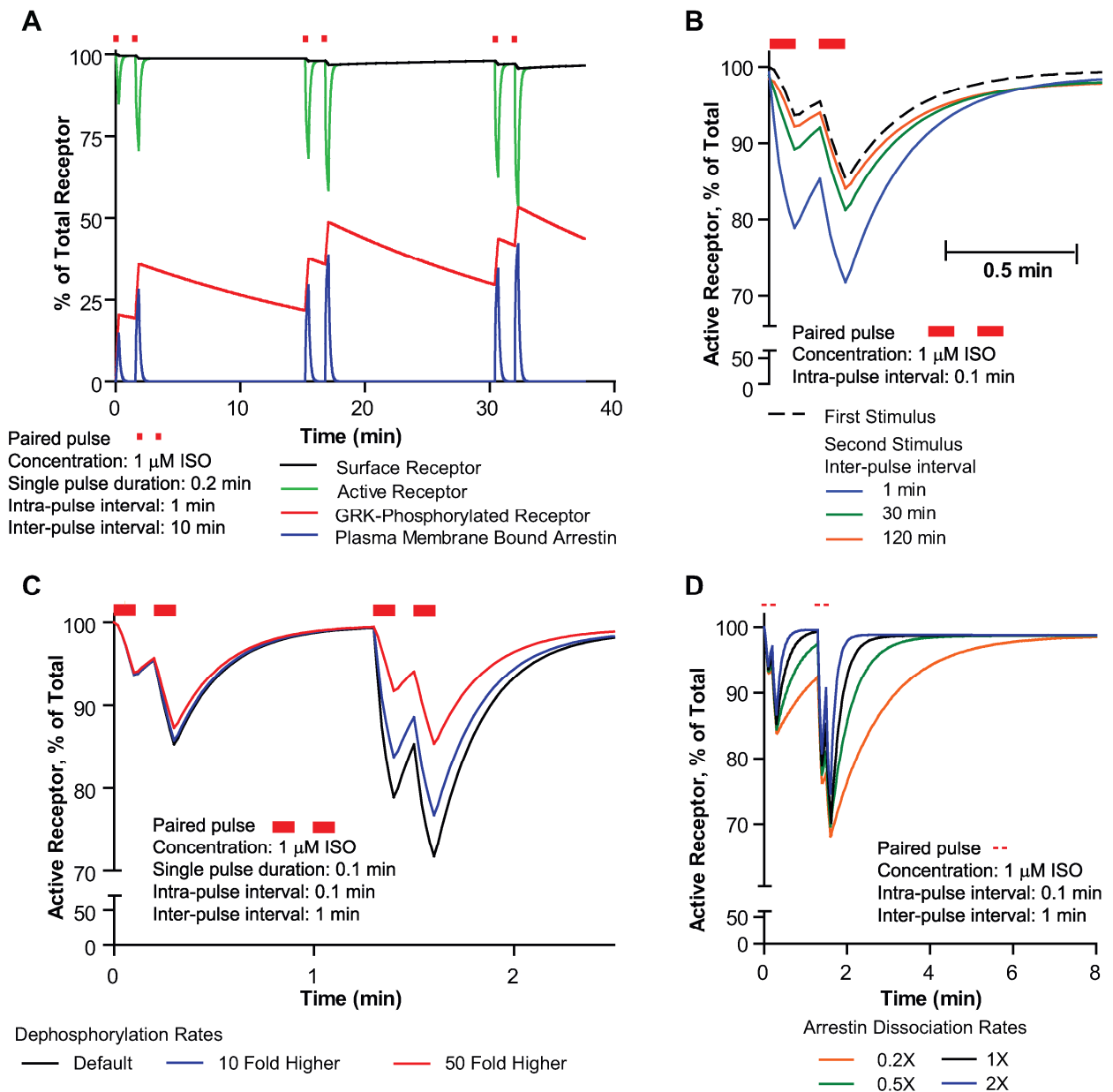
Figure 3.12 Basis for "Cellular Memory" in the β2AR Signalling Machinery.

(A) Simulation of activation of β2AR by paired pulses of 1 µM isoproterenol. Higher desensitisation is obtained for the second and third pulse. Colours indicate simulated receptor species as indicated in the figure. **(B)** Decay in memory of prior stimuli on increase in inter-pulse period from 1–120 min. **(C)** Effect of up to 50 fold increase in surface dephosphorylation rates on memory of prior stimuli. Default dephosphorylation rate is 0.036/min. **(D)** Effect of arrestin-β2AR complex stability on desensitisation time courses simulated by varying arrestin

dissociation rates from the ligand-free complex on the surface. Default arrestin surface

dissociation rate from the ligand-free complex is 11/min.

Figure and Figure Legend Source: http://dx.doi.org/10.1371/journal.pcbi.1000647.g007

"Quantitative Modeling of GRK-Mediated β2AR Regulation." Vayttaden SJ, Friedman J, Tran

TM, Rich TC, Dessauer CW, Clark RB (2010) PLoS Comput Biol 6(1): e1000647.

doi:10.1371/journal.pcbi.1000647
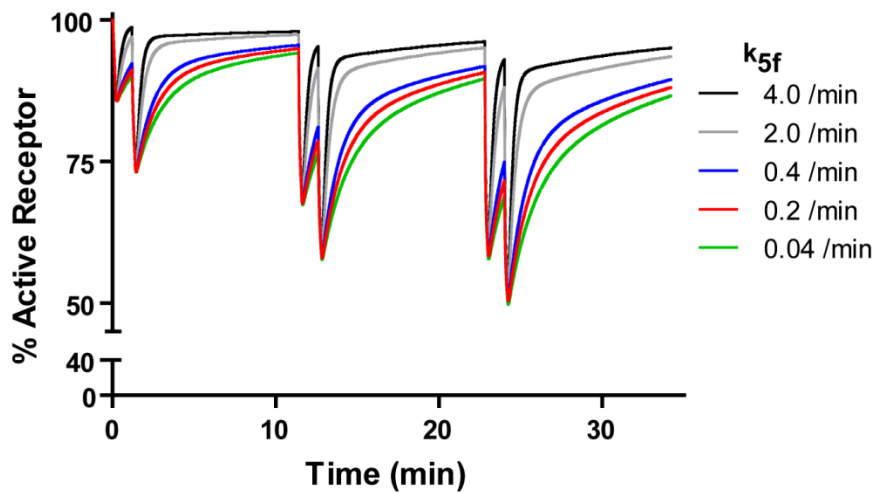
Figure 3.13 Sensitivity of Simulated "Cellular Memory" to the Stability of Arrestin-Receptor/Ligand Complex.

Simulation of activation of β2AR by paired pulses of 1 µM Isoproterenol. Higher desensitisation is obtained for the second and third pulse even on 100 fold increased stability of the arrestin-receptor/ligand complex.

Figure and Figure Legend Source:

http://dx.doi.org/10.1371/journal.pcbi.1000647#pcbi.1000647.s006

"Quantitative Modeling of GRK-Mediated β2AR Regulation." Vayttaden SJ, Friedman J, Tran TM, Rich TC, Dessauer CW, Clark RB (2010) PLoS Comput Biol 6(1): e1000647.

doi:10.1371/journal.pcbi.1000647

Some GPCRs have a higher affinity for arrestin than β2AR causing a slower release of arrestin from the receptor post internalisation (Moore, Milano et al. 2007). To investigate the effects of slow arrestin release from β2AR on latent memory I decreased the dissociation rate of arrestin from the β2AR (Figure 3.1, Table 3.1; k_{3b}, k_{6f}, k_{9f}) thereby mimicking a high affinity complex. The time required for resensitisation was directly proportional to the affinity of arrestin for the β2AR (Figure 3.12D). Next I increased the stability of the ligand/β2AR /arrestin complex by a 100 fold reduction in the ligand off-rate (Figure 3.1, Table 3.1; k_{5f}). This did not diminish the extent of memory, but it did increase the recovery time between each paired pulse (Figure 3.13). In summary, the predicted latent memory was due to (i) slow β2AR dephosphorylation (0.036 /min); and (ii) rapid arrestin dissociation from ligand free β2AR (11.0 /min).

3.4.6. Model Limitations

My model ignores effects of adenylyl cyclase or PDE regulation and PKA mediated β2AR phosphorylation. In the absence of the PKA/PDE module the current model fails to capture the behaviour of the β2AR signalling machinery at low agonist concentrations as shown in Figure 3.3A inset (red bar graphs). Our group has shown that at high agonist concentrations GRK phosphorylation appears to decrease PKA site phosphorylation of the β2AR (Vaughan, Millman et al. 2006). Prestimulation of PKA mediated β2AR phosphorylation with forskolin on the other hand does not affect GRK mediated β2AR phosphorylation (Tran, Friedman et al. 2004). So clearly there is some interplay between PKA and GRK phosphorylation of the β2AR and this cannot be

explored in the current model. I have modelled only receptor-level desensitisation and as a consequence omitted downstream regulatory events like adenylyl cyclase regulation.

On account of lack of relevant kinetic data my model ignores multi-site phosphorylation of the receptor in that it considers phosphorylation and dephosphorylation of S365, 366 as a single event and ignores phosphorylation at other sites by GRK or PKA. As a consequence of this simplification this model cannot be used to explore effects of phosphosignature on receptor sorting and varied receptor activity.

In this model I collapse internalisation of arrestin-bound, GRK-phosphorylated ligand-bound β2AR and post-internalisation ligand dissociation into the same step since internalisation is slower than ligand dissociation rates for full agonists like epinephrine/isoproterenol. This model in its current state cannot be used to simulate post-internalisation effects on treatment with a partial agonist like salmeterol that quasi-irreversibly bind to the β2AR.

The simplistic ligand-induced two-state receptor activation model used here can be used to credibly simulate a variety of biochemical events that the receptor undergoes like GRK phosphorylation/dephosphorylation, receptor trafficking, desensitisation/resensitisation. This representation of receptor activation is not amenable to studying biased signalling of the receptor on account of lack of representation of other signalling states of the receptor and lack of downstream signalling proteins like the elements of the MAPK cascade.

Due to the use of pseudo-first order reactions to simulate ligand -, arrestin- and GRK-binding the receptor the model in its current form cannot be used to study the effects of prolonged membrane accumulation of lipophilic ligands like salmeterol and formoterol that could persist even after internalisation of the receptor. This model also cannot explore effects of agonist treatment on GRK and arrestin trafficking and recruitment to the plasma membrane bound receptor.

I have shown that preventing plasma membrane receptor dephosphorylation and recycling of the GRK phosphorylated receptor is antithetical with my modeling and our previous experimental results. A point to note is that my model does not have a significant basal internalisation. Agonist-independent internalisation does occur in GPCRs like the melanocortin MC4 receptor (Mohammad, Baldini et al. 2007) and cannabinoid CB1 receptor (McDonald, Henstridge et al. 2007). Our group has shown that in HEK293s there is no detectable basal internalisation of the β2AR (Morrison, Moore et al. 1996). Others have detected agonist-independent internalisation in HeLa cells transiently transfected with M3R or β2AR (Scarselli and Donaldson 2009). It needs to be examined if agonist-independent β2AR internalisation occurs in other cell lines, and if it does the current model would hold true only for β2AR signalling in HEK293s.

4. Partial Agonist Models

Agonist-induced activation of a GPCR leads to a change in the relative orientations of the transmembrane helices leading to induction of a signal transduction function. The efficiency with which these ligands induce the downstream signal transduction is called coupling efficiency. Partial agonists are ligands that give sub-maximal receptor activation on account of lower coupling efficiency even at receptor saturation. For β2AR, isoproterenol (Isuprel[®]) and epinephrine (endogenous ligand) are examples of full agonists while salmeterol (Servent[®]) and albuterol (Ventolin[®], Proventil[®]) are examples of partial agonists. Except for cyclopentylbutanephrine, the initial rate of GRK-mediated β2AR phosphorylation is proportional to the coupling efficiency of partial agonists (January, Seibold et al. 1997; Tran, Friedman et al. 2004; Drake, Violin et al. 2008).

4.1. Relative Efficacies

I used the GRK-mediated β2AR regulation model developed in Chapter 3 to model partial agonist induced GRK-mediated β2AR phosphorylation. To do this I set the coupling efficiencies of the partial agonist relative to epinephrine/isoproterenol (α in Table 2.1 for parameter k_{2f}). The relative coupling efficiencies for partial agonists are given in Table 4.1.

Figure 4.1A shows that the simulated time course of salmeterol and albuterol induced GRK-mediated β2AR phosphorylation matches experimental data over 30 minutes. In figure 4.1B I show that the simulation results match well the GRK-

mediated β2AR phosphorylation at 2 min normalised to 10 µM epinephrine. These

results are additional validation for Model 1 presented in Chapter 3.

Table 4.1. Relative Coupling Efficiencies and Kds of β-Agonists

Agonist	Coupling Efficiencies Relative to Epinephrine[a]	Kd (nM) [b]
Epinephrine	1	450
Isoproterenol	1	283
Fenoterol	0.66	133
Formoterol	0.63	5
Terbutaline	0.33	1835
Zinterol	0.33	8.6
Albuterol	0.25	420
Salmeterol	0.13	< 2
Dobutamine	0.04	589
Ephedrine	0.03	2674

[a] The relative coupling efficiencies are calculated as described by our group previously (Tran, Friedman et al. 2004).

[b] Kds as estimated in HEK293 cells stably overexpressing β2AR.
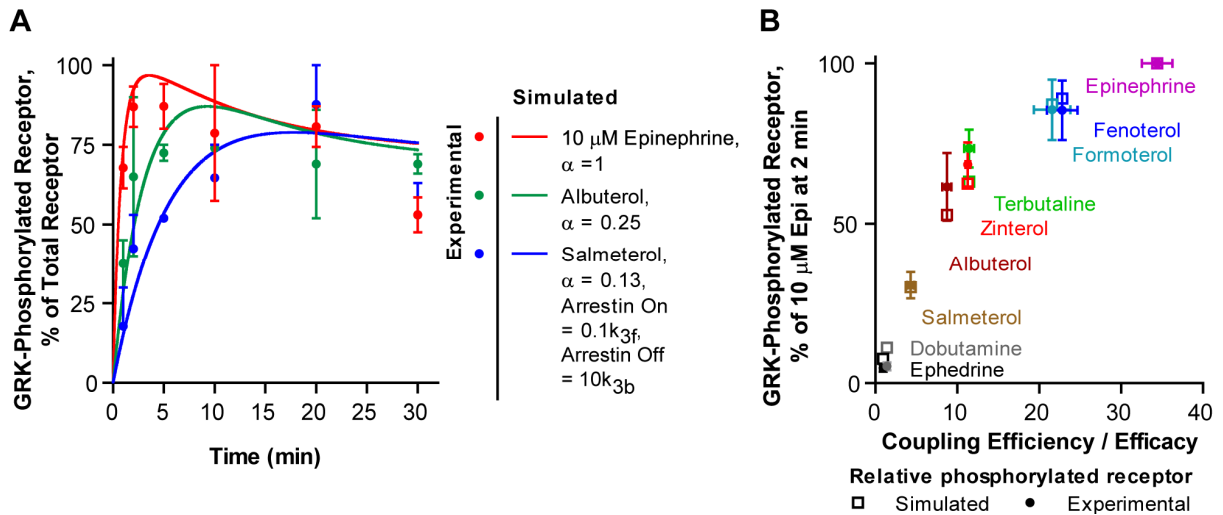
Figure 4.1 Comparison of Simulated Time Course of GRK Site Phosphorylation with Experimentally Measured Phosphorylation in Response to Various Agonists.

(A) The simulated time course of GRK site phosphorylation of the β2AR in response to various agonists is compared with experimentally measured phosphorylation (Tran, Friedman et al. 2004). (B) Comparison of simulated and experimentally measured GRK-mediated β2AR phosphorylation at 2 min of agonist treatment normalised to phosphorylation achieved with 10 μM epinephrine (Tran, Friedman et al. 2004).

Figure and Figure Legend Source:

http://dx.doi.org/10.1371/journal.pcbi.1000647#pcbi.1000647.s001

"Quantitative Modeling of GRK-Mediated β2AR Regulation." Vayttaden SJ, Friedman J, Tran TM, Rich TC, Dessauer CW, Clark RB (2010) PLoS Comput Biol 6(1): e1000647. doi:10.1371/journal.pcbi.1000647

4.2. Previous Models of Salmeterol Action on the Receptor

Salmeterol is a partial agonist that is extensively used clinically in maintenance therapy of asthma along with a steroid. Due to the clinical importance of salmeterol there have been a few phenomenological models of salmeterol. All models of salmeterol action must reconcile with two important phenomena of salmeterol action, viz. (i) long action (8-12 hours) as described in the section above; and (ii) reassertion of salmeterol action following first treatment with antagonist (that fully inhibits salmeterol action), and second, washout of antagonist without addition of new salmeterol (Ball, Brittain et al. 1991; Anderson 1993). Additionally clinical models of salmeterol must also explain the reason for delayed onset of salmeterol action (Ball, Brittain et al. 1991; Johnson, Butchers et al. 1993; Nials, Coleman et al. 1993). In contrast to slow onset of salmeterol action in patients and tissue explants, salmeterol shows no noticeable lag in monolayer cell culture experiments (McCrea and Hill 1993; Clark, Allal et al. 1996; McCrea and Hill 1996). Therefore, we have not attempted to model the torturous path of salmeterol to the relevant sites of action on the receptor.

A detailed discussion of the merits of the different models of salmeterol action can be found elsewhere (Anderson, Linden et al. 1994; Szczuka, Wennerberg et al. 2009). Briefly, salmeterol action has been explained by **three models**. Salmeterol is lipohilic and reversibly incorporates in the plasma membrane, resulting in a partition of drugs between a membrane and an aqueous phase (Rhodes, Newton et al. 1992). Due to membrane partitioning of salmeterol, the membrane can act as a salmeterol reservoir and this forms the basis of the **microkinetic model (MM)**

(Anderson, Linden et al. 1994) (Figure 4.2). Due to the high membrane partitioning

of salmeterol and its slow rate of release from the membrane, $t_{1/2}$ = 25 mins

(synthetic membranes) – 3 hours (tracheal strips) (Rhodes, Newton et al. 1992;

Austin, Barton et al. 2003) it is posited that salmeterol reaches the receptor by

lateral diffusion through the membrane (Anderson, Linden et al. 1994) since by the

time salmeterol traverses the length of the airways to reach the target bronchii it

would have bound to the membrane on account of its lipophilicity.

Per the **exosite model (EM)** (Figure 4.4) the saligenin head of salmeterol (Figure

1.2) and the hydrophobic phenylalkoxyalkyl side chain binds the β2AR at two

spatially distinct sites. The site of saligenin head binding is identified as the active

site and the site of hydrophobic phenylalkoxyalkyl side chain binding is called an

exosite. In the exosite model tethering of the phenylalkoxyalkyl chain to the exosite

is quasi-irreversible while the binding of the saligenin head to the active site is

rapidly reversible. This model also allows agonist or antagonist binding to the

active site when the exosite is occupied by salmeterol's hydrophobic tail (Figure

6.1). To allow the flipping in and out of the saligenin head from the active site, the

exosite has been posited to be in the central core of the β2AR (Jack 1991). Both

site directed mutagenesis studies involving replacement of β2AR central domains

with β1AR (Green, Spasoff et al. 1996; Isogaya, Yamagiwa et al. 1998) and

photoaffinity labeling with [125I]iodoazido-salmeterol (Rong, Arbabian et al. 1999)

lend credence to the idea that the exosite is further into the transmembrane

domains toward the cytosol than the active site.

The **rebinding model** posits that a high local concentration of salmeterol is maintained on account of rapid rebinding (Szczuka, Wennerberg et al. 2009). This model wouldn't be able to explain the reassertion phenomenon when a competing ligand is present without invoking another mechanism to retain salmeterol in the proximity of the receptor.

Given the importance of salmeterol in treating asthma and COPD (as discussed in Section 1.3) I developed phenomenological models to describe the effects of membrane retention of salmeterol, exosite binding or a composite of the two **(combined model - CM)**. I then coupled these models to an adaptation of the GRK-mediated β2AR regulation model developed in Chapter 3 and then tested them to see if properties of salmeterol long action and reassertion still held true.

4.2.1. Model Assumptions

4.2.1.1. Isoproterenol Partitioning (Valid for MM/EM/CM)

I presume that isoproterenol "sees" the plasma membrane as an inert substratum for the β2AR. As a consequence of this there is no partitioning of isoproterenol from the aqueous phase into the plasma membrane. Washout of isoproterenol from the aqueous phase results in no lingering free isoproterenol concentration in the plasma membrane. To mimic addition of isoproterenol in an *in silico* experiment I initialise free isoproterenol concentration in the aqueous phase to the concentration used in the *in vitro* experiment. To mimic washout of isoproterenol in an *in silico* experiment I buffer free isoproterenol concentration in the aqueous phase to zero.

4.2.1.2. Salmeterol Partitioning (Valid for MM/CM)

I have modelled salmeterol partitioning into the plasma membrane as a first order reaction. Partitition coefficient for a molecule is defined as the ratio of concentrations of a molecule in the phases of a mixture of immiscible solvents at equilibrium. Membrane based partition coefficient ($K_{p(mem)}$) for salmeterol has been determined to be 22500 from unilamellar liposomes (Rhodes, Newton et al. 1992; Lombardi, Cuenoud et al. 2009). Using dioleoyl phosphatidylcholine it has been estimated that under ideal conditions the association coefficient (K_a) would be ~ 1.24 X $K_{p(mem)}$(Rhodes, Newton et al. 1992). Thus the K_a of salmeterol would be ~ 27900.

The $t_{1/2}$ for salmeterol release from membranes ranges between ~ 60 min from unilamellar liposomes to ~ 180 min from multilamellar liposomes (Rhodes, Newton et al. 1992). I used the $t_{1/2}$ of 180 min to calculate a rate of salmeterol release from the membrane because (i) the $t_{1/2}$ is comparable to that from tracheal strips (Austin, Barton et al. 2003), and (ii) partition coefficients for other systems are not affected by lamellarity of membranes (Rhodes, Newton et al. 1992). Using a $t_{1/2}$ of 180 min the rate of release of salmeterol from the plasma membrane (k_{rel}) is approximated to 0.004 /min. Once k_{rel} is known the rate of plasma membrane association for salmeterol (k_{in}) can be approximated to 107 /min from K_a.

4.2.1.3. Salmeterol Exosite Binding (Valid for EM/CM)

I have assumed that the rate of salmeterol binding to the exosite is same as the rate of plasma membrane association for salmeterol and hence both are denoted by k_{in} with a $t_{1/2} \sim 0.006$/min. This is a simplification since based on the rate of appearance of the increase in basal adenylyl cylase activity in washed membranes after salmeterol treatment of intact cells we have estimated a $t_{1/2} \sim 0.14$/min. (Clark, Allal et al. 1996)

Also I have assumed that the rate of release of salmeterol from the exosite is the same as the rate of salmeterol release from the plasma membrane, and hence both are denoted by k_{rel}. This too is a gross oversimplification since while we do know that the $t_{1/2}$ of release of salmeterol from synthetic liposomes is ~180 min (Rhodes, Newton et al. 1992) k_{rel} from the exosite is quasi-irreversible making a measure of release of salmeterol from the exosite difficult (Clark, Allal et al. 1996). Further this rate is inextricably mixed in with release from the membranes. As a consequence of these simplifications it is possible to run the simulations for a shorter period of time and it is possible to compare the microkinetic and exosite models on the same timescales.

Salmeterol can bind either the active site or the exosite of a naïve receptor. Again for ease of simulations I have ignored the receptor state that has salmeterol bound to the active-site alone (c.f.Figure 4.4. Reactions 6 and 7). Since I am exploring the effects of long term salmetereol action, at the time

courses being simulated, both active and exo-site of the receptor will be occupied.

4.2.1.4. Ligand Binding (Valid for MM/EM/CM)

Since we had an estimate of K_d for epinephrine to be ~ 450 nM (Vayttaden, Friedman et al. 2010) the off-rates were calculated to give the appropriate K_d. The on-rates of isoproterenol were assumed to be similar to epinephrine and then using a Kd of ~ 283 nM (Vayttaden, Friedman et al. 2010) appropriate off-rates were calculated. I assumed that salmeterol binds β2AR on the active site at the same rate as isoproterenol. Based upon the K_d for salmeterol (2 nM) (Rong, Arbabian et al. 1999), off-rates were calculated. In the exosite model Sal:R$_{Eam}$ (salmeterol bound only to the exosite) can transition into Sal:R$_{EAm}$ (salmeterol bound to both active site and exosite on the β2AR). This transition is a first order reaction and its rate must match the second order rate for salmeterol binding β2AR (8.4e+08 /M.min). I estimated the first order transition rates to be ~ 20 /min by matching the $t_{1/2}$ for both reactions at saturating agonist concentration. Using this calculation we note that the off rate for salmeterol is about 1400 times slower that for isopreoterenol/epinephrine.

4.2.1.5. Ligand Dissociation (Valid for MM/EM/CM)

I ignored ligand dissociation from membrane bound, GRK phosphorylated β2AR with or without arrestin in the larger models that have microkinetics or exosite binding introduced into the GRK-mediated β2AR regulation. This

was done to reduce the number of receptor states and reactions. The reactions that I have ignored have negligible fluxes under saturating agonist concentrations since under these conditions GRK phosphorylation and arrestin binding are favoured. Therefore I've validated the model only to GRK phosphorylation under saturating levels of agonist. Due to these modifications, under washout conditions there will be an exaggeration of membrane retention of agonists and residual receptor activity on account of accumulation of ligand bound GRK-phosphorylated β2AR. Arrestin kinetics will be unaffected by these modifications. It is not known if the assumption of saturating concentration of salmeterol might bear out under pharmacological conditions. The recommended dose of Advair HFA gives 42 μg of salmeterol base which amounts to 60.90 μg of salmeterol xinafoate (GlaxoSmithKline 2008). Peak plasma concentrations from 21 μg of salmeterol base is about 510 pg/mL but due to the lipophilicity of salmeterol it is anybody's guess what the actual concentrations are in the plasma membranes.

4.2.2. Microkinetic Model (MM)

The hallmark of the microkinetic model (Figure 4.2) is the partitioning of salmeterol into the plasma membrane which then serves as a reservoir for prolonged salmeterol action (Anderson, Linden et al. 1994). Table 4.2 lists the parameters used in my representation of the microkinetic model. Figure 4.3 shows that this representation of the microkinetic model can recapitulate both long action and reassertion of salmeterol post treatment with a competing ligand.

R1. $\mathrm{Sal_o} \;\underset{k_{rel}}{\overset{k_{in}}{\rightleftharpoons}}\; \mathrm{Sal_m}$

R2. $\mathrm{Sal_o + R_m} \;\underset{k_{Sal\,off}}{\overset{k_{Sal\,on}}{\rightleftharpoons}}\; \mathrm{Sal{:}R_m}$

R3. $\mathrm{Sal_m + R_m} \;\underset{k_{Sal\,off}}{\overset{k_{Sal\,on}}{\rightleftharpoons}}\; \mathrm{Sal{:}R_m}$

R4. $\mathrm{Iso_o + R_m} \;\underset{k_{Iso\,off}}{\overset{k_{Iso\,on}}{\rightleftharpoons}}\; \mathrm{Iso{:}R_m}$
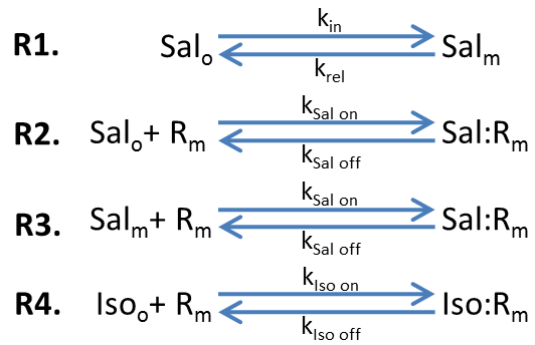
Figure 4.2 Reaction Diagram of the Microkinetic Model (MM)

The membrane acts as depot for salmeterol ($\mathrm{Sal_m}$) from where it is steadily released. $\mathrm{Sal_o}$ = Sal outside the cell; $\mathrm{R_m}$ = membrane bound β2AR; $\mathrm{Sal{:}R_m}$ = salmeterol bound to β2AR on the membrane; $\mathrm{Iso_o}$ = isoproterenol in the aqueous phase; $\mathrm{Iso{:}R_m}$ = isoproterenol bound to β2AR on the membrane.

Table 4.2 Parameters of the Microkinetic Model

Reaction Name	Parameter	Reference/Rationale
Salmeterol association rate (to plasma membrane)	k_{in}= 107 min^{-1}	$K_{p(mem)}$ = 22500 (Rhodes, Newton et al. 1992)
Salmeterol release rate (from plasma membrane)	k_{rel} = 0.004 min^{-1}	$t_{1/2}$ ~ 180 min (Rhodes, Newton et al. 1992; Austin, Barton et al. 2003)
Salmeterol On	$k_{Sal\ on}$ = 8.4e+07 M^{-1}.min^{-1}	Rate of salmeterol binding β2AR assumed to similar to isoproterenol
Salmeterol Off	$k_{Sal\ off}$ = 0.168 min^{-1}	Kd ~ 2 nM (Rong, Arbabian et al. 1999)
Isoproterenol On	$k_{Iso\ on}$ = 8.4e+07 M^{-1}.min^{-1}	Kf set to achieve ~ 47 msec τ for 10μM isoproterenol binding (Reiner, Ambrosio et al. 2010)
Isoproterenol Off	$k_{Iso\ off}$ = 235.2 min^{-1}	Kd ~ 283 nM (Vayttaden, Friedman et al. 2010)
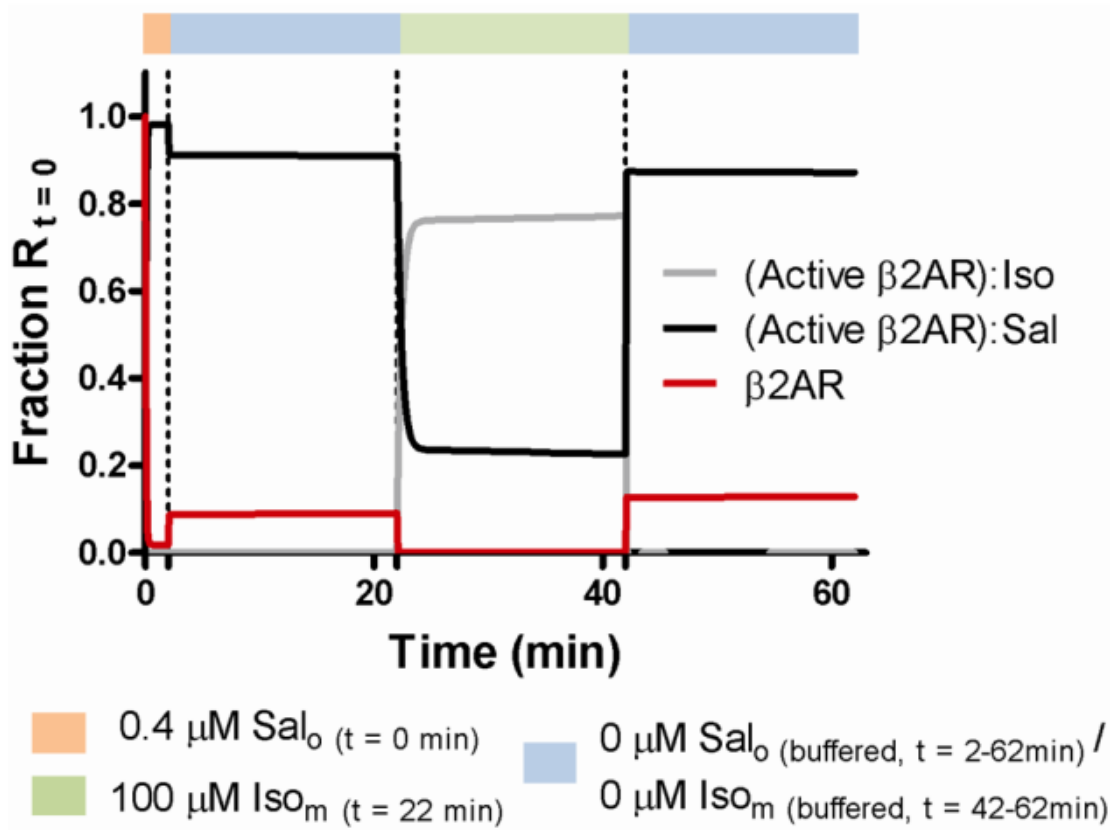
Figure 4.3 Microkinetic Model – Salmeterol Long Action and Reassertion

Simulations based on Figure 4.2 and Table 4.2. **Long Action** – Salmeterol bound active β2AR

(black line) persists after 2 min treatment. **Reassertion** – Salmeterol bound active β2AR

(black line) reappears even after 20 min washout and 20 min isoproterenol treatment followed

by a 20 min second washout.

4.2.3. Exosite Model (EM)

The exosite model (Figure 4.4) is characterised by the binding of salmeterol on the receptor at a site that is by necessity adjacent to the saligenin site. This exosite binding enables preferable partitioning of salmeterol into the plasma membrane which then serves as a reservoir for prolonged salmeterol action (Jack 1991). A key difference between the exosite and microkinetic model is that in the microkinetic model partitioning of salmeterol into the plasma membrane is driven by the drug's lipophilicity whereas in the exosite model it is dependent upon the receptor concentration.

Table 4.3 lists the parameters used in my representation of the exosite model. Figure 4.5 shows that this representation of the exosite model can recapitulate both long action and reassertion of salmeterol post treatment with a competing ligand.

R1. $Sal_o + R_{eam}$ $\underset{k_{rel}}{\overset{k_{in}}{\rightleftharpoons}}$ $Sal:R_{Eam}$

R2. $Sal:R_{Eam}$ $\underset{k_{Sal\,off}}{\overset{k_{Sal\,on}}{\rightleftharpoons}}$ $Sal:R_{EAm}$

R3. $Iso_o + R_{eam}$ $\underset{k_{Iso\,off}}{\overset{k_{Iso\,on}}{\rightleftharpoons}}$ $Iso:R_{eAm}$

R4. $Sal_o + Iso:R_{eAm}$ $\underset{k_{rel}}{\overset{k_{in}}{\rightleftharpoons}}$ $Sal:Iso:R_{EAm}$

R5. $Iso_o + Sal:R_{Eam}$ $\underset{k_{Iso\,off}}{\overset{k_{Iso\,on}}{\rightleftharpoons}}$ $Sal:Iso:R_{EAm}$

R6. $Sal_o + R_{eam}$ $\underset{k_{Sal\,off}}{\overset{k_{Sal\,on}}{\rightleftharpoons}}$ $Sal:R_{eAm}$

R7. $Sal:R_{eAm}$ $\underset{k_{rel}}{\overset{k_{in}}{\rightleftharpoons}}$ $Sal:R_{EAm}$
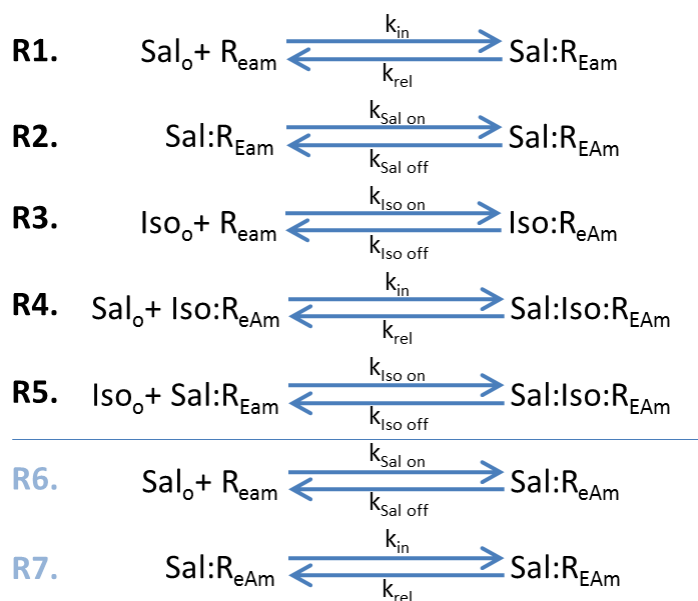
Figure 4.4 Reaction Diagram of the Exosite Model (EM)

The β2AR has an exosite to which salmeterol is bound and retained in the membrane. The subscript m denotes that the species is retained on the plasma membrane and the subscript o denotes that the species is in the aqueous phase. R denotes the β2AR and it is followed by subscripts *eam, EAm, Eam* and *eAm* where *e/E* and *a/A* denote the exosite and active site respectively and the case denotes whether these sites are empty or occupied. A lower case denotes that the site is empty and an upper case denotes that the site is occupied. Thus R_{eam} = β2AR with empty active- and exo-sites; $Sal:R_{EAm}$ = Salmeterol bound to both active- and exo-site on the β2AR; $Sal:R_{Eam}$ = Salmeterol bound to only exo-site on the β2AR; $Sal:R_{eAm}$ = Salmeterol bound to only active-site on the β2AR; $Iso:R_{eAm}$ = Isoproterenol bound to active-site on the β2AR; $Sal:Iso:R_{eAm}$ = Isoproterenol bound to active-site on the β2AR. Reactions 6 and 7 are ignored in the simulations since at longer treatments active site should be occupied and exosite should be quasi-irreversibly occupied.

Table 4.3 Parameters of the Exosite Model

Reaction Name	Parameter	Reference/Rationale
Salmeterol association rate (to β2AR exosite)	k_{in} = 8e+07 M^{-1}.min^{-1}	Set to match τ (at 4e-07 M salmeterol and 3e-07 M naïve β2AR) for membrane association of salmeterol in microkinetic model
Salmeterol release rate (from β2AR exosite)	k_{exo} = 0.004 min^{-1}	$t_{1/2}$ ~ 180 min (Rhodes, Newton et al. 1992; Austin, Barton et al. 2003)
Salmeterol On (to β2AR active site)	$k_{Sal\ on}$ = 20 min^{-1}	Set to match τ (at 4e-07 M salmeterol and 3e-07 M naïve β2AR) for salmeterol binding β2AR in microkinetic model
Salmeterol Off (from β2AR active site)	$k_{Sal\ off}$ = 0.168 min^{-1}	Kd ~ 2 nM (Rong, Arbabian et al. 1999)
Isoproterenol On	$k_{Iso\ on}$ = 8.4e+07 M^{-1}.min^{-1}	Kf set to achieve ~ 47 msec τ for 10μM isoproterenol binding (Reiner, Ambrosio et al. 2010)
Isoproterenol Off	$k_{Iso\ off}$ = 235.2 min^{-1}	Kd ~ 283 nM (Vayttaden, Friedman et al. 2010)

Figure 4.5 Exosite Model – Salmeterol Long Action and Reassertion

Simulations based on Figure 4.4 and Table 4.2. **Long Action** – Salmeterol bound active β2AR

(black line) persists after 2 min treatment. **Reassertion** – Salmeterol bound active β2AR

(black line) reappears even after 20 min washout and 20 min isoproterenol treatment.

4.2.4. Combined Model (CM)

The third model proposed for salmeterol action was the rebinding model (Szczuka, Wennerberg et al. 2009). This model explains long action of salmeterol by rapid rebinding of the released salmeterol to an adjacent receptor. As recognised by the proponents of this model, rebinding cannot by itself explain reassertion properties of salmeterol when a competing ligand is present. It is now generally accepted that the properties of salmeterol are due to a combination of microkinetics, exosite binding to the receptor and rebinding. I have thus made a composite model that allows for all three events to occur. The combined model is shown in Figure 4.6 and its ability to capture long action and reassertion properties of salmeterol is shown in Figure 4.7. Table 4.4 lists the parameters used in my representation of the combined model.

R1. $\text{Sal}_o \underset{k_{rel}}{\overset{k_{in}}{\rightleftharpoons}} \text{Sal}_m$

R2. $\text{Sal}_o + R_{eam} \underset{k_{rel}}{\overset{k_{in}'}{\rightleftharpoons}} \text{Sal:}R_{Eam}$

R3. $\text{Sal}_m + R_{eam} \underset{k_{rel}}{\overset{k_{in}'}{\rightleftharpoons}} \text{Sal:}R_{Eam}$

R4. $\text{Sal:}R_{Eam} \underset{k_{Sal\,off}}{\overset{k_{Sal\,on}'}{\rightleftharpoons}} \text{Sal:}R_{EAm}$

R5. $\text{Iso}_o + R_{eam} \underset{k_{Iso\,off}}{\overset{k_{Iso\,on}}{\rightleftharpoons}} \text{Iso:}R_{eAm}$

R6. $\text{Sal}_o + \text{Iso:}R_{eAm} \underset{k_{rel}}{\overset{k_{in}'}{\rightleftharpoons}} \text{Sal:Iso:}R_{EAm}$

R7. $\text{Sal}_m + \text{Iso:}R_{eAm} \underset{k_{rel}}{\overset{k_{in}'}{\rightleftharpoons}} \text{Sal:Iso:}R_{EAm}$

R8. $\text{Iso}_o + \text{Sal:}R_{Eam} \underset{k_{Iso\,off}}{\overset{k_{Iso\,on}}{\rightleftharpoons}} \text{Sal:Iso:}R_{EAm}$

R9. $\text{Sal}_o + R_{eam} \underset{k_{Sal\,off}}{\overset{k_{Sal\,on}}{\rightleftharpoons}} \text{Sal:}R_{eAm}$

R10. $\text{Sal}_m + R_{eam} \underset{k_{Sal\,off}}{\overset{k_{Sal\,on}}{\rightleftharpoons}} \text{Sal:}R_{eAm}$

R11. $\text{Sal:}R_{eAm} \underset{k_{rel}}{\overset{k_{in}'}{\rightleftharpoons}} \text{Sal:}R_{EAm}$

Figure 4.6 Reaction Diagram of the Combined Model (CM)

The β2AR has an exosite to which salmeterol is bound and retained in the membrane. The membrane also acts as depot for salmeterol (Sal_m) from where it is steadily released. R denotes the β2AR and it is followed by subscripts *eam, EAm, Eam* and *eAm* where *e/E* and *a/A* denote the exosite and active site respectively and the case denotes whether these sites are empty or occupied. A lower case denotes that the site is empty and an upper case denotes that the site is occupied. Thus R_{eam} = β2AR with empty active- and exo-sites; $\text{Sal:}R_{EAm}$ =

Salmeterol bound to both active- and exo-site on the β2AR; Sal:R_{Eam} = Salmeterol bound to only exo-site on the β2AR; Sal:R_{eAm} = Salmeterol bound to only active-site on the β2AR; Iso:R_{eAm} = Isoproterenol bound to active-site on the β2AR; Sal:Iso:R_{eAm} = Isoproterenol bound to active-site on the β2AR. Reactions 9 - 11 are ignored in the simulations since at longer treatments active site should be occupied and salmeterol exosite binding is quasi-irreversible. Iso_o = isoproterenol in the aqueous phase

Table 4.4 Parameters of the Combined Model

Reaction Name	Parameter	Reference/Rationale
Salmeterol association rate (to β2AR exosite)	$k_{in}' = 8e+07\ M^{-1}.min^{-1}$	Set to match τ (at 4e-07 M salmeterol and 3e-07 M naïve β2AR) for membrane association of salmeterol in microkinetic model
Salmeterol association rate (to plasma membrane)	$k_{in} = 107\ min^{-1}$	$K_{p(mem)} = 22500$ (Rhodes, Newton et al. 1992)
Salmeterol release rate (from β2AR exosite or from plasma membrane)	$k_{exo} = k_{rel} = 0.004\ min^{-1}$	$t_{1/2} \sim$ 180 min (Rhodes, Newton et al. 1992; Austin, Barton et al. 2003)
Salmeterol On (to β2AR active site)	$k_{Sal\ on}' = 20\ min^{-1}$	Set to match τ (at 4e-07 M salmeterol and 3e-07 M naïve β2AR) for salmeterol binding β2AR in microkinetic model (see below)
Salmeterol On (to β2AR active site)	$k_{Sal\ on} = 8.4e+07\ M^{-1}.min^{-1}$	Rate of salmeterol binding β2AR assumed to similar to isoproterenol
Salmeterol Off (from β2AR active site)	$k_{Sal\ off} = 0.168\ min^{-1}$	Kd ~ 2 nM (Rong, Arbabian et al. 1999)
Isoproterenol On	$k_{Iso\ on} = 8.4e+07\ M^{-1}.min^{-1}$	Kf set to achieve ~ 50 msec τ for 10µM isoproterenol binding (Reiner, Ambrosio et al. 2010)
Isoproterenol Off	$k_{Iso\ off} = 235.2\ min^{-1}$	Kd ~ 283 nM (Vayttaden, Friedman et al. 2010)
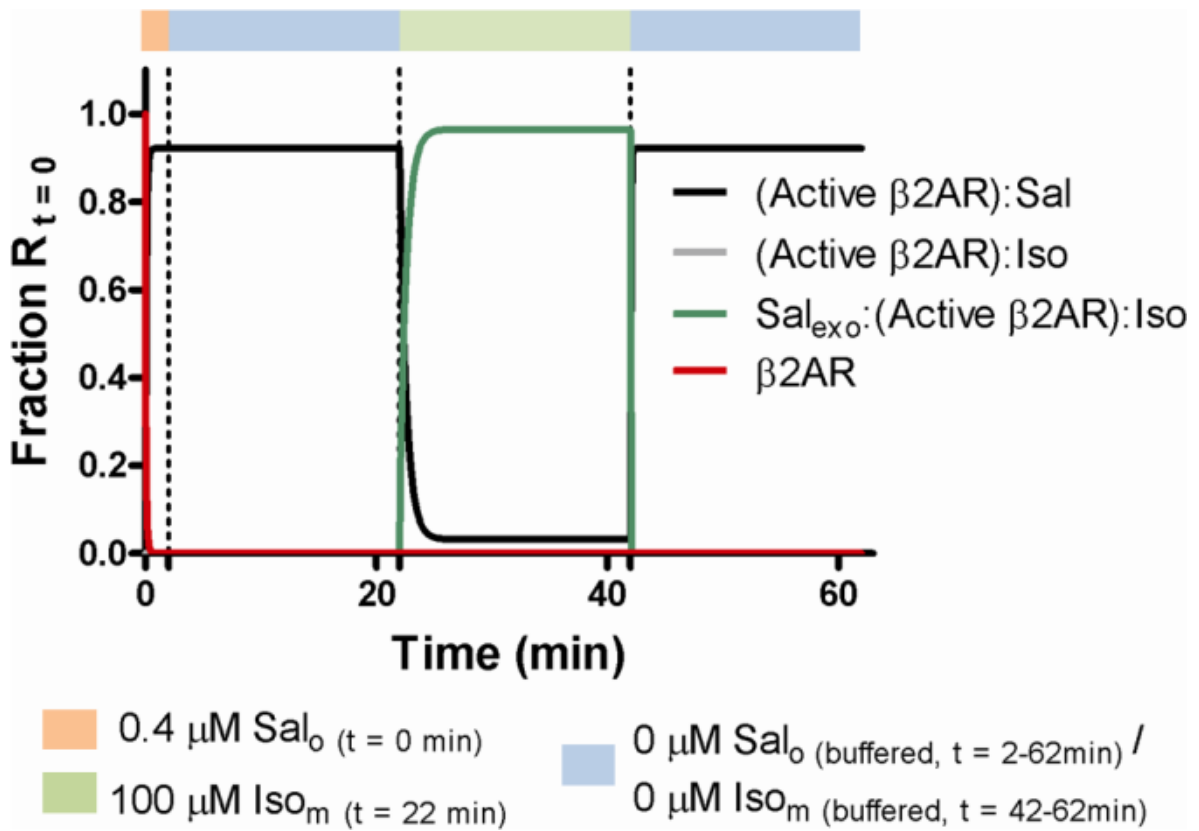
Figure 4.7 Combined Model – Salmeterol Long Action and Reassertion

Simulations based on Figure 4.6 and Table 4.4. **Long Action** – Salmeterol bound active β2AR

(black line) persists after 2 min treatment. **Reassertion** – Salmeterol bound active β2AR

(black line) reappears even after 20 min washout and 20 min isoproterenol treatment.

4.2.5. Salmeterol β2AR Binding Models Coupled to the GRK Model

Since all the three salmeterol models presented thus far in Section 4.2 deal only with events at the receptor ligand interaction level it is necessary to follow up these models to see if the simulated behaviour of salmeterol action holds true when downstream signalling events are introduced. Towards that end I created three new models (Figure 4.8, Models 8-10) that looked at the effects of coupling GRK-mediated β2AR regulation to the existing models (MM/EM/CM). Since the Combined Model coupled to the GRK model encompasses both exosite and microkinetics I have discussed only that variation of the model in detail below. The exosite model and the microkinetic model coupled by itself to the GRK model showed similar results (data not shown).

To validate these phenomenological models I simulated isoproterenol- and salmeterol-induced GRK-mediated β2AR phosphorylation at saturating agonist concentrations. All three models (8-10) have a general match to the phosphorylation kinetics. Figure 4.9 shows results from only the combined model.
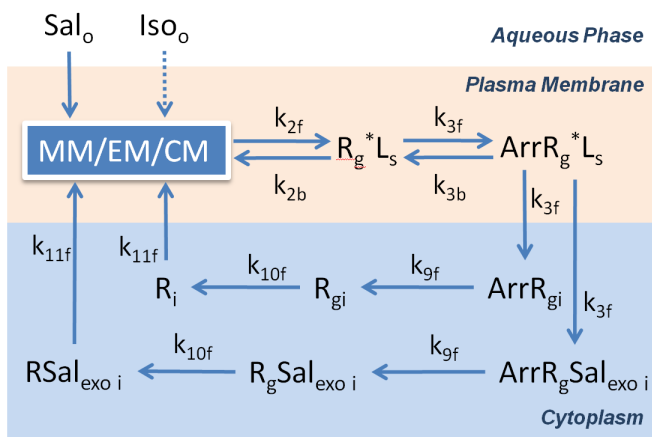
Figure 4.8 Reaction Diagram of the MM/EM/CM Coupled to GRK-Mediated β2AR Regulation

L is ligand (salmeterol/isoproterenol); the blue box with the letterings MM/EM/CM denotes the microkinetic, exosite and combined models for ligand receptor interactions presented above; Reaction numbers are as described in Table 3.1 (c.f. Chapter 3). Iso_o = isoproterenol outside the cell; Sal_o = salmeterol outside the cell, Arr = arrestin; surface species are denoted with a subscript s; internalised species are denoted with a subscript i, GRK phosphorylated species are denoted with a subscript g.
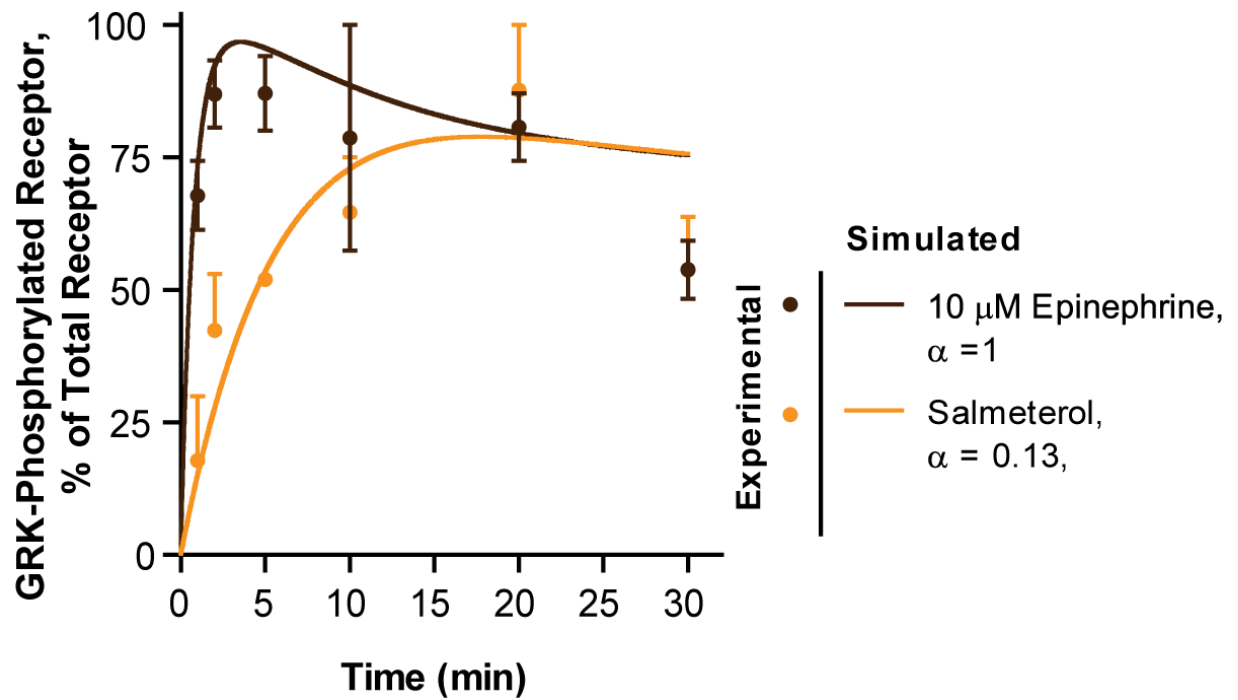
Figure 4.9 Simulated Time Course of GRK Site Phosphorylation

Simulations of GRK phosphorylation on treatment with 10μM epinephrine (brown lines) or

0.4μM salmeterol (orange lines) in the Combined-GRK (Model 10) model. The experimental

results are shown as discrete points.

These validated models were then tested for salmeterol properties of long action and reassertion. All three models show reassertion capabilities but none of them were now able to show considerable long action. Figure 4.10A shows the results for the Combined-GRK model. This can be explained by the simulated rapid arrestin binding to the ligand bound phosphorylated β2AR as measured for isoproterenol (Krasel, Bunemann et al. 2005). In the absence of information to the contrary I had assumed that salmeterol-induced recruitment of arrestin would be as rapid as isoproterenol-induced arrestin recruitment. When I now used the Combined-GRK model to simulate salmeterol induced receptor internalisation (Figure 4.10B) I see that arrestin affinity for the salmeterol-bound receptor had to be reduced 100 fold to match experimentally measured salmeterol-induced receptor internalisation.

We had previously shown that contrary to isoproterenol behaviour, there is negligible β2AR internalisation on treating with saturating salmeterol concentrations. This negligible salmeterol-induced internalisation can be rescued by overexpression of arrestin without affecting internalisation induced by other agonists (Moore, Millman et al. 2007). I had previously shown that a 100-fold reduction in arrestin affinity for salmeterol/β2AR complex was needed to simulate the negligible internalisation, and this did not affect the simulated phosphorylation kinetics (Vayttaden, Friedman et al. 2010). This supports our idea that salmeterol stabilises an alternate conformation of the receptor where eventually the GRK phosphorylation matches the levels attained by full agonists but arrestin affinity of the salmeterol/β2AR complex is markedly reduced. In the light of this I modified

models 8-10 by a ten-fold reduction of arrestin on rate and a ten-fold increase of arrestin on rate to salmeterol/β2AR complex. These modified models were all able to now recapitulate both long action and reassertion effects of salmeterol. Figure 4.10C shows the results of only the Combined-GRK model with the abrogation of internalisation.
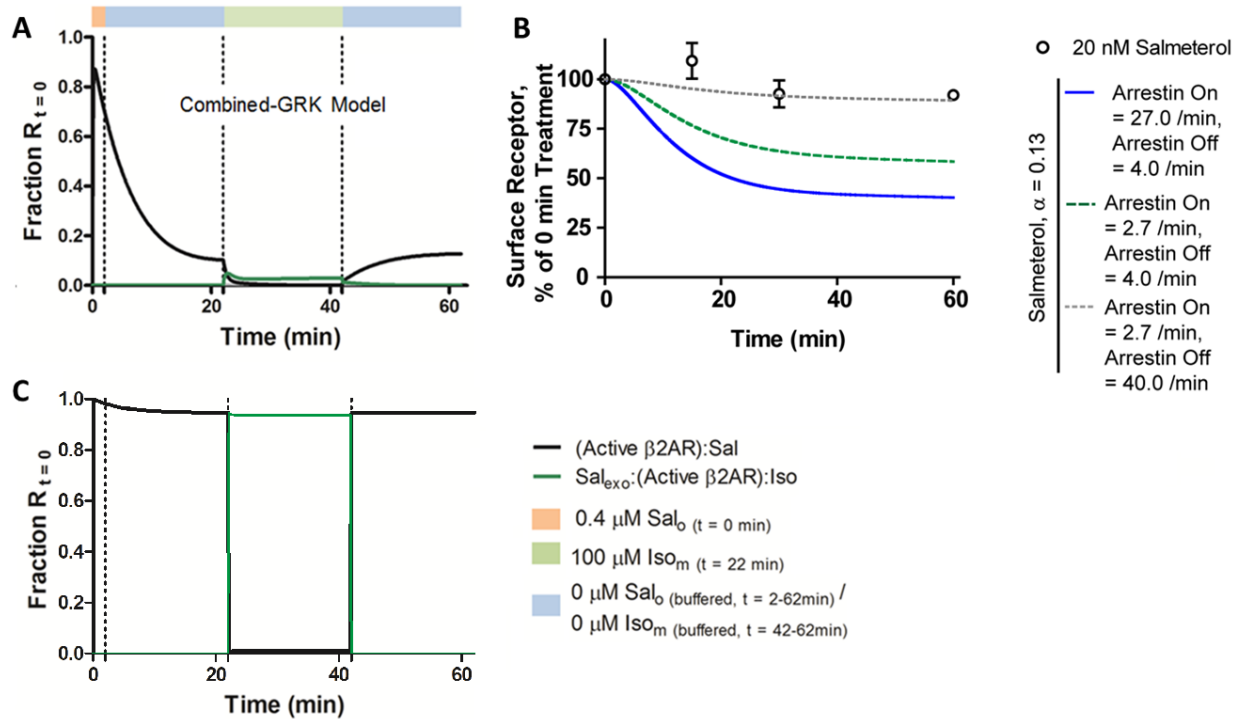
Figure 4.10 Simulated Salmeterol Long Action, Reassertion and Salmeterol-Induced Internalisation

Simulations based on Figure 4.8 and Tables 2.1and 4.1-3. **Long Action** – Salmeterol bound active β2AR (black line) persists after 2 min treatment only in C. **Reassertion** – Salmeterol bound active β2AR (black line) reappears even after 20 min washout and 20 min in A and C. **(A)** Combined-GRK models with default arrestin kinetics; **(B)** Sal-induced internalisation, with varying arrestin kinetics and **(C)** Combined-GRK model with 100 fold lower arrestin affinity for salmeterol/ β2AR complex with internalisation inhibited.

In summary, all existing models of salmeterol action deal solely with receptor ligand events. When we consider downstream signalling events none of these models can effectively explain salmeterol long action. It becomes necessary to invoke reduced arrestin affinity for the salmeterol/β2AR complex in order to simulate experimentally measured salmeterol-induced β2AR internalisation (Vayttaden, Friedman et al. 2010) and to rescue loss of long action (Section 4.2 of this thesis).

4.3. Model Limitations

For ease of comparison of microkinetic and exosite models on the same time scales I assumed that the two mechanisms have the same rates even though we know that the $t_{1/2}$ for salmeterol release from synthetic membranes is ~ 3 hrs (Rhodes, Newton et al. 1992) and for exosite binding is possibly 2-3 fold longer. In spite of these assumptions the models described herein can be used to provide important proof-of-concept simulations about the necessity of reduced arrestin affinity for salmeterol bound β2AR complex.

Figure 4.11 shows experimental measures of cyclic AMP on both short term (30 mins) and long term (12 hrs) treatment with salmeterol in the presence of IBMX to inhibit PDE activity. The experimental data clearly shows that in spite of lower coupling efficiency of salmeterol activated β2AR it is still able to activate significant amount of adenylyl cyclases to show measureable cAMP in the presence of PDE inhibitors. Inspite of the use of IBMX the PDE inhibition is not complete, so by 30 minutes we see a drop in cAMP levels in human airways smooth muscle (HASM) cells treated with saturating isoproterenol (Figure 4.11B). Our data also shows that

a 12 hour pre-treatment with salmeterol does bring about significant desensitisation of the cAMP synthesis machinery. My models of salmeterol action encompass only the G-protein independent GRK-mediated β2AR regulation and so cannot explain the experimental measurements shown in Figure 4.11. From my simulations (Section 4.2 of this thesis) and our experimental data (Moore, Millman et al. 2007) it is clear that the GRK-mediated β2AR regulation does not bring about significant receptor desensitisation on account of weak arrestin affinity so the reduction in cAMP synthesis seen in Figure 4.11B is due to other parts of the signaling machinery. Therefore to better capture the dynamics of salmeterol-induced β2AR desensitisation it is necessary to include PKA- and PDE-mediated regulatory components in the model.

Since salmeterol association and dissociation kinetics from both the active- and exo-site are difficult to measure it is necessary to do a thorough analysis on the effects of variations in these rates on the simulated properties of salmeterol long action and reassertion in models 8-10, although only varying the exosite release is of real consequence over the long treatment periods since we could get good measures of active site on/off from the Kd. Also it would be necessary to include salmeterol dissociation from the GRK phosphorylated β2AR species with or without arrestin so that dephosphorylation and recycling experiments can be simulated. This would have predictive value on account of the difficulties in washing out salmeterol in an experiment. In the next chapter I show very preliminary work towards creating a model that is aimed at explaining the effects of GRK-/PKA-/Arrestin-/PDE-mediated regulation of β2AR signaling.
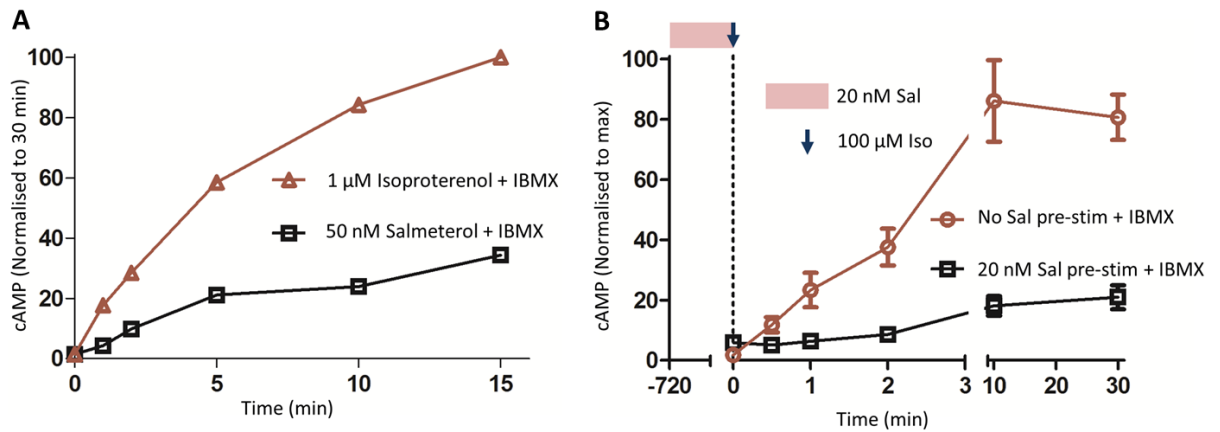
Figure 4.11 cAMP Measured in HASMs in Response to Salmeterol and Isoproterenol Treatment[*]

(A) cAMP measured in response to 1 µM Isoproterenol or 50 nM Salmeterol treatment for 30 minutes when the cells have been pre-treated with IBMX for 30 mins to inhibit PDE activity. **(B)** cAMP measured in response to 100 µM Isoproterenol treatment ± 12 hour pre-treatment with 20 nM Salmeterol. Sal-induced internalisation, with varying arrestin kinetics and **(C)** Combined-GRK model with100 fold lower arrestin affinity for salmeterol/ β2AR complex.

[*] Experiments performed by Ms.Jacqueline Friedman

5. Unified Model for PKA-/PDE-/GRK-Mediated Regulation of β2AR Signalling

This chapter presents preliminary work towards combining models from

"Quantitative Modeling of GRK-Mediated β2AR Regulation." Vayttaden SJ, Friedman J, Tran TM, Rich TC, Dessauer CW, Clark RB (2010) PLoS Comput Biol 6(1): e1000647. doi:10.1371/journal.pcbi.1000647and "Roles of GRK and PDE4 activities in the regulation of beta2 adrenergic signaling" Xin W, Tran TM, Richter W, Clark RB, Rich TC J Gen Physiol. 2008 Apr;131(4):349-64.

My work presented in Chapter 4 suggests that arrestin-mediated desensitisation cannot be the major mode of desensitisation for partial agonists like salmeterol. My work presented in Chapter 3 shows that the rapid arrestin-mediated desensitisation with transient levels of high concentrations of a full agonist like isoproterenol is fully reversible on washout of the agonists and that there is increased desensitisation on repeated agonist delivery inspite of near complete resensitisation during washouts. To understand the effects of prolonged salmeterol maintenance treatment and isoproterenol rescue treatment and to identify the dominant β2AR desensitisation pathways under these different therapeutic regimens it then becomes necessary to follow PKA-/PDE-/GRK-/Arrestin-mediated regulation of β2AR signaling in HASMs.

Due to the low receptor number of HASMs the measure of GRK- and PKA-mediated β2AR phosphorylation and β2AR internalisation in HASMs is inherently noisy. These measurements can be made in our stable β2AR overexpressions in HEK293 cells. It is

possible to measure cAMP profiles in HASMs in response to treatment with various β-agonists in the presence or absence of PDE inhibitors. The use of PDE inhibitors is not without difficulties in that inhibitors like IBMX do not completely inhibit all PDE activity in the cells (Figure 5.1). In our stable β2AR overexpressions in HEK293s the basal PDE activity is up regulated to compensate for the β2AR overexpression. Thus due to the difficulties in obtaining experimental readouts of PKA-/PDE-/GRK-/Arrestin signaling modules in β2AR regulation in a single cell line, it becomes necessary to pool experimental data from both HASMs and stable β2AR overexpressions in HEK293s.

A mathematical representation of the β2AR regulation involving PKA-/PDE-/GRK-/Arrestin signaling modules working together in a single model can then be used to simulate the behaviour of the modules for which data is missing in either HEKs or HASMs. The individual signalling modules of the model can be validated against appropriate data sets while varying receptor number in the model depending on whether HASM data or HEK293 data is being used. This combination of experiments across different cell lines and modeling is expected to yield insight into which of the signalling modules plays a major role in β2AR desensitisation during various treatment regimens.
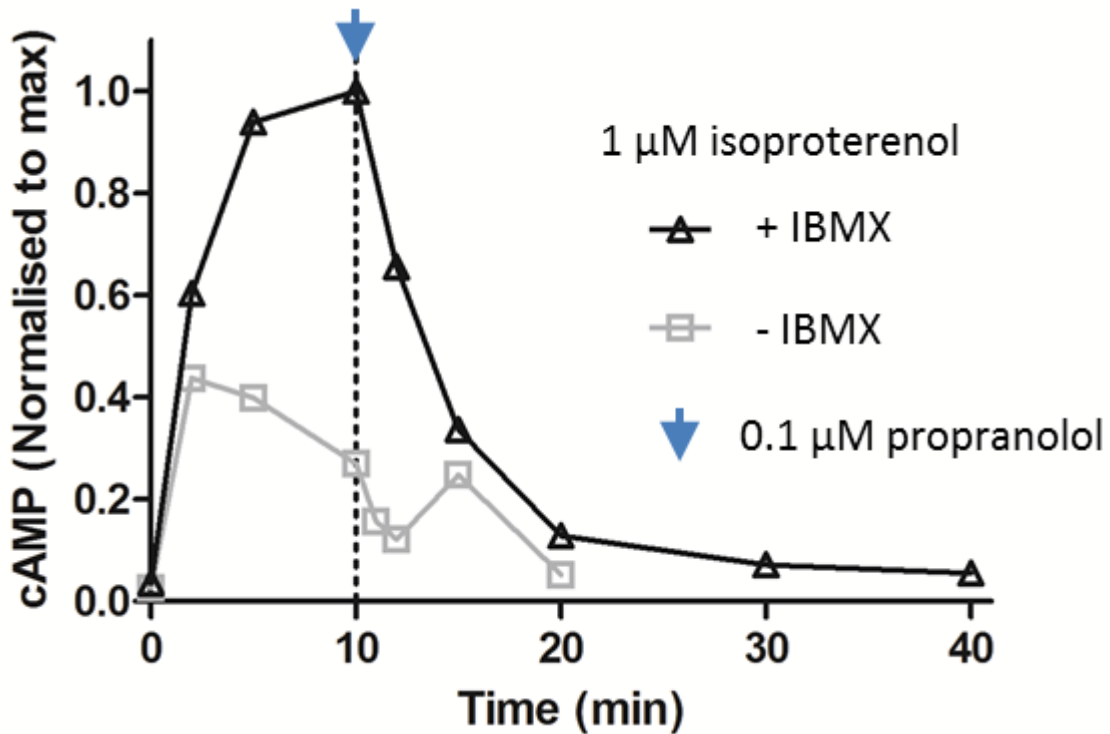
Figure 5.1 cAMP in Response to Isoproterenol Treatment.[*]

cAMP measured in response to 1 μM isoproterenol ± IBMX pretreatment for 30 mins to inhibit PDE activity. At 10 mins post isoproterenol treatment 0.1 μM propranolol is added to displace isoproterenol and abrogate β2AR activated adenylyl cyclase activity. If IBMX inhibition of PDEs were 100% then the cAM levels post propranolol treatment wouldn't have deacayed significantly.

[*] Experiments performed by Ms.Jacqueline Friedman in HASMs.

Some of the weaknesses of this approach are; 1) there will always be unknown variability from one cell line to the other, this will make creating a unique model to explain all datasets very challenging; 2) the number of species and reactions in this model will be higher than any of the previously discussed models which could result in longer computation times; 3) there will also be an increase in unknown parameter values which will require parameter estimation; 4) the large model size will require multiple iterations of the model building exercise before we can settle on the simplest model that can simulate the behavior of all the signalling modules that we are interested in. To create a consensus model I combined my model of the GRK/Arrestin modules (Vayttaden, Friedman et al. 2010) with that of the PKA/PDE modules that our group had published previously (Xin, Tran et al. 2008). The reaction diagram for the unified model as it pertains to experimental measurements of agonist-induced GRK-mediated β2AR-phosphorylation, PKA-mediated β2AR-phosphorylation, β2AR-dephosphorylation, -trafficking, -desensitisation, -resensitisation and -cAMP profile is given in Figures 5.2-5.5 and Table 5.1 lists its parameters.
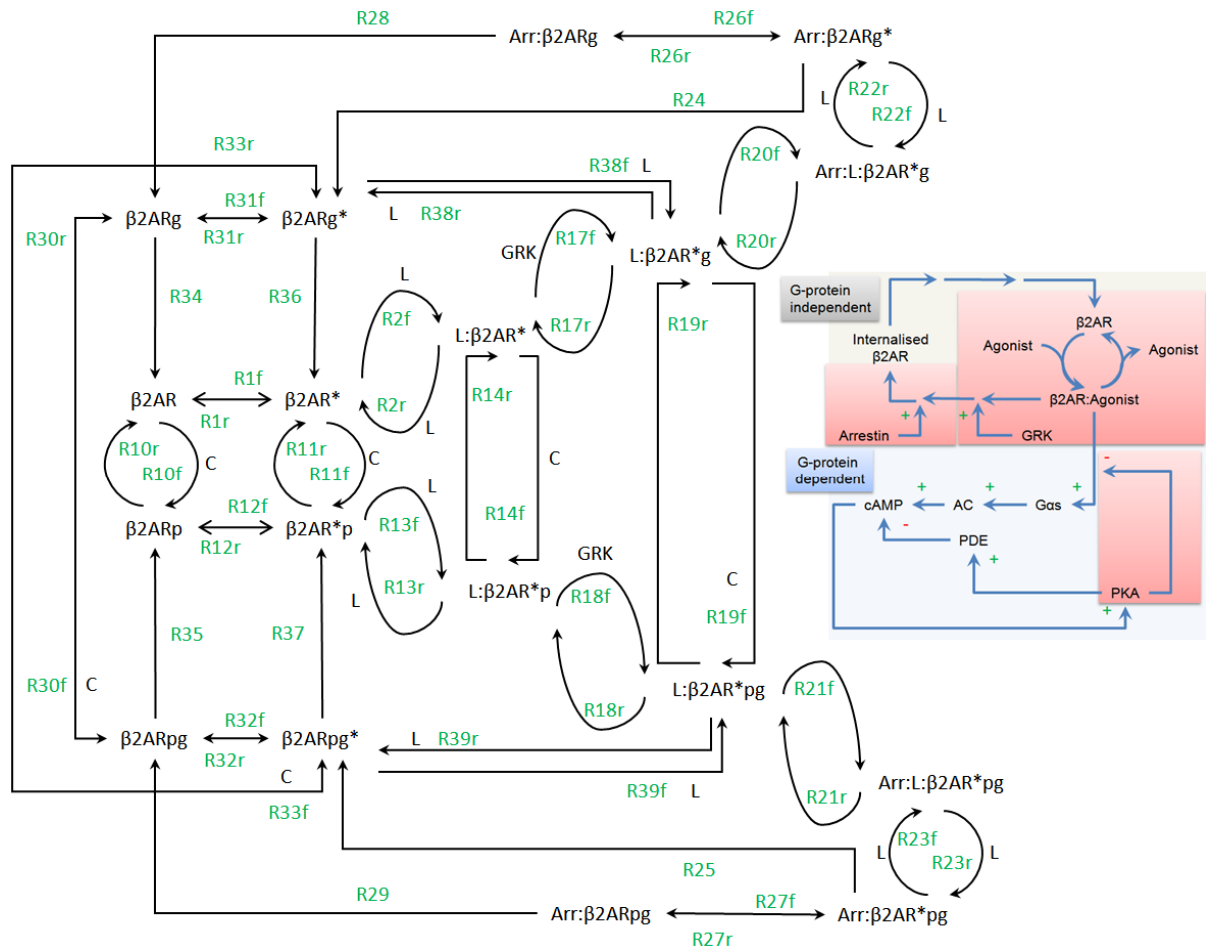
Figure 5.2 Reaction Diagram of β2AR Level Regulation at the Plasma Membrane.

This reaction diagram describes the β2AR level regulation modules at the plasma membrane as highlighted in red in the inset. L is ligand; $\beta2AR^*$ is active state of β2AR; $\beta2AR_g$ is GRK-phosphorylated β2AR; $\beta2AR_p$ is PKA-phosphorylated β2AR; Arr is arrestin; C is catalytic subunit of PKA. The reaction numbers in green correspond to rate constants described in Table 5.1.
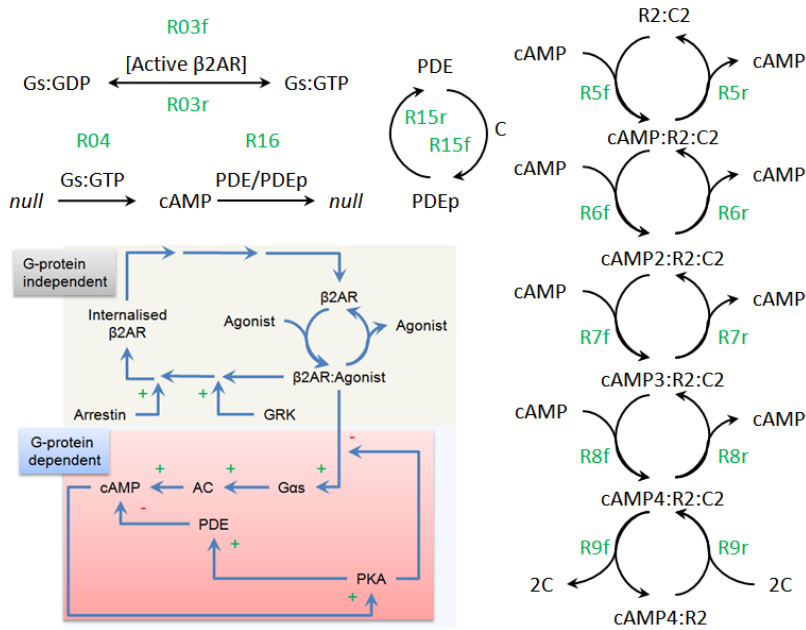
Figure 5.3 Reaction Diagram of Gs/PKA/PDE Activation Modules in β2AR Regulation.

This reaction diagram describes the Gs/PKA/PDE activation modules in β2AR regulation at the plasma membrane as highlighted in red in the inset. Gs is G protein αs; null indicates an implicit substrate or product; R is the regulatory subunit of PKA; C is catalytic subunit of PKA; PDEp indicates PKA phosphorylated PDE. The reaction numbers in green correspond to rate constants described in Table 5.1.
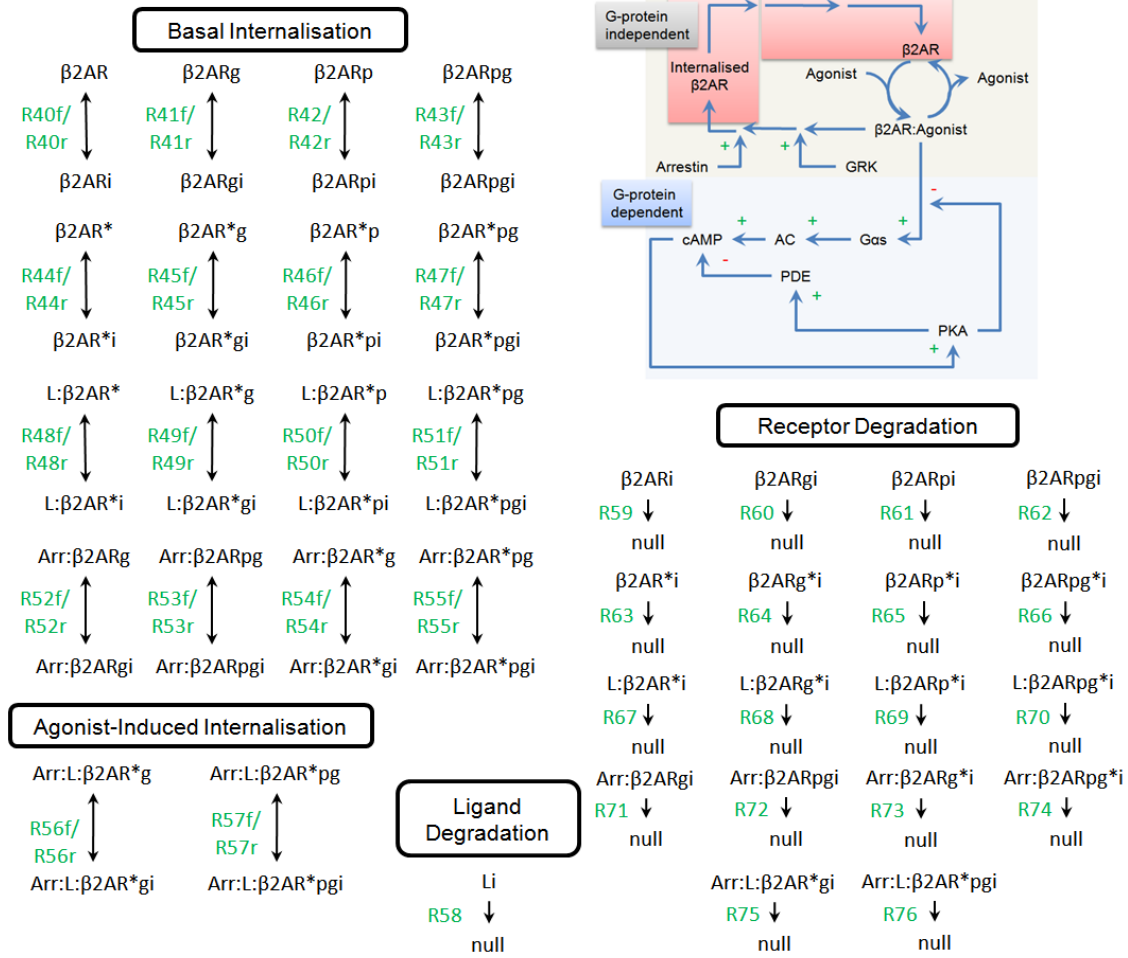
Figure 5.4 Reaction Diagram of β2AR-Trafficking and Degradation.

This reaction diagram describes the β2AR-trafficking and degradation modules in β2AR regulation as highlighted in red in the inset. $β2AR_i$ indicates an internalised β2AR; L_i indicates an internalised ligand; null indicates an implicit product; $β2AR^*$ is active state of β2AR; $β2AR_g$ is GRK-phosphorylated β2AR; $β2AR_p$ is PKA-phosphorylated β2AR; Arr is arrestin. The reaction numbers in green correspond to rate constants described in Table 5.1.

Figure 5.5 Reaction Diagram of Post-Internalisation Events in β2AR Regulation.

This reaction diagram describes the post-internalisation events of β2AR regulation as highlighted in red in the inset. $β2AR_i$ indicates an internalised β2AR; L_i indicates an internalised ligand; $β2AR^*$ is active state of β2AR; $β2AR_g$ is GRK-phosphorylated β2AR; $β2AR_p$ is PKA-phosphorylated β2AR; Arr is arrestin. The reaction numbers in green correspond to rate constants described in Table 5.1.

Table 5.1 Parameters for the Unified PKA-/GRK-/PDE-Mediated β2AR Regulation Model

No.	Parameter Name	Value	Reference/Rationale	Fig. No.
1	R1f: β2AR Activation	40 /sec	Rates adjusted to achieve appropriate levels of basal active β2AR.	5.2
2	R1r: β2AR* Inactivation	200 /sec		
3	R2f: L On β2AR*	14 $\mu M^{-1}.sec^{-1}$	Rates adjusted to achieve appropriate τ (Reiner, Ambrosio et al. 2010) and K_{ds} (Vayttaden, Friedman et al. 2010).	5.2
4	R2r: L Off L:β2AR*	6.3 sec^{-1}		
5	R3f: G_s Activation	K_c = 15 μM; k_{act} = 15 sec^{-1}; k_h = 0.8 sec^{-1}	(K_c) Equilibrium constant for activated β2AR and G_s; (k_{act}) Rate constant of G_s activation by active β2AR; (k_h) Rate constant of GTP hydrolysis (Xin, Tran et al. 2008).	5.3
6	R3r: G_s:GTP Hydrolysis			

$[G_s{:}GTP] = k_{act} \times (([Fraction\ Active\ \beta 2AR] \times [G_s{:}GDP])/K_c) - k_h \times [G_s{:}GTP]$

Adapted from equations 2, 5 and 6 (Xin, Tran et al. 2008).

No.	Parameter Name	Value	Reference/Rationale	Fig. No.
7	R4: cAMP Production	AC_{syn} = 10 $\mu M.sec^{-1}$; K_{GsAC} = 315 μM	(AC_{syn}) cAMP synthesis rate; (K_{GsAC}) Equilibrium constant for G_s:GTP and AC (Xin, Tran et al. 2008).	5.3

$k_4 = (AC_{syn} \times [G_s{:}GTP])/K_{GsAC}$; Adapted from equation 8 (Xin, Tran et al. 2008).

No.	Parameter Name	Value	Reference/Rationale	Fig. No.
8	R5f: cAMP On R2:C2	0.4 $\mu M^{-1}.sec^{-1}$	(Xin, Tran et al. 2008)	5.3
9	R5r: cAMP Off cAMP:R2:C2	0.2 sec^{-1}	(Xin, Tran et al. 2008)	5.3
10	R6f: cAMP On cAMP:R2:C2	0.4 $\mu M^{-1}.sec^{-1}$	(Xin, Tran et al. 2008)	5.3
11	R6r: cAMP Off cAMP2:R2:C2	0.2 sec^{-1}	(Xin, Tran et al. 2008)	5.3
12	R7f: cAMP On cAMP2:R2:C2	5 $\mu M^{-1}.sec^{-1}$	(Xin, Tran et al. 2008)	5.3
13	R7r: cAMP Off cAMP3:R2:C2	1 sec^{-1}	(Xin, Tran et al. 2008)	5.3
14	R8f: cAMP On cAMP3:R2:C2	5 $\mu M^{-1}.sec^{-1}$	(Xin, Tran et al. 2008)	5.3

Table 5.1 (contd.) Parameters for the Unified PKA-/GRK-/PDE-Mediated β2AR Regulation Model

No.	Parameter Name	Value	Reference/Rationale	Fig. No.
15	R8r: cAMP Off cAMP4:R2:C2	1 sec^{-1}	(Xin, Tran et al. 2008)	5.3
16	R9f: 2C Off cAMP4:R2:C2	70 sec^{-1}	(Xin, Tran et al. 2008)	5.3
17	R9r: 2C On cAMP4:R2	0.75 μM^{-2}.sec^{-1}	(Xin, Tran et al. 2008)	5.3
18	R10f: PKA Phosphorylation β2AR	[Fraction Active PKA]*83 sec^{-1}	(Tran, Friedman et al. 2004)	5.2
19	R10r: PKA Dephosphorylation β2ARp	0.036 sec^{-1}	Phosphorylated receptor $t_{1/2}$ = 18 min (Tran, Friedman et al. 2004; Tran, Friedman et al. 2007)	5.2
20	R11f: PKA Phosphorylation β2AR*	[Fraction Active PKA]*83 sec^{-1}	(Tran, Friedman et al. 2004)	5.2
21	R11r: PKA Dephosphorylation β2AR*p	0.036 sec^{-1}	Phosphorylated receptor $t_{1/2}$ = 18 min (Tran, Friedman et al. 2004; Tran, Friedman et al. 2007)	5.2
22	R12f: β2ARp Activation	40 /sec	Rates adjusted to achieve appropriate levels of basal active β2AR.	5.2
23	R12r: β2AR*p Inactivation	200 /sec		
24	R13f: L On β2AR*	14 μM^{-1}.sec^{-1}	Rates adjusted to achieve appropriate τ (Reiner, Ambrosio et al. 2010) and K_{ds} (Vayttaden, Friedman et al. 2010).	5.2
25	R13r: L Off L:β2AR*	6.3 sec^{-1}		
26	R14f: PKA Phosphorylation L:β2AR*	[Fraction Active PKA]*83 sec^{-1}	(Tran, Friedman et al. 2004)	5.2
27	R14r: PKA Dephosphorylation L:β2AR*p	0.036 sec^{-1}	Phosphorylated receptor $t_{1/2}$ = 18 min (Tran, Friedman et al. 2004; Tran, Friedman et al. 2007)	5.2

Table 5.1 (contd.) Parameters for the Unified PKA-/GRK-/PDE-Mediated β2AR Regulation Model

No.	Parameter Name	Value	Reference/Rationale	Fig. No.
28	R15f: PKA Phosphorylation PDE	[Fraction Active PKA]*0.015 sec^{-1}	Rates need to be adjusted for my system (Xin, Tran et al. 2008)	5.3
29	R15r: PKA Dephosphorylation PDEp	0.005 sec^{-1}	Rates need to be adjusted for my system (Xin, Tran et al. 2008)	5.3
30	R16: PDE Activity	k_{PDE} =0.15 µM.sec^{-1}; k_{PDEp} =2.5 X (k_{PDE}); I =Appropriate PDE inhibitor concentration as used in experiment ; K_I=0.1 µM (for Rolipram)	(Xin, Tran et al. 2008)	5.3

$$k_{16f} = \frac{[PDE] \times [cAMP] \times k_{PDE}}{[cAMP] + \left(K_{m\,PDE} \times \left(1 + \frac{[I]}{K_I} \right) \right)} + \frac{[PDE_p] \times [cAMP] \times k_{PDEp}}{[cAMP] + \left(K_{m\,PDEp} \times \left(1 + \frac{[I]}{K_I} \right) \right)}$$

Adapted from equation 9 (Xin, Tran et al. 2008).

No.	Parameter Name	Value	Reference/Rationale	Fig. No.
31	R17f: GRK Phosphorylation L:β2AR*	8.4 sec^{-1}	(Tran, Friedman et al. 2004)	5.2
32	R17r: GRK Dephosphorylation β2AR*g	0.036 sec^{-1}	Phosphorylated receptor t$_{1/2}$ = 18 min (Tran, Friedman et al. 2004; Tran, Friedman et al. 2007)	5.2
33	R18f: GRK Phosphorylation L:β2AR*p	8.4 sec^{-1}	(Tran, Friedman et al. 2004)	5.2
34	R18r: GRK Dephosphorylation L:β2AR*pg	0.036 sec^{-1}	Phosphorylated receptor t$_{1/2}$ = 18 min (Tran, Friedman et al. 2004; Tran, Friedman et al. 2007)	5.2

Table 5.1 (contd.) Parameters for the Unified PKA-/GRK-/PDE-Mediated β2AR Regulation Model

No.	Parameter Name	Value	Reference/Rationale	Fig. No.
35	R19f: PKA Phosphorylation L:β2AR*g	[Fraction Active PKA]*83 sec^{-1}	(Tran, Friedman et al. 2004)	5.2
36	R19r: PKA Dephosphorylation L:β2AR*pg	0.036 sec^{-1}	Phosphorylated receptor $t_{1/2}$ = 18 min (Tran, Friedman et al. 2004; Tran, Friedman et al. 2007)	5.2
37	R20f: Arrestin On L:β2AR*g	1620 sec^{-1}	Rate of arrestin binding = 26.6 ± 5.9 /min (Krasel, Bunemann et al. 2005)	5.2
38	R20r: Arrestin Off Arr:L:β2AR*g	240 sec^{-1}	Rate of arrestin dissociation assumed to match measured K_d.	5.2
39	R21f: Arrestin On L:β2AR*pg	1620 sec^{-1}	Rate of arrestin binding = 26.6 ± 5.9 /min (Krasel, Bunemann et al. 2005)	5.2
40	R21r: Arrestin Off Arr:L:β2AR*pg	240 sec^{-1}	Rate of arrestin dissociation assumed to match measured K_d.	5.2
41	R22f: L On Arr:β2AR*g	14 µM^{-1}.sec^{-1}	Rates adjusted to achieve appropriate τ (Reiner, Ambrosio et al. 2010) and K_{ds} (Vayttaden, Friedman et al. 2010).	5.2
42	R22r: L Off Arr:L:β2AR*g	6.3 sec^{-1}		
43	R23f: L On Arr:β2AR*pg	14 µM^{-1}.sec^{-1}	Rates adjusted to achieve appropriate τ (Reiner, Ambrosio et al. 2010) and K_{ds} (Vayttaden, Friedman et al. 2010).	5.2
44	R23r: L Off Arr:L:β2AR*pg	6.3 sec^{-1}		
45	R24: Arrestin Off Arr: β2AR*g	660 sec^{-1}	Rate of arrestin dissociation = 10.86 ± 1.2 /min (Krasel, Bunemann et al. 2005).	5.2
46	R25: Arrestin Off Arr: β2AR*pg	660 sec^{-1}	Rate of arrestin dissociation = 10.86 ± 1.2 /min (Krasel, Bunemann et al. 2005).	5.2

Table 5.1 (contd.) Parameters for the Unified PKA-/GRK-/PDE-Mediated β2AR Regulation Model

No.	Parameter Name	Value	Reference/Rationale	Fig. No.
47	R26f: Arr:β2ARg Activation	40 /sec	Rates adjusted to achieve appropriate levels of basal active β2AR.	5.2
48	R26r: Arr:β2AR*g Inactivation	200 /sec		
49	R27f: Arr:β2ARpg Activation	40 /sec	Rates adjusted to achieve appropriate levels of basal active β2AR.	5.2
50	R27r: Arr:β2AR*pg Inactivation	200 /sec		
51	R28: Arrestin Off Arr: β2AR*g	660 sec^{-1}	Rate of arrestin dissociation = 10.86 ± 1.2 /min (Krasel, Bunemann et al. 2005).	5.2
52	R29: Arrestin Off Arr: β2AR*pg	660 sec^{-1}	Rate of arrestin dissociation = 10.86 ± 1.2 /min (Krasel, Bunemann et al. 2005).	5.2
53	R30f: PKA Phosphorylation β2ARg	[Fraction Active PKA]*83 sec^{-1}	(Tran, Friedman et al. 2004)	5.2
54	R30r: PKA Dephosphorylation β2ARpg	0.036 sec^{-1}	Phosphorylated receptor $t_{1/2}$ = 18 min (Tran, Friedman et al. 2004; Tran, Friedman et al. 2007)	5.2
55	R31f: β2ARg Activation	40 /sec	Rates adjusted to achieve appropriate levels of basal active β2AR.	5.2
56	R31r: β2AR*g Inactivation	200 /sec		
57	R32f: β2ARpg Activation	40 /sec	Rates adjusted to achieve appropriate levels of basal active β2AR.	5.2
58	R32r: β2AR*pg Inactivation	200 /sec		
59	R33f: PKA Phosphorylation β2AR*g	[Fraction Active PKA]*83 sec^{-1}	(Tran, Friedman et al. 2004)	5.2
60	R33r: PKA Dephosphorylation β2AR*pg	0.036 sec^{-1}	Phosphorylated receptor $t_{1/2}$ = 18 min (Tran, Friedman et al. 2004; Tran, Friedman et al. 2007)	5.2

Table 5.1 (contd.) Parameters for the Unified PKA-/GRK-/PDE-Mediated β2AR Regulation Model

No.	Parameter Name	Value	Reference/Rationale	Fig. No.
61	R34: GRK Dephosphorylation β2ARg	0.036 sec^{-1}	Phosphorylated receptor $t_{1/2}$ = 18 min (Tran, Friedman et al. 2004; Tran, Friedman et al. 2007)	5.2
62	R35: GRK Dephosphorylation β2ARpg	0.036 sec^{-1}	Phosphorylated receptor $t_{1/2}$ = 18 min (Tran, Friedman et al. 2004; Tran, Friedman et al. 2007)	5.2
63	R36: GRK Dephosphorylation β2ARg	0.036 sec^{-1}	Phosphorylated receptor $t_{1/2}$ = 18 min (Tran, Friedman et al. 2004; Tran, Friedman et al. 2007)	5.2
64	R37: GRK Dephosphorylation β2ARpg	0.036 sec^{-1}	Phosphorylated receptor $t_{1/2}$ = 18 min (Tran, Friedman et al. 2004; Tran, Friedman et al. 2007)	5.2
65	R38f: L On β2AR*g	$14 \text{ µM}^{-1}.\text{sec}^{-1}$	Rates adjusted to achieve appropriate τ (Reiner, Ambrosio et al. 2010) and K_{ds} (Vayttaden, Friedman et al. 2010).	5.2
66	R38r: L Off L:β2AR*g	6.3 sec^{-1}		
67	R39f: L On β2AR*pg	$14 \text{ µM}^{-1}.\text{sec}^{-1}$	Rates adjusted to achieve appropriate τ (Reiner, Ambrosio et al. 2010) and K_{ds} (Vayttaden, Friedman et al. 2010).	5.2
68	R39r: L Off L:β2AR*pg	6.3 sec^{-1}		
69	R40f: β2AR Basal Internalisation	0.51 sec^{-1}	Rates used to match negligible basal internalisation (Morrison, Moore et al. 1996).	5.4
70	R40r: β2ARi Recycling	5.4 sec^{-1}	k_f = 0.09 /min (Tran, Friedman et al. 2004).	5.4
71	R41f: β2ARg Basal Internalisation	0.51 sec^{-1}	Rates used to match negligible basal internalisation (Morrison, Moore et al. 1996).	5.4
72	R41r: β2ARgi Recycling	5.4 sec^{-1}	k_f = 0.09 /min (Tran, Friedman et al. 2004).	5.4
73	R42f: β2ARp Basal Internalisation	0.51 sec^{-1}	Rates used to match negligible basal internalisation (Morrison, Moore et al. 1996).	5.4

Table 5.1 (contd.) Parameters for the Unified PKA-/GRK-/PDE-Mediated β2AR Regulation Model

No.	Parameter Name	Value	Reference/Rationale	Fig. No.
74	R42r: β2ARpi Recycling	5.4 sec^{-1}	k_f = 0.09 /min (Tran, Friedman et al. 2004).	5.4
75	R43f: β2ARpg Basal Internalisation	0.51 sec^{-1}	Rates used to match negligible basal internalisation (Morrison, Moore et al. 1996).	5.4
76	R43r: β2ARpgi Recycling	5.4 sec^{-1}	k_f = 0.09 /min (Tran, Friedman et al. 2004).	5.4
77	R44f: β2AR* Basal Internalisation	0.51 sec^{-1}	Rates used to match negligible basal internalisation (Morrison, Moore et al. 1996).	5.4
78	R44r: β2AR*i Recycling	5.4 sec^{-1}	k_f = 0.09 /min (Tran, Friedman et al. 2004).	5.4
79	R45f: β2AR*g Basal Internalisation	0.51 sec^{-1}	Rates used to match negligible basal internalisation (Morrison, Moore et al. 1996).	5.4
80	R45r: β2AR*gi Recycling	5.4 sec^{-1}	k_f = 0.09 /min (Tran, Friedman et al. 2004).	5.4
81	R46f: β2AR*p Basal Internalisation	0.51 sec^{-1}	Rates used to match negligible basal internalisation (Morrison, Moore et al. 1996).	5.4
82	R46r: β2AR*pi Recycling	5.4 sec^{-1}	k_f = 0.09 /min (Tran, Friedman et al. 2004).	5.4
83	R47f: β2AR*pg Basal Internalisation	0.51 sec^{-1}	Rates used to match negligible basal internalisation (Morrison, Moore et al. 1996).	5.4
84	R47r: β2AR*pgi Recycling	5.4 sec^{-1}	k_f = 0.09 /min (Tran, Friedman et al. 2004).	5.4
85	R48f: L:β2AR* Basal Internalisation	0.51 sec^{-1}	Rates used to match negligible basal internalisation (Morrison, Moore et al. 1996).	5.4
86	R48r: L:β2AR*i Recycling	5.4 sec^{-1}	k_f = 0.09 /min (Tran, Friedman et al. 2004).	5.4

Table 5.1 (contd.) Parameters for the Unified PKA-/GRK-/PDE-Mediated β2AR Regulation Model

No.	Parameter Name	Value	Reference/Rationale	Fig. No.
87	R49f: L:β2AR*g Basal Internalisation	0.51 sec^{-1}	Rates used to match negligible basal internalisation (Morrison, Moore et al. 1996).	5.4
88	R49r: L:β2AR*gi Recycling	5.4 sec^{-1}	k_f = 0.09 /min (Tran, Friedman et al. 2004).	5.4
89	R50f: L:β2AR*p Basal Internalisation	0.51 sec^{-1}	Rates used to match negligible basal internalisation (Morrison, Moore et al. 1996).	5.4
90	R50r: L:β2AR*pi Recycling	5.4 sec^{-1}	k_f = 0.09 /min (Tran, Friedman et al. 2004).	5.4
91	R51f: L:β2AR*pg Basal Internalisation	0.51 sec^{-1}	Rates used to match negligible basal internalisation (Morrison, Moore et al. 1996).	5.4
92	R51r: L:β2AR*pgi Recycling	5.4 sec^{-1}	k_f = 0.09 /min (Tran, Friedman et al. 2004).	5.4
93	R52f: Arr:β2ARg Basal Internalisation	0.51 sec^{-1}	Rates used to match negligible basal internalisation (Morrison, Moore et al. 1996).	5.4
94	R52r: Arr:β2ARgi Recycling	5.4 sec^{-1}	k_f = 0.09 /min (Tran, Friedman et al. 2004).	5.4
95	R53f: Arr:β2ARpg Basal Internalisation	0.51 sec^{-1}	Rates used to match negligible basal internalisation (Morrison, Moore et al. 1996).	5.4
96	R53r: Arr:β2ARpgi Recycling	5.4 sec^{-1}	k_f = 0.09 /min (Tran, Friedman et al. 2004).	5.4
97	R54f: Arr:β2AR*g Basal Internalisation	0.51 sec^{-1}	Rates used to match negligible basal internalisation (Morrison, Moore et al. 1996).	5.4
98	R54r: Arr:β2AR*gi Recycling	5.4 sec^{-1}	k_f = 0.09 /min (Tran, Friedman et al. 2004).	5.4
99	R55f: Arr:β2AR*pg Basal Internalisation	0.51 sec^{-1}	Rates used to match negligible basal internalisation (Morrison, Moore et al. 1996).	5.4

Table 5.1 (contd.) Parameters for the Unified PKA-/GRK-/PDE-Mediated β2AR Regulation Model

No.	Parameter Name	Value	Reference/Rationale	Fig. No.
100	R55r: Arr:β2AR*pgi Recycling	5.4 sec^{-1}	k_f = 0.09 /min (Tran, Friedman et al. 2004).	5.4
101	R56f: Arr:L:β2AR*g Internalisation	13.2 sec^{-1}	k_f = 0.22 /min (Tran, Friedman et al. 2004).	5.4
102	R56r: Arr:L:β2AR*gi Recycling	5.4 sec^{-1}	k_f = 0.09 /min (Tran, Friedman et al. 2004).	5.4
103	R57f: Arr:L:β2AR*pg Internalisation	13.2 sec^{-1}	k_f = 0.22 /min (Tran, Friedman et al. 2004).	5.4
104	R57r: Arr:L:β2AR*pgi Recycling	5.4 sec^{-1}	k_f = 0.09 /min (Tran, Friedman et al. 2004).	5.4
105	R58: Li Degradation	100 sec^{-1}	Catecholamine group should degrade rapidly. Arbitrarily set high to prevent persistent ligand rebinding post internalisation	5.4
106	R59: β2ARi Degradation	0.24 sec^{-1}	$t_{1/2}$ = 3-4 hours (Liang, Hoang et al. 2008)	5.4
107	R60: β2ARgi Degradation	0.24 sec^{-1}	$t_{1/2}$ = 3-4 hours (Liang, Hoang et al. 2008)	5.4
108	R61: β2ARpi Degradation	0.24 sec^{-1}	$t_{1/2}$ = 3-4 hours (Liang, Hoang et al. 2008)	5.4
109	R62: β2ARpgi Degradation	0.24 sec^{-1}	$t_{1/2}$ = 3-4 hours (Liang, Hoang et al. 2008)	5.4
110	R63: β2AR*i Degradation	0.24 sec^{-1}	$t_{1/2}$ = 3-4 hours (Liang, Hoang et al. 2008)	5.4
111	R64: β2AR*gi Degradation	0.24 sec^{-1}	$t_{1/2}$ = 3-4 hours (Liang, Hoang et al. 2008)	5.4
112	R65: β2AR*pi Degradation	0.24 sec^{-1}	$t_{1/2}$ = 3-4 hours (Liang, Hoang et al. 2008)	5.4
113	R66: β2AR*pgi Degradation	0.24 sec^{-1}	$t_{1/2}$ = 3-4 hours (Liang, Hoang et al. 2008)	5.4
114	R67: L:β2AR*i Degradation	0.24 sec^{-1}	$t_{1/2}$ = 3-4 hours (Liang, Hoang et al. 2008)	5.4

Table 5.1 (contd.) Parameters for the Unified PKA-/GRK-/PDE-Mediated β2AR Regulation Model

No.	Parameter Name	Value	Reference/Rationale	Fig. No.
115	R68: L:β2AR*gi Degradation	0.24 sec^{-1}	t$_{1/2}$ = 3-4 hours (Liang, Hoang et al. 2008)	5.4
116	R69: L:β2AR*pi Degradation	0.24 sec^{-1}	t$_{1/2}$ = 3-4 hours (Liang, Hoang et al. 2008)	5.4
117	R70: L:β2AR*pgi Degradation	0.24 sec^{-1}	t$_{1/2}$ = 3-4 hours (Liang, Hoang et al. 2008)	5.4
118	R71: Arr:β2ARgi Degradation	0.24 sec^{-1}	t$_{1/2}$ = 3-4 hours (Liang, Hoang et al. 2008)	5.4
119	R72: Arr:β2ARpgi Degradation	0.24 sec^{-1}	t$_{1/2}$ = 3-4 hours (Liang, Hoang et al. 2008)	5.4
120	R73: Arr:β2AR*gi Degradation	0.24 sec^{-1}	t$_{1/2}$ = 3-4 hours (Liang, Hoang et al. 2008)	5.4
121	R74: Arr:β2AR*pgi Degradation	0.24 sec^{-1}	t$_{1/2}$ = 3-4 hours (Liang, Hoang et al. 2008)	5.4
122	R75: Arr:L:β2AR*gi Degradation	0.24 sec^{-1}	t$_{1/2}$ = 3-4 hours (Liang, Hoang et al. 2008)	5.4
123	R76: Arr:L:β2AR*pgi Degradation	0.24 sec^{-1}	t$_{1/2}$ = 3-4 hours (Liang, Hoang et al. 2008)	5.4
124	R77f: β2ARi Activation	40 /sec	Rates adjusted to achieve appropriate levels of basal active β2AR.	5.5
125	R77r: β2AR*i Inactivation	200 /sec		
126	R78f: L On β2AR*i	14 µM^{-1}.sec^{-1}	Rates adjusted to achieve appropriate τ (Reiner, Ambrosio et al. 2010) and K$_{ds}$ (Vayttaden, Friedman et al. 2010).	5.5
127	R78r: L Off L:β2AR*i	6.3 sec^{-1}		
128	R79: GRK Dephosphorylation L:β2AR*gi	0.036 sec^{-1}	Phosphorylated receptor t$_{1/2}$ = 18 min (Tran, Friedman et al. 2004; Tran, Friedman et al. 2007)	5.5
129	R80f: Arrestin On L:β2AR*gi	1620 sec^{-1}	Rate of arrestin binding = 26.6 ± 5.9 /min (Krasel, Bunemann et al. 2005)	5.5

Table 5.1 (contd.) Parameters for the Unified PKA-/GRK-/PDE-Mediated β2AR Regulation Model

No.	Parameter Name	Value	Reference/Rationale	Fig. No.
130	R80r: Arrestin Off Arr:L:β2AR*gi	240 sec^{-1}	Rate of arrestin dissociation assumed to match measured K_d.	5.5
131	R81f: L On Arr:β2AR*gi	14 µM^{-1}.sec^{-1}	Rates adjusted to achieve appropriate τ (Reiner, Ambrosio et al. 2010) and K_{ds} (Vayttaden, Friedman et al. 2010).	5.5
132	R81r: L Off Arr:L:β2AR*gi	6.3 sec^{-1}		
133	R82f: Arr:β2ARgi Activation	40 /sec	Rates adjusted to achieve appropriate levels of basal active β2AR.	5.5
134	R82r: Arr:β2AR*gi Inactivation	200 /sec		
135	R83: Arrestin Off Arr:β2ARgi	660 sec^{-1}	Rate of arrestin dissociation = 10.86 ± 1.2 /min (Krasel, Bunemann et al. 2005).	5.5
136	R84: Arrestin Off Arr:β2AR*gi	660 sec^{-1}	Rate of arrestin dissociation = 10.86 ± 1.2 /min (Krasel, Bunemann et al. 2005).	5.5
137	R85f: L On β2AR*gi	14 µM^{-1}.sec^{-1}	Rates adjusted to achieve appropriate τ (Reiner, Ambrosio et al. 2010) and K_{ds} (Vayttaden, Friedman et al. 2010).	5.5
138	R85r: L Off L:β2AR*gi	6.3 sec^{-1}		
139	R86f: β2ARi Activation	40 /sec	Rates adjusted to achieve appropriate levels of basal active β2AR.	5.5
140	R86r: β2AR*i Inactivation	200 /sec		
141	R87: GRK Dephosphorylation β2ARgi	0.036 sec^{-1}	Phosphorylated receptor $t_{1/2}$ = 18 min (Tran, Friedman et al. 2004; Tran, Friedman et al. 2007)	5.5
142	R88: GRK Dephosphorylation β2AR*gi	0.036 sec^{-1}	Phosphorylated receptor $t_{1/2}$ = 18 min (Tran, Friedman et al. 2004; Tran, Friedman et al. 2007)	5.5
143	R89f: β2ARpi Activation	40 /sec	Rates adjusted to achieve appropriate levels of basal active β2AR.	5.5
144	R89r: β2AR*pi Inactivation	200 /sec		

153

Table 5.1 (contd.) Parameters for the Unified PKA-/GRK-/PDE-Mediated β2AR Regulation Model

No.	Parameter Name	Value	Reference/Rationale	Fig. No.
145	R90f: L On β2AR*pi	14 µM^{-1}.sec^{-1}	Rates adjusted to achieve appropriate τ (Reiner, Ambrosio et al. 2010) and K$_{ds}$ (Vayttaden, Friedman et al. 2010).	5.5
146	R90r: L Off L:β2AR*pi	6.3 sec^{-1}		
147	R91: GRK Dephosphorylation L:β2AR*pgi	0.036 sec^{-1}	Phosphorylated receptor t$_{1/2}$ = 18 min (Tran, Friedman et al. 2004; Tran, Friedman et al. 2007)	5.5
148	R92f: Arrestin On L:β2AR*pgi	1620 sec^{-1}	Rate of arrestin binding = 26.6 ± 5.9 /min (Krasel, Bunemann et al. 2005)	5.5
149	R92r: Arrestin Off Arr:L:β2AR*pgi	240 sec^{-1}	Rate of arrestin dissociation assumed to match measured K$_d$.	5.5
150	R93f: L On Arr:β2AR*pgi	14 µM^{-1}.sec^{-1}	Rates adjusted to achieve appropriate τ (Reiner, Ambrosio et al. 2010) and K$_{ds}$ (Vayttaden, Friedman et al. 2010).	5.5
151	R93r: L Off Arr:L:β2AR*pgi	6.3 sec^{-1}		
152	R94f: Arr:β2ARpgi Activation	40 /sec	Rates adjusted to achieve appropriate levels of basal active β2AR.	5.5
153	R94r: Arr:β2AR*pgi Inactivation	200 /sec		
154	R95: Arrestin Off Arr: β2ARpgi	660 sec^{-1}	Rate of arrestin dissociation = 10.86 ± 1.2 /min (Krasel, Bunemann et al. 2005).	5.2
155	R96: Arrestin Off Arr: β2AR*pgi	660 sec^{-1}	Rate of arrestin dissociation = 10.86 ± 1.2 /min (Krasel, Bunemann et al. 2005).	5.2
156	R97f: L On β2AR*pgi	14 µM^{-1}.sec^{-1}	Rates adjusted to achieve appropriate τ (Reiner, Ambrosio et al. 2010) and K$_{ds}$ (Vayttaden, Friedman et al. 2010).	5.5
157	R97r: L Off L:β2AR*pgi	6.3 sec^{-1}		
158	R98f: β2ARpgi Activation	40 /sec	Rates adjusted to achieve appropriate levels of basal active β2AR.	5.5
159	R98r: β2AR*pgi Inactivation	200 /sec		

Table 5.1 (contd.) Parameters for the Unified PKA-/GRK-/PDE-Mediated β2AR Regulation Model

No.	Parameter Name	Value	Reference/Rationale	Fig. No.
160	R99: GRK Dephosphorylation β2ARpgi	0.036 sec^{-1}	Phosphorylated receptor $t_{1/2}$ = 18 min (Tran, Friedman et al. 2004; Tran, Friedman et al. 2007)	5.5
161	R100: GRK Dephosphorylation β2AR*pgi	0.036 sec^{-1}	Phosphorylated receptor $t_{1/2}$ = 18 min (Tran, Friedman et al. 2004; Tran, Friedman et al. 2007)	5.5
162	R101: PKA Dephosphorylation β2ARpgi	0.036 sec^{-1}	Phosphorylated receptor $t_{1/2}$ = 18 min (Tran, Friedman et al. 2004; Tran, Friedman et al. 2007)	5.2
163	R102: PKA Dephosphorylation β2ARpi	0.036 sec^{-1}	Phosphorylated receptor $t_{1/2}$ = 18 min (Tran, Friedman et al. 2004; Tran, Friedman et al. 2007)	5.2
164	R103: PKA Dephosphorylation β2AR*pi	0.036 sec^{-1}	Phosphorylated receptor $t_{1/2}$ = 18 min (Tran, Friedman et al. 2004; Tran, Friedman et al. 2007)	5.2
165	R104: PKA Dephosphorylation β2AR*pgi	0.036 sec^{-1}	Phosphorylated receptor $t_{1/2}$ = 18 min (Tran, Friedman et al. 2004; Tran, Friedman et al. 2007)	5.2
166	R105: PKA Dephosphorylation L:β2AR*pi	0.036 sec^{-1}	Phosphorylated receptor $t_{1/2}$ = 18 min (Tran, Friedman et al. 2004; Tran, Friedman et al. 2007)	5.2
167	R106: PKA Dephosphorylation L:β2AR*pgi	0.036 sec^{-1}	Phosphorylated receptor $t_{1/2}$ = 18 min (Tran, Friedman et al. 2004; Tran, Friedman et al. 2007)	5.2

No.	Parameter Name	Value	Reference/Rationale	Fig. No.
	Table 5.1 (contd.) Parameters for the Unified PKA-/GRK-/PDE-Mediated β2AR Regulation Model			
168	$\beta2AR_{t=0;\ HASMs}$	1µM	Arbitrarily set (Xin, Tran et al. 2008). Need to lower to 0.003µM per my calculations	5.2
169	$\beta2AR_{t=0;\ HEK293s\ (over\ expression)}$	100µM	Arbitrarily set (Xin, Tran et al. 2008). Need to lower to 0.3µM per my calculations	5.2
170	$PDE_{t=0;\ HASMs\ /\ HEK293s\ (over\ expression)}$	1µM	Arbitrarily set (Xin, Tran et al. 2008).	5.3
171	$R2:C2_{t=0;\ HASMs\ /\ HEK293s\ (over\ expression)}$	1µM	(Xin, Tran et al. 2008).	5.3
172	$Gs:GDP_{t=0;\ HASMs\ /\ HEK293s\ (over\ expression)}$	4µM	(Xin, Tran et al. 2008).	5.3

5.1. Assumptions

5.1.1. Receptor Activation

I assumed a ligand-induced stabilisation model for β2AR activation. Here β2AR denotes the inactive receptor on the plasma membrane, β2AR* the spontaneously active receptor and L:β2AR, the agonist-induced stable active receptor. This was done to accommodate the differences in basal activity with varying receptor levels. The limitations of the two-state model are that it cannot account for ligand induced differential signalling or bias wherein a wide spectrum of receptor conformations is stabilised by different agonists to varying extents and thereby capable of differential signalling.

5.1.2. Ligand On/Off

The ligand binding rates were set in COPASI (COmplex PAthway SImulator) (Hoops, Sahle et al. 2006) to achieve appropriate $t_{1/2}$ of 47 msec for 10 µM epinephrine (Reiner, Ambrosio et al. 2010). Since we had an estimate of K_d for epinephrine to be ~ 450 nM (Vayttaden, Friedman et al. 2010) the off-rates were calculated to give the appropriate K_d. The on-rates of isoproterenol were assumed to be similar to epinephrine and then using a Kd of ~ 283 nM (Vayttaden, Friedman et al. 2010) appropriate off-rates were calculated.

5.1.3. Receptor Activity

In the current version of the model I have assumed only two receptor states – active or inactive. Contrary to the GRK-mediated β2AR regulation model

presented in chapter 3, I haven't considered intermediate receptor activity levels dependent on phosphorylation status. In its current version the model will not be able to capture the effects of PKA phosphorylation of the β2AR on desensitisation. This simplification was done to reduce the complexity of the model to capture first the effects of PKA-mediated PDE activation on treatment with 1 – 100 μM isoproterenol (c.f. Figure 4.11) since at these concentrations PKA phosphorylation of the β2AR would be saturated (Tran, Friedman et al. 2004). The effects of phosphorylation dependent variable receptor activity will have to be explored in later versions of the model. I also assume that arrestin binding and/or internalisation completely uncouples the receptor from Gαs and therefore these species have no activity.

5.1.4. β2AR-Phosphorylation Kinetics

In my model the rate of PKA phosphorylation is dependent on [C] which is the fraction of activated PKA. We've measured 0.01 – 100 nM epinephrine-induced PKA-mediated β2AR phosphorylation $t_{1/2}$ to ~ range from 1–2/min (Tran, Friedman et al. 2004). I assume that isoproterenol induced β2AR phosphorylation rates will be in the same range since epinephrine and isoproterenol have comparable efficacies.

I assumed that ligand activation of β2AR results in only a single event of GRK phosphorylation where both serines 355 and 356 are simultaneously phosphorylated. The anti-phosphosite antibody used in our β2AR phosphorylation studies detects only dual phosphorylation of serines 355, 356.

Use of our antibody for studying GRK-mediated β2AR phosphorylation kinetics has been validated by various groups (Tran, Friedman et al. 2004; Shenoy, Drake et al. 2006; Violin, Ren et al. 2006; Pontier, Percherancier et al. 2008; Woo, Wang et al. 2009). The disadvantage of this assumption is that it is no longer possible to project multi-phosphorylation states of the receptor that could play a role in receptor sorting post-internalisation selecting for recycling vs. receptor degradation. Also assuming a single phosphorylation event prevents assigning multiple phosphorylation site specific activities to the receptor, this could in turn affect the quality of simulation fits.

We've measured epinephrine-induced GRK-mediated β2AR phosphorylation to range from 0.7–1.4/min (Tran, Friedman et al. 2004). I assume that isoproterenol induced β2AR phosphorylation rates will be in the same range since epinephrine and isoproterenol have comparable efficacies.

We have previously shown that both the plasma membrane and endosomal fraction of β2AR can undergo dephosphorylation (Iyer, Tran et al. 2006; Tran, Friedman et al. 2007). Therefore I allow both plasma membrane and cytosolic dephosphorylation of β2AR in my model (c.f. Footnote of Table 3.1).

5.1.5. PKA Activation Kinetics

Generic PKA activation is modelled here through a series of 10 reactions. The kinetics of cAMP binding/unbinding to the PKA regulatory subunit and the rate of release and rebinding of catalytic subunit binding to the regulatory subunit of PKA in HASMs is assumed to match the rates determined using purified dimer

of regulatory subunit of PKA I from rabbit skeletal muscle (Doskeland and Ogreid 1984). These rates will have to be adjusted to match PKA activation in our cell lines as measured by PKA phosphorylation of the β2AR.

5.1.6. PDE Activation Kinetics

Generic PKA-mediated activation of PDE is modelled here through PKA phosphorylation of PDE and PDE dephosphorylation. The kinetics of these two reactions is arbitrarily set to match the cAMP kinetics observed in HEK293 cells overexpressing the C460W/E583M CNG channel (Xin, Tran et al. 2008). These rates will have to be adjusted to match cAMP levels in our cell lines in the presence and absence of PDE inhibitors.

5.1.7. Post-Internalisation Events

I have assumed that there is no PKA or GRK activity post-internalisation so no new phosphorylation is achieved post-internalisation. Consistent with the rapid on/off-rates and high K_ds of epinephrine or isoproterenol (Mueller, Motulsky et al. 1988; Devanathan, Yao et al. 2004) I assumed ligand dissociation post β2AR internalisation to be very rapid. We have previously shown negligible rates of basal β2AR internalisation (Morrison, Moore et al. 1996).

I allow arrestin-free internalised β2AR to recycle independent of its phosphorylation status (Tran, Friedman et al. 2007). Currently the precise mechanisms and pathways of β2AR downregulation are unclear even though we have shown it to be biphasic (Williams, Barber et al. 2000). Thus to simplify downregulation reactions in the model I assume that all internalised β2AR

species can undergo downregulation ($t_{1/2}$ = 3–4 hours) (Morrison, Moore et al. 1996; Williams, Barber et al. 2000; Liang, Hoang et al. 2008).

5.2. Model Validation

My unified model of GRK-/PKA-/PDE-mediated β2AR regulation has 167 reactions and 4 initial species. The model has currently been subjected to only phenomenological validation; extensive quantitative validation is required for this model as part of future works. Figure 5.6A shows the simulated results of 1 µM isoproterenol stimulation and figure 5.6B shows cAMP profile in HASMs on treatment with 1 µM isoproterenol.
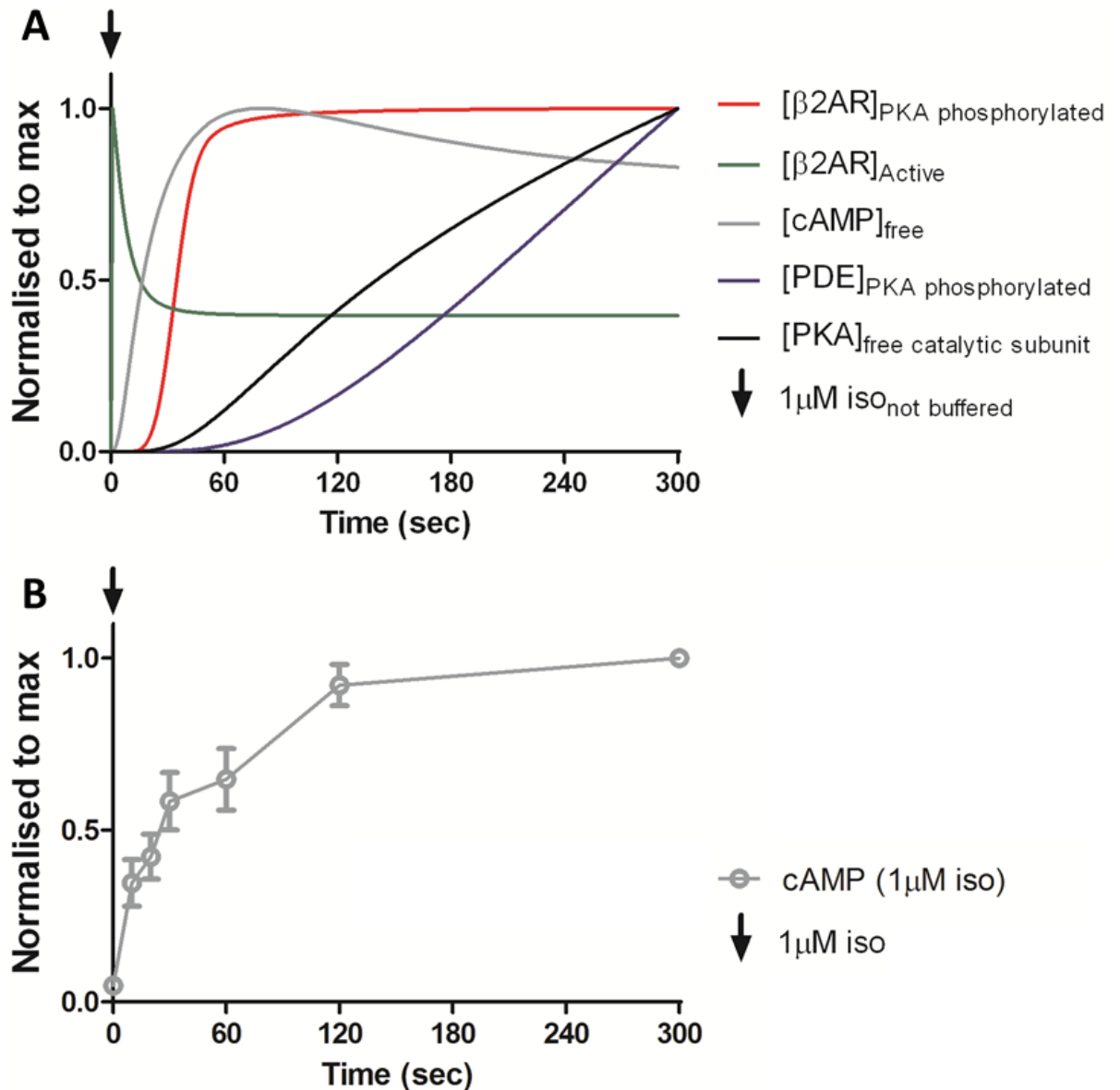
Figure 5.6 1 μM Isoproterenol Stimulation of HASMs

This reaction diagram shows the effect of treatment of HASM with 1 μM isoproterenol. **A)** Simulated profiles of: total PKA phosphorylated β2AR (red line); active β2AR (green line); free cAMP (grey line); PKA-activated PDE (blue line); free catalytic subunit of PKA (black line); $β2AR_{t0=1μM}$. **B)** cAMP in HASMs normalised to maximum levels obtained with 0-300 sec of 1 μM isoproterenol treatment.

The model shows that receptor activation is near instantaneous and transient. After a minute of stimulation, active receptor levels reach a steady state of roughly 50 % of maximal active levels. This is likely a modelling artifact on account of not considering intermediate receptor activity levels dependent on phosphorylation status and ignoring arrestin binding. Figure 3.2D clearly shows that 1μM isoproterenol treatment causes internalisation of close to 40 % of surface β2AR after minutes. Had I considered arrestin binding in these simulations then the active β2AR levels would have dropped close to zero within the first five minutes of treatment with 1μM isoproterenol. This simplification was done to reduce the complexity of the model to capture first the effects of β2AR-mediated AC activation on treatment within the first 5 minutes. We know that there is both a high-potency PKA-mediated desensitisation, and an occupancy-dependent desensitisation mediated by GRKs (Clark, Knoll et al. 1999). Seeing that we have maximal PKA phosphorylation of the receptor in a minute, there would be significant PKA-mediated desensitisation at the receptor level which is currently being ignored. Incorporating partial receptor activities based on phosphorylation status should lower the high steady state receptor activities. The fact that PKA phosphorylation reaches steady state within 1 minute is congruent with experimental observations that PKA phosphorylation of receptor reaches near steady state within 1-2 mins on treatment with 100 nM epinephrine (Tran, Friedman et al. 2004). The simulated PKA-phosphorylated PDE follows PKA activation. We don't have an experimental measure of PKA-phosphorylated PDE in our cell lines. The time course of PKA-phosphorylated β2AR and PKA-phosphorylated PDE don't match on account of the

different phosphorylation rates used in the model. The rate of PKA phosphorylation of the β2AR in our HEK293 cells that stably overexpress the β2AR is ~ 83/sec (Tran, Friedman et al. 2004). The rate of PKA phosphorylation of PDE in our cells is unknown. I used a rate of ~ 0.015/sec based on our previous models for the HEK293 cells (Xin, Tran et al. 2008). The rates of PDE phosphorylation will have to be adjusted to help match the experimental measured cAMP in response to varying concentrations of isoproterenol. The simulated cAMP profile reaches maximal levels in ~ 1 minute and the experimentally measured cAMP profile reaches maximal levels after about 2 minutes. The fact that simulated cAMP levels rise faster than our experimental measures could be because of one of two reasons (i) very high AC activity; and (ii) low basal PDE activity. This will have to be fine-tuned in future simulations. Inspite of this divergence from measured behaviour simulated cAMP levels at 5 min can be used to study the effects of varying receptor concentrations to mimic differences between HASMs and HEK293s that stably over express the β2AR.

5.3. Effect of Varying β2AR Levels

There is ~ 100-fold difference in β2AR levels between stable overexpressions in HEK293s and endogenous levels in HASMs (Clark and Knoll 2002). I've simulated in Figure 5.7 the effect of variation in receptor levels and of inhibiting GRK-/PKA-/PDE-modules when the GRK/arrestin modules are functioning properly.
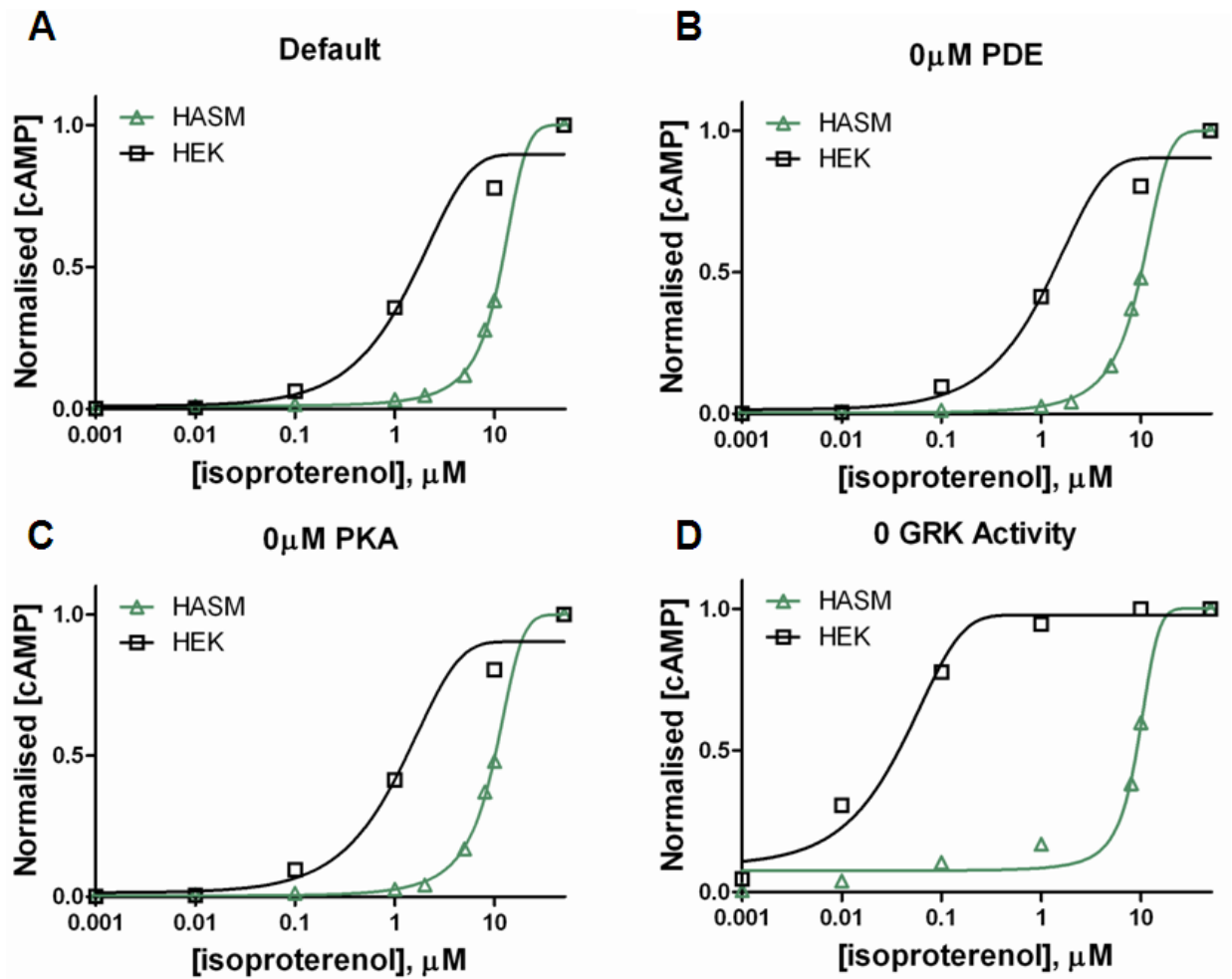
Figure 5.7 Effect of [β2AR] Variation in Unified Model Under Different Inhibition Protocols

This reaction diagram shows the simulated profiles of normalised cAMP in HASMs ($\beta2AR_{t=0}$ = 1 µM; green triangle/line) and HEK293s ($\beta2AR_{t=0}$ = 100 µM; black square/line). **(A)** Parameters as per Table 3.1; **(B)** $PDE_{t=0}$ = 0 µM; **(C)** $R2:C2_{t=0}$ = 0 µM; **(D)** GRK Phosphorylation Rate = 0 sec^{-1}.

As expected from Figure 5.6 basal PDE activity is very low in the model. Therefore inhibiting PDE by setting initial PDE concentrations to 0 µM does not affect cAMP at 5 min, hence Figure 5.7A and Figure 5.7B are same. Due to ignoring PKA effects on the receptor any PKA-mediated desensitisation is through PDE activation. Figure 5.6 shows that there is a delay in accumulation of catalytic subunit of PKA and PKA-phosphorylated PDE, because of this there won't be any significant effect of inhibiting PKA on the cAMP profile in the first 5 mins post-stimulus. Therefore Figure 5.7C will be same as Figure 5.7A. Post ligand treatment GRK phosphorylation of the receptor is a prerequisite for arrestin binding the receptor (Krasel, Bunemann et al. 2005). Arrestin binding to the receptor is rapid and assumed to completely uncouple the receptor from Gαs. Therefore in the absence of GRK phosphorylation there won't be any arrestin binding and arrestin-mediated desensitisation. Figure 5.7D shows that GRK-/arrestin-mediated β2AR desensitisation is the dominant mode of β2AR desensitisation in the over expression system.

5.4. Model Limitations

My model currently ignores effects of PKA mediated β2AR phosphorylation. Incorporation of variable receptor activity dependent upon phosphorylation status of the receptor is necessary to capture better the behaviour of the β2AR signaling machinery at low agonist concentrations. At high agonist concentrations GRK-phosphorylation of the β2AR leads to arrestin recruitment and complete uncoupling of the Gαs from the β2AR thereby reducing the β2AR coupling efficieny for Gs to zero

Currently the simulated AC activity is too high and basal PDE activity is too low and this leads to a faster peak in cAMP production. AC activity and basal PDE activity can be corrected while validating the model to cAMP profile ± PDE inhibitors.

The model of PDE-mediated β2AR regulation previously developed by our group (Xin, Tran et al. 2008) used arbitrary concentrations for β2AR levels in HASMs (1 µM) and HEK293s (100 µM). Estimates of local concentrations of membrane bound proteins are error-prone. One needs an estimate of the plasma membrane volume and assume point distribution of the protein of interest. My crude estimates (c.f. Equations 5.1 and 5.2) based on an ideal spherical cell and measured total protein levels in our cells put the receptor concentration at the ball park range of 0.003 µM for HASMs and 0.3 µM for HEK293s. I'll have to validate the model for cAMP profile ± PDE inhibitors for a range of receptor concentrations and verify if the simulated properties of overexpression are a function of absolute receptor concentrations or they are dependent upon the ratio of concentrations.

Given the preponderance of reactions (167!) in this model it is necessary to do a sensitivity analysis to help prune the model. Stoichiometric analysis will also help in reducing the number of receptor states in the model.

6. Conclusions and Future Work

The β2AR is a G-protein coupled receptor that activates smooth muscle relaxation through both cAMP-dependent and independent pathways (Katsuki and Murad 1977; Wong and Buckner 1978; Rinard, Rubinfeld et al. 1979; Zhou, Newsholme et al. 1992). Asthma is a chronic disease characterised by; 1) bronchial hyper-responsiveness which leads to increased contraction of the airway smooth muscles; 2) inflammation; and 3) airway remodelling. Due to its role in smooth muscle relaxation β-agonists are used in treatment of asthma and COPD (Connors, Dawson et al. 1996; Celli and MacNee 2004; Donohue 2004). Short acting β-agonists are used as a rescue agent to bring about immediate airway smooth muscle relaxation to relieve airway distress. Long acting β-agonists are used in combination with inhaled corticosteroids on a daily basis as a maintenance therapy to avoid recurrence of asthmatic episodes. The hallmark of these treatments is that they are only palliative and so they alleviate the symptom of airway distress and don't cure the underlying cause of the symptoms. Due to this, during asthma treatment regimen a patient is repeatedly exposed to the drugs. Excessive and prolonged use of β-agonists leads to tachyphylaxis – which is characterised by a tolerance or subsensitivity to the drug leading to the loss of both broncholdilatory (lung inflation post airway smooth muscle relaxation) and bronchoprotective (resistance to contraction on inhalation of a bronchioconstrictor) effects of the drug (Keighley 1966; Van Metre 1969; Davis and Conolly 1980; Sears 2002; Abramson, Walters et al. 2003). For β-agonists, tachyphylaxis occurs due to β-desensitisation and downregulation. In order to understand why clinical tachyphylaxis

happens in response to β-agonists it becomes necessary to understand agonist specific activation of the various β2AR desensitisation pathways. These studies are difficult and extremely time consuming to perform in vivo or in vitro on account of multiple isoforms and cross-reactions in signalling pathways. Our group's long-term goal has been to understand the regulatory mechanisms of the β2AR machinery in response to both short- and long-acting β-agonists. The ten models that I have developed and described in the previous chapters represent a significant advance toward this goal.

In Chapter 3 I have modelled the GRK/Arrestin module of the β2AR regulation as it pertains to experimental measures of agonist-induced GRK-mediated β2AR-phosphorylation, β2AR-dephosphorylation, -trafficking, -desensitisation and -resensitisation (Figure 3.1). Table 3.1 lists the parameters used to model and simulate the consensus GRK pathway in response to various agonists at different concentrations and durations. The data simulated were from 90+ independent experiments on our stable overexpressions of human β2AR in HEK 293 cells.

GRK and arrestin isoforms have been frequently targeted for overexpression or knockdown in different cells types (Ahn, Nelson et al. 2003; Penela, Ribas et al. 2003; Reiter and Lefkowitz 2006; Violin, Ren et al. 2006; Luo, Busillo et al. 2008). These proteins also differ in their overall expression levels and localisation (Zhang, Barak et al. 1997; Komori, Cain et al. 1998). They also undergo post-translational modifications (Lin, Krueger et al. 1997; Lin, Chen et al. 2002; Penela, Ribas et al. 2003; Shenoy, Drake et al. 2006). Given that there is wide variability in the level or activity of these two β2AR regulatory proteins in different cell types I was interested in the effect of this

variability on the modelling results. In Figure 3.7 I explored the effects of varying GRK phosphorylation and arrestin binding over a hundred-fold range around rates mentioned in Table 3.1 and plotted its effects on β2AR phosphorylation, desensitisation and internalisation over a 0–30 min time course.

The major discoveries from these computational analyses were that steady states of GRK phosphorylated β2AR were unaffected over hundred-fold variation in GRK phosphorylation rates (Figure 3.7 A-C) on treatment with saturating concentration (10 µM) of epinephrine. This pointed out a flaw in how most GRK overexpression and knockdown studies are performed. These usually tend to measure β2AR phosphorylation at steady state with saturating agonist concentrations; my model suggests that this would increase the risk of false negative results. A more exacting measure for the effects of GRK overexpression and knockdown experiments would be an estimate of the initial rates of GRK-mediated receptor phosphorylation at sub-saturating ligand concentrations.

I presented models to test various reaction topologies for GRK-mediated β2AR regulation. This was done since the possibility of cell surface dephosphorylation of the GRK phosphorylated β2AR and the recycling of the phosphorylated β2AR has been a contentious issue (Yu, Lefkowitz et al. 1993; Pippig, Andexinger et al. 1995; Krueger, Daaka et al. 1997; Iyer, Tran et al. 2006; Kelly 2006). Our group has shown that 1) blocking internalisation does not prevent β2AR dephosphorylation (Iyer, Tran et al. 2006), and 2) that β2AR dephosphorylation can occur even at undetectable levels of internalisation (Tran, Friedman et al. 2007). I have determined GRK site β2AR

dephosphorylation rates at the membrane to be ~0.04/min per method described in 2.1.1.

To investigate the effects of membrane dephosphorylation and phosphorylated receptor recycling I created six different models (Figure 3.9A-F) that vary different reactions as described in the footnote of Table 3.1. In Figure 3.9A I modelled our default reaction topology that allowed for both dephosphorylation of the receptor at the plasma membrane and phosphorylated receptor recycling. I contrasted this with Figure 3.9F where I modelled a reaction topology that did not allow for both plasma membrane dephosphorylation and recycling of phosphorylated receptor. This was in keeping with the prevalent view around early 2000s (Krupnick and Benovic 1998; Billington and Penn 2003). I showed that under these conditions the system failed to achieve more than 50% β2AR dephosphorylation which was discordant with our experimental measurements (Tran, Friedman et al. 2007). Increasing the cytosolic dephosphorylation rate did not help in rescuing the simulated dephosphorylation curves. Thus through modeling I was able to show that the prevalent model of early 2000s was not able to explain dephosphorylation measurements done in our lab. I further explored if random variations in β2AR dephosphorylation and recycling reaction topologies could explain our experimental results. Through my analyses using these models I clarified the necessity for β2AR dephosphorylation at the membrane and the recycling of the GRK phosphorylated receptor.

I further used the models described in Chapter 3 to explore the effects of various frequencies of agonist treatment since under physiological conditions based on the target tissue the β2AR "sees" different frequencies and amplitudes of stimuli. Synaptic

β2AR "sees" high norepinephrine concentrations in a pulsatile fashion (Trendelenburg, Gaiser et al. 1999; Stjarne 2000) due to the small synaptic volumes, rapid removal and reuptake of norepinephrine. In contrast to the synaptic stimuli, the bloodstream concentrations of agonist post epinephrine secretion from the adrenal gland are much lower but for relatively longer periods. The most exciting results from these computational analyses were that during pulsatile activation of the β2AR, the signalling machinery "remembered" prior exposure to an agonist and desensitised much more strongly on subsequent exposures (Figure 3.11A). This memory of prior stimuli could be attributed to the accumulation of the GRK phosphorylated β2AR due to slower dephosphorylation. In subsequent figures (Figure 3.12-3.13) I explored the basis of this cellular memory and showed (Figure 3.12B) that this memory was robust even after 2 hours of treatment. Thus this phenomenon could be responsible for the reduced drug efficacy on repeated use of short acting β-agonists.

After exploring short acting β-agonists in chapter 3 in chapter 4 I developed models of salmeterol action, a long acting β-agonist used in combination with inhaled corticosteroids during maintenance therapy of asthma. Briefly, salmeterol action has been explained by three models. Salmeterol is lipohilic and reversibly incorporates in the plasma membrane, resulting in a partition of drugs between a membrane and an aqueous phase (Rhodes, Newton et al. 1992). Due to membrane partitioning of salmeterol, the membrane can act as a salmeterol reservoir and this forms the basis of the **microkinetic model (MM)** (Anderson, Linden et al. 1994) (Figure 4.2). Due to the high membrane partitioning of salmeterol and its slow rate of release from the membrane, $t_{1/2}$ = 25 mins (synthetic membranes) – 3 hours (tracheal strips) (Rhodes,

Newton et al. 1992; Austin, Barton et al. 2003) it is posited that salmeterol reaches the

receptor by lateral diffusion through the membrane (Anderson, Linden et al. 1994)

since by the time salmeterol traverses the length of the airways to reach the target

bronchii it would have bound to the membrane on account of its lipophilicity.

Per the **exosite model (EM)** (Figure 4.4) the saligenin head of salmeterol (Figure 1.2)

and the hydrophobic phenylalkoxyalkyl side chain binds the β2AR at two spatially

distinct sites. The site of saligenin head binding is identified as the active site and the

site of hydrophobic phenylalkoxyalkyl side chain binding is called an exosite. In the

exosite model tethering of the phenylalkoxyalkyl chain to the exosite is quasi-

irreversible while the binding of the saligenin head to the active site is rapidly

reversible. This model also allows agonist or antagonist binding to the active site when

the exosite is occupied by salmeterol's hydrophobic tail (Figure 6.1). To allow the

flipping in and out of the saligenin head from the active site, the exosite has been

posited to be in the central core of the β2AR (Jack 1991). Both site directed

mutagenesis studies involving replacement of β2AR central domains with β1AR

(Green, Spasoff et al. 1996; Isogaya, Yamagiwa et al. 1998) and photoaffinity labeling

with [^{125}I]iodoazido-salmeterol (Rong, Arbabian et al. 1999) lend credence to the idea

that the exosite is further into the transmembrane domains toward the cytosol than the

active site.

The **rebinding model** posits that a high local concentration of salmeterol is

maintained on account of rapid rebinding (Szczuka, Wennerberg et al. 2009). This

model wouldn't be able to explain the reassertion phenomenon when a competing

ligand is present without invoking another mechanism to retain salmeterol in the vicinity of the receptor.

Given the importance of salmeterol in treating asthma and COPD I developed phenomenological models to describe the effects of membrane retention of salmeterol, exosite binding or a composite of the two **(combined model - CM)**. I then coupled these models to an adaptation of the GRK-mediated β2AR regulation model developed in Chapter 3 and then tested them to see if properties of salmeterol long action and reassertion still held true. Using these models I show (Figure 4.10A) that none of the three currently accepted models can sufficiently explain the long action of salmeterol or significantly reduced β2AR internalisation (Figure 4.10B) on treatment with saturating concentrations of salmeterol. It becomes necessary to invoke decreased arrestin affinity for salmeterol bound β2AR complex in order to simulate experimentally measured salmeterol-induced β2AR internalisation (Vayttaden, Friedman et al. 2010) and to rescue loss of long action to explain the long action of salmeterol (Figure 4.10C).

In Chapter 5 I described an alpha version of the unified model of GRK-/PKA-/PDE-mediated β2AR regulation. This model explores the effect of variation in receptor number (Figure 5.6). Once validated, this model will be an important tool to study the effects of various beta agonists on GRK- and PKA-mediated β2AR regulation in HASMs where the low receptor number makes phosphorylation experiments difficult. This model can eventually be used to discover the relative contribution of PKA, GRK, PDE, arrestin and internalisation to the total β2AR desensitisation on treatment with various beta agonists. This information in turn would be valuable in deciding what

desensitisation modules are best targeted pharmacologically for most effective use of individual beta agonists.

A well tested comprehensive model of β2AR regulation would aid in: (i) understanding tissue specific mechanistic differences in β2AR response; (ii) in-silico estimation of tachyphylaxis associated with prolonged use of different β2AR agonists; (iii) hypothesis testing and in-silico prediction of experimental results. Some of the future work planned to understand β2AR regulation is described below.

6.1. Salmeterol Models

The salmeterol models presented in Chapter 4 deals only with GRK-mediated β2AR regulation. Since the GRK-mediated β2AR phosphorylation profile at saturating salmeterol concentrations are similar to that obtained with about 50 nM isoproterenol, it is expected that PKA- and PDE-modules would be significant players in β2AR regulation. I need to expand the combined model (Model 9) representing salmeterol exosite, microkinetic and rebinding effects to include PKA- and PDE-mediated β2AR regulation.
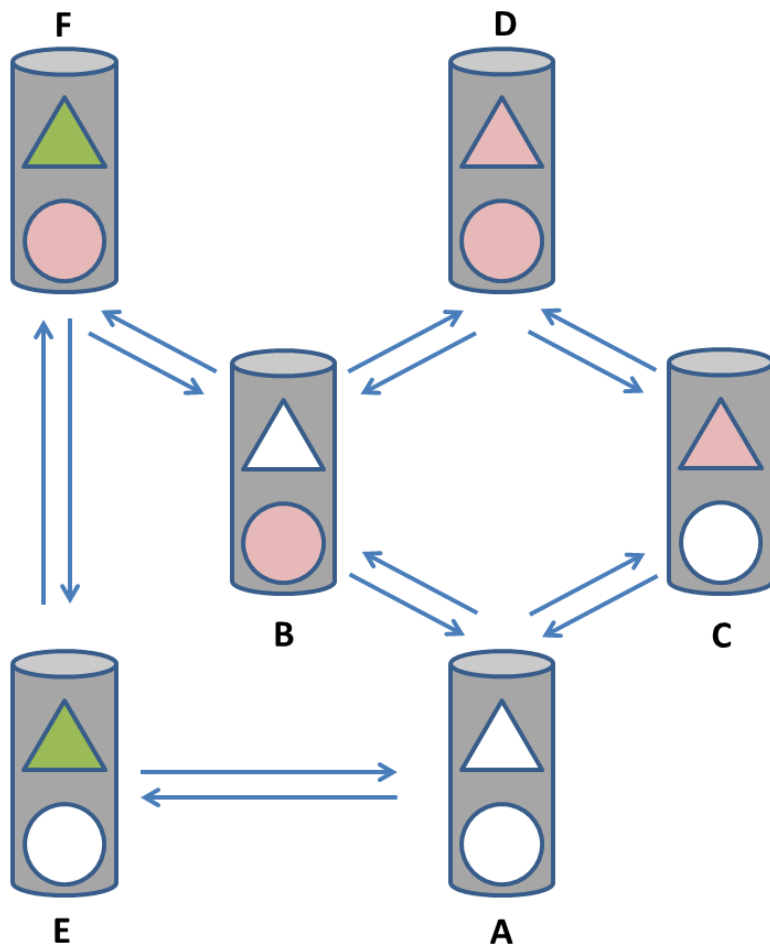
Figure 6.1 Model of Salmeterol Bitopic Action.

Grey cylinders = β2AR; white triangle = empty active site; white circle = empty exosite; green triangle = active site occupied by isoproterenol; red triangle = active site occupied by salmeterol; red circle = exosite occupied by salmeterol. A = naïve β2AR; B = salmeterol bound to an exosite on the β2AR; C = salmeterol bound to the active site on the β2AR; D = salmeterol bound to both the active- and exo-site on the β2AR; E = isoproterenol bound to the active site on the β2AR; F = β2AR having isoproterenol bound to the active site and salmeterol to the exosite.

Salmeterol is a bitopic ligand since it binds the β2AR both at an active site and an

exosite (Johnson, Butchers et al. 1993; Green, Spasoff et al. 1996; Isogaya,

Yamagiwa et al. 1998; Rong, Arbabian et al. 1999). In Figure 6.1 I have shown the

minimum number of β2AR states to accommodate isoproterenol and salmeterol

binding per the exosite model. In the interest of simplification, in the models

simulated in Chapter 4 I've ignored a β2AR state that has salmeterol bound only to

the active site with an empty exosite (state D in Figure 6.1) since I expect all

exosite to be occupied by salmeterol when β2AR is treated with saturating

concentrations of salmeterol for long periods of time. The number of β2AR states

now increases exponentially while allowing for GRK- and PKA-mediated β2AR

phosphorylation, arrestin binding and internalisation of the β2AR. Thus a unified

GRK-/PKA-/PDE-mediated β2AR regulation model that simulates salmeterol

exosite, microkinetic and rebinding effects is not easily tractable on account of an

exponential increase in receptor species. Such a model is best attempted after the

unified GRK-/PKA-/PDE-mediated β2AR regulation model for monotopic ligands as

described in Chapter 5 is well validated and constrained. Since salmeterol

treatment is for longer durations and it brings about negligible β2AR internalisation

I'd have to incorporate additional reactions to capture the β2AR degradation

kinetics.

6.2. GRK-/PKA-/PDE-Mediated Regulation

The model of GRK-/PKA-/PDE-mediated regulation of β2AR signalling described in Chapter 5 has 167 reactions. There are a few quality control measures that need to be taken. I need to do a stoichiometric state analysis to calculate mass conservation. Since my model is implemented in COPASI I'll be using the Householder reduction method (Householder 1958; Vallabhajosyula, Chickarmane et al. 2006). The model also needs to be subjected to sensitivity analysis similar to analysis done in Figures 2.5-6 and for cAMP profile. The results of the stoichiometric state analysis and sensitivity analysis will help determine if reactions need to be pruned.

Currently I have only done a rudimentary phenomenological validation of the model. I need to extend the model validation to a more exhaustive set of time course profiles that cover PKA- and GRK-mediated β2AR phosphorylation, cAMP profile (± PDE inhibitors ± propranolol), β2AR trafficking (internalisation and recycling), and β2AR activity (desensitisation and resensitisation) for different monotopic agonists and concentrations. Once the model has been well constrained through experimental validation, stoichiometric state analysis and sensitivity analysis I will use the model to predict the percent contribution of each regulatory module to total β2AR desensitisation.

6.3. β2AR and Pro-Inflammatory Signalling Pathway Crosstalk

Currently little is known about how salmeterol-mediated β2AR desensitisation pathways are altered with co-treatment of corticosteroids or under conditions of inflammation. The effect of corticosteroid and pro-inflammation mediated signalling on agonist induced β2AR desensitisation is important given that LABAs such as salmeterol are used clinically in asthmatic patients as a chronic medication in combination with inhaled corticosteroids. Recently, the Penn group has published data regarding the effect of PKA on the HASM transcriptome. They determined transcriptional changes using mRNA array technology following the introduction of a genetic inhibitor of PKA (GFP-PKI) under pro-inflammatory conditions and in the presence or absence of corticosteroids. A major finding of this study was that PKA is a critical modulator of the transcriptional changes induced by pro-inflammatory cytokines, particularly with regard to their promitogenic effects (Misior, Deshpande et al. 2009). They have also shown that corticosteroids can suppress β agonist-induced PKA activity thus inhibiting the mitogenic effects of cytokines (Misior, Yan et al. 2008) and that the anti-mitogenic effects of β-agonists (including salmeterol) are mediated by PKA (Yan, Deshpande et al. 2011). Modelling the crosstalk between salmeterol-mediated β2AR regulatory pathways and pro-inflammatory signalling pathways will have to be complemented with experiments. Salmeterol-mediated β2AR desensitisation will have to be measured in the presence of corticosteroid like fluticasone propionate in both naïve cells as well as under cytokine-mediated inflammatory conditions, to mimic signaling in the asthmatic airway. The application of these results to my quantitative model will provide a

more complete picture of how β2AR signaling functions in disease states and an improved understanding of β agonist mediated crosstalk with pro-inflammatory pathways.

7. Bibliography

Abramson, M. J., J. Walters, et al. (2003). "Adverse effects of beta-agonists: are they clinically relevant?" Am J Respir Med 2(4): 287-297.

Ahn, S., C. D. Nelson, et al. (2003). "Desensitization, internalization, and signaling functions of beta-arrestins demonstrated by RNA interference." Proc Natl Acad Sci U S A 100(4): 1740-1744.

Ahn, S., S. K. Shenoy, et al. (2004). "Differential kinetic and spatial patterns of beta-arrestin and G protein-mediated ERK activation by the angiotensin II receptor." J Biol Chem 279(34): 35518-35525.

Anderson, G. P. (1993). "Long acting inhaled beta-adrenoceptor agonists the comparative pharmacology of formoterol and salmeterol." Agents Actions Suppl 43: 253-269.

Anderson, G. P. (2006). "Current issues with beta2-adrenoceptor agonists: pharmacology and molecular and cellular mechanisms." Clin Rev Allergy Immunol 31(2-3): 119-130.

Anderson, G. P., A. Linden, et al. (1994). "Why are long-acting beta-adrenoceptor agonists long-acting?" Eur Respir J 7(3): 569-578.

Attwood, T. K. and J. B. Findlay (1994). "Fingerprinting G-protein-coupled receptors." Protein Eng 7(2): 195-203.

Austin, R. P., P. Barton, et al. (2003). "QSAR and the rational design of long-acting dual D2-receptor/beta 2-adrenoceptor agonists." J Med Chem 46(15): 3210-3220.

Azzi, M., P. G. Charest, et al. (2003). "Beta-arrestin-mediated activation of MAPK by inverse agonists reveals distinct active conformations for G protein-coupled receptors." Proc Natl Acad Sci U S A 100(20): 11406-11411.

Ball, D. I., R. T. Brittain, et al. (1991). "Salmeterol, a novel, long-acting beta 2-adrenoceptor agonist: characterization of pharmacological activity in vitro and in vivo." Br J Pharmacol 104(3): 665-671.

Barak, L. S., M. Tiberi, et al. (1994). "A highly conserved tyrosine residue in G protein-coupled receptors is required for agonist-mediated beta 2-adrenergic receptor sequestration." J Biol Chem 269(4): 2790-2795.

Barber, R., T. J. Goka, et al. (1992). "Positively cooperative cAMP phosphodiesterase attenuates cellular cAMP responses." Second Messengers Phosphoproteins 14(1-2): 77-97.

Barlic, J., J. D. Andrews, et al. (2000). "Regulation of tyrosine kinase activation and granule release through beta-arrestin by CXCRI." Nat Immunol 1(3): 227-233.

Beach, J. R., C. L. Young, et al. (1992). "A comparison of the speeds of action of salmeterol and salbutamol in reversing methacholine-induced bronchoconstriction." Pulm Pharmacol 5(2): 133-135.

Beaulieu, J. M., S. Marion, et al. (2008). "A beta-arrestin 2 signaling complex mediates lithium action on behavior." Cell 132(1): 125-136.

Beaulieu, J. M., T. D. Sotnikova, et al. (2005). "An Akt/beta-arrestin 2/PP2A signaling complex mediates dopaminergic neurotransmission and behavior." Cell 122(2): 261-273.

Benovic, J. L., H. Kuhn, et al. (1987). "Functional desensitization of the isolated beta-adrenergic receptor by the beta-adrenergic receptor kinase: potential role of an analog of the retinal protein arrestin (48-kDa protein)." Proc Natl Acad Sci U S A 84(24): 8879-8882.

Benovic, J. L., L. J. Pike, et al. (1985). "Phosphorylation of the mammalian beta-adrenergic receptor by cyclic AMP-dependent protein kinase. Regulation of the rate of receptor phosphorylation and dephosphorylation by agonist occupancy and effects on coupling of the receptor to the stimulatory guanine nucleotide regulatory protein." J Biol Chem 260(11): 7094-7101.

Benovic, J. L., R. H. Strasser, et al. (1986). "Beta-adrenergic receptor kinase: identification of a novel protein kinase that phosphorylates the agonist-occupied form of the receptor." Proc Natl Acad Sci U S A 83(9): 2797-2801.

Berg, K. A., S. Maayani, et al. (1998). "Effector pathway-dependent relative efficacy at serotonin type 2A and 2C receptors: evidence for agonist-directed trafficking of receptor stimulus." Mol Pharmacol 54(1): 94-104.

Bhalla, U. S. (2002). "Use of Kinetikit and GENESIS for modeling signaling pathways." Methods Enzymol 345: 3-23.

Bhattacharya, M., P. H. Anborgh, et al. (2002). "Beta-arrestins regulate a Ral-GDS Ral effector pathway that mediates cytoskeletal reorganization." Nat Cell Biol 4(8): 547-555.

Billington, C. K., S. K. Joseph, et al. (1999). "Modulation of human airway smooth muscle proliferation by type 3 phosphodiesterase inhibition." Am J Physiol 276(3 Pt 1): L412-419.

Billington, C. K., I. R. Le Jeune, et al. (2008). "A major functional role for phosphodiesterase 4D5 in human airway smooth muscle cells." Am J Respir Cell Mol Biol 38(1): 1-7.

Billington, C. K. and R. B. Penn (2003). "Signaling and regulation of G protein-coupled receptors in airway smooth muscle." Respir Res 4: 2.

Bingham, J., S. Sudarsanam, et al. (2006). "Profiling human phosphodiesterase genes and splice isoforms." Biochem Biophys Res Commun 350(1): 25-32.

Bjarnadottir, T. K., D. E. Gloriam, et al. (2006). "Comprehensive repertoire and phylogenetic analysis of the G protein-coupled receptors in human and mouse." Genomics 88(3): 263-273.

Black, J. L., B. G. Oliver, et al. (2009). "Molecular mechanisms of combination therapy with inhaled corticosteroids and long-acting beta-agonists." Chest 136(4): 1095-1100.

Bockaert, J. and J. P. Pin (1999). "Molecular tinkering of G protein-coupled receptors: an evolutionary success." EMBO J 18(7): 1723-1729.

Bohn, L. M., R. J. Lefkowitz, et al. (2002). "Differential mechanisms of morphine antinociceptive tolerance revealed in (beta)arrestin-2 knock-out mice." J Neurosci 22(23): 10494-10500.

Bohn, L. M., R. J. Lefkowitz, et al. (1999). "Enhanced morphine analgesia in mice lacking beta-arrestin 2." Science 286(5449): 2495-2498.

Bolger, G. B., A. McCahill, et al. (2003). "The unique amino-terminal region of the PDE4D5 cAMP phosphodiesterase isoform confers preferential interaction with beta-arrestins." J Biol Chem 278(49): 49230-49238.

Boswell-Smith, V., M. Cazzola, et al. (2006). "Are phosphodiesterase 4 inhibitors just more theophylline?" J Allergy Clin Immunol 117(6): 1237-1243.

Bouvier, M., W. P. Hausdorff, et al. (1988). "Removal of phosphorylation sites from the beta 2-adrenergic receptor delays onset of agonist-promoted desensitization." Nature 333(6171): 370-373.

Bower, J. M. and D. Beeman (2007). "Constructing realistic neural simulations with GENESIS." Methods Mol Biol 401: 103-125.

Bresnahan, S. J., J. L. Borowitz, et al. (1975). "Some steric factors affecting smooth muscle relaxation by cAMP analogs." Arch Int Pharmacodyn Ther 218(2): 180-185.

Brindley, D. N. and D. W. Waggoner (1996). "Phosphatidate phosphohydrolase and signal transduction." Chem Phys Lipids 80(1-2): 45-57.

Broadley, K. J. (1999). "Review of mechanisms involved in the apparent differential desensitization of beta1- and beta2-adrenoceptor-mediated functional responses." J Auton Pharmacol 19(6): 335-345.

Brondello, J. M., A. Brunet, et al. (1997). "The dual specificity mitogen-activated protein kinase phosphatase-1 and -2 are induced by the p42/p44MAPK cascade." J Biol Chem 272(2): 1368-1376.

Bruynzeel, P. L. (1984). "Changes in the beta-adrenergic system due to beta-adrenergic therapy: clinical consequences." Eur J Respir Dis Suppl 135: 62-71.

Bruynzeel, P. L., H. Meurs, et al. (1985). "Some fundamental points concerning the clinical aspects of desensitization." Bull Eur Physiopathol Respir 21(5): 45s-52s.

Camps, M., A. Carozzi, et al. (1992). "Isozyme-selective stimulation of phospholipase C-beta 2 by G protein beta gamma-subunits." Nature 360(6405): 684-686.

Cazzola, M., S. Picciolo, et al. (2011). "Roflumilast in chronic obstructive pulmonary disease: evidence from large trials." Expert Opin Pharmacother 11(3): 441-449.

Celli, B. R. and W. MacNee (2004). "Standards for the diagnosis and treatment of patients with COPD: a summary of the ATS/ERS position paper." Eur Respir J 23(6): 932-946.

Cherezov, V., D. M. Rosenbaum, et al. (2007). "High-resolution crystal structure of an engineered human beta2-adrenergic G protein-coupled receptor." Science 318(5854): 1258-1265.

Chong, J., P. Poole, et al. (2011). "Phosphodiesterase 4 inhibitors for chronic obstructive pulmonary disease." Cochrane Database Syst Rev(5): CD002309.

Choo-Kang, Y. F., W. T. Simpson, et al. (1969). "Controlled comparison of the bronchodilator effects of three beta-adrenergic stimulant drugs administered by inhalation to patients with asthma." Br Med J 2(5652): 287-289.

Clark, R. B., C. Allal, et al. (1996). "Stable activation and desensitization of beta 2-adrenergic receptor stimulation of adenylyl cyclase by salmeterol: evidence for quasi-irreversible binding to an exosite." Mol Pharmacol 49(1): 182-189.

Clark, R. B., J. Friedman, et al. (1987). "Beta-adrenergic receptor desensitization of wild-type but not cyc lymphoma cells unmasked by submillimolar Mg2+." FASEB J 1(4): 289-297.

Clark, R. B. and B. J. Knoll (2002). "Measurement of receptor desensitization and internalization in intact cells." Methods Enzymol 343: 506-529.

Clark, R. B., B. J. Knoll, et al. (1999). "Partial agonists and G protein-coupled receptor desensitization." Trends Pharmacol Sci 20(7): 279-286.

Clark, R. B., M. W. Kunkel, et al. (1988). "Activation of cAMP-dependent protein kinase is required for heterologous desensitization of adenylyl cyclase in S49 wild-type lymphoma cells." Proc Natl Acad Sci U S A 85(5): 1442-1446.

Conner, D. A., M. A. Mathier, et al. (1997). "beta-Arrestin1 knockout mice appear normal but demonstrate altered cardiac responses to beta-adrenergic stimulation." Circ Res 81(6): 1021-1026.

Connors, A. F., Jr., N. V. Dawson, et al. (1996). "Outcomes following acute exacerbation of severe chronic obstructive lung disease. The SUPPORT investigators (Study to Understand Prognoses and Preferences for Outcomes and Risks of Treatments)." Am J Respir Crit Care Med 154(4 Pt 1): 959-967.

Conti, M., W. Richter, et al. (2003). "Cyclic AMP-specific PDE4 phosphodiesterases as critical components of cyclic AMP signaling." J Biol Chem 278(8): 5493-5496.

Conway, B. R., L. K. Minor, et al. (1999). "Quantification of G-Protein Coupled Receptor Internatilization Using G-Protein Coupled Receptor-Green Fluorescent Protein Conjugates with the ArrayScantrade mark High-Content Screening System." J Biomol Screen 4(2): 75-86.

Cooper, P., R. Kurten, et al. (2011). "Formoterol and salmeterol induce a similar degree of beta(2) -adrenoceptor tolerance in human small airways but via different mechanisms." Br J Pharmacol 163(3): 521-532.

Cowie, R. L., L. P. Boulet, et al. (2007). "Tolerability of a salmeterol xinafoate/fluticasone propionate hydrofluoroalkane metered-dose inhaler in adolescent and adult patients with persistent asthma: a 52-week, open-label, stratified, parallel-group, multicenter study." Clin Ther 29(7): 1390-1402.

Davis, C. and M. E. Conolly (1980). "Tachyphylaxis to beta-adrenoceptor agonists in human bronchial smooth muscle: studies in vitro." Br J Clin Pharmacol 10(5): 417-423.

DeFea, K. A., Z. D. Vaughn, et al. (2000). "The proliferative and antiapoptotic effects of substance P are facilitated by formation of a beta -arrestin-dependent scaffolding complex." Proc Natl Acad Sci U S A 97(20): 11086-11091.

DeFea, K. A., J. Zalevsky, et al. (2000). "beta-arrestin-dependent endocytosis of proteinase-activated receptor 2 is required for intracellular targeting of activated ERK1/2." J Cell Biol 148(6): 1267-1281.

Deshpande, D. A. and R. B. Penn (2006). "Targeting G protein-coupled receptor signaling in asthma." Cell Signal 18(12): 2105-2120.

Devanathan, S., Z. Yao, et al. (2004). "Plasmon-waveguide resonance studies of ligand binding to the human beta 2-adrenergic receptor." Biochemistry 43(11): 3280-3288.

Donohue, J. F. (2004). "Therapeutic responses in asthma and COPD. Bronchodilators." Chest 126(2 Suppl): 125S-137S; discussion 159S-161S.

Doskeland, S. O. and D. Ogreid (1984). "Characterization of the interchain and intrachain interactions between the binding sites of the free regulatory moiety of protein kinase I." J Biol Chem 259(4): 2291-2301.

Drake, M. T., J. D. Violin, et al. (2008). "beta-arrestin-biased agonism at the beta2-adrenergic receptor." J Biol Chem 283(9): 5669-5676.

Duringer, C., G. Grundstrom, et al. (2009). "Agonist-specific patterns of beta 2-adrenoceptor responses in human airway cells during prolonged exposure." Br J Pharmacol 158(1): 169-179.

Ferguson, S. S., W. E. Downey, 3rd, et al. (1996). "Role of beta-arrestin in mediating agonist-promoted G protein-coupled receptor internalization." Science 271(5247): 363-366.

Flower, D. R. (1999). "Modelling G-protein-coupled receptors for drug design." Biochim Biophys Acta 1422(3): 207-234.

Francis, S. H., B. D. Noblett, et al. (1988). "Relaxation of vascular and tracheal smooth muscle by cyclic nucleotide analogs that preferentially activate purified cGMP-dependent protein kinase." Mol Pharmacol 34(4): 506-517.

Gardella, T. J., M. D. Luck, et al. (1996). "Inverse agonism of amino-terminally truncated parathyroid hormone (PTH) and PTH-related peptide (PTHrP) analogs revealed with constitutively active mutant PTH/PTHrP receptors." Endocrinology 137(9): 3936-3941.

Gardner, B., Z. F. Liu, et al. (2001). "The role of phosphorylation/dephosphorylation in agonist-induced desensitization of D1 dopamine receptor function: evidence for a novel pathway for receptor dephosphorylation." Mol Pharmacol 59(2): 310-321.

Gesty-Palmer, D., M. Chen, et al. (2006). "Distinct beta-arrestin- and G protein-dependent pathways for parathyroid hormone receptor-stimulated ERK1/2 activation." J Biol Chem 281(16): 10856-10864.

Gesty-Palmer, D., H. El Shewy, et al. (2005). "beta-Arrestin 2 expression determines the transcriptional response to lysophosphatidic acid stimulation in murine embryo fibroblasts." J Biol Chem 280(37): 32157-32167.

Gesty-Palmer, D. and L. M. Luttrell (2008). "Heptahelical terpsichory. Who calls the tune?" J Recept Signal Transduct Res 28(1-2): 39-58.

Giembycz, M. A. and J. Diamond (1990). "Partial characterization of cyclic AMP-dependent protein kinases in guinea-pig lung employing the synthetic heptapeptide substrate, kemptide. In vitro sensitivity of the soluble enzyme to isoprenaline, forskolin, methacholine and leukotriene D4." Biochem Pharmacol 39(8): 1297-1312.

Gilman, A. G. (1987). "G proteins: transducers of receptor-generated signals." Annu Rev Biochem 56: 615-649.

GlaxoSmithKline. (2008). "Advair Hfa (fluticasone propionate and salmeterol xinafoate) Aerosol, Metered

[GlaxoSmithKline] "   Retrieved Sept 28, 2011, 2011, from http://dailymed.nlm.nih.gov/dailymed/archives/fdaDrugInfo.cfm?archiveid=8926.

Goldberg, N. D., R. F. O'Dea, et al. (1973). "Cyclic GMP." Adv Cyclic Nucleotide Res 3: 155-223.

Green, S. A., A. P. Spasoff, et al. (1996). "Sustained activation of a G protein-coupled receptor via "anchored" agonist binding. Molecular localization of the salmeterol exosite within the 2-adrenergic receptor." J Biol Chem 271(39): 24029-24035.

Guldberg, C. M. (1864). ""Concerning the Laws of Chemical Affinity"." Forhandlinger i Videnskabs-Selskabet i Christiania

Gurevich, V. V. and J. L. Benovic (1993). "Visual arrestin interaction with rhodopsin. Sequential multisite binding ensures strict selectivity toward light-activated phosphorylated rhodopsin." J Biol Chem 268(16): 11628-11638.

Gurevich, V. V., S. B. Dion, et al. (1995). "Arrestin interactions with G protein-coupled receptors. Direct binding studies of wild type and mutant arrestins with rhodopsin, beta 2-adrenergic, and m2 muscarinic cholinergic receptors." J Biol Chem 270(2): 720-731.

Gurevich, V. V., R. Pals-Rylaarsdam, et al. (1997). "Agonist-receptor-arrestin, an alternative ternary complex with high agonist affinity." J Biol Chem 272(46): 28849-28852.

Hansen, G., S. Jin, et al. (2000). "Absence of muscarinic cholinergic airway responses in mice deficient in the cyclic nucleotide phosphodiesterase PDE4D." Proc Natl Acad Sci U S A 97(12): 6751-6756.

Hanson, S. M. and V. V. Gurevich (2006). "The differential engagement of arrestin surface charges by the various functional forms of the receptor." J Biol Chem 281(6): 3458-3462.

Hardman, J. G., G. A. Robison, et al. (1971). "Cyclic nucleotides." Annu Rev Physiol 33: 311-336.

Harris, A. L., M. J. Connell, et al. (1989). "Role of low Km cyclic AMP phosphodiesterase inhibition in tracheal relaxation and bronchodilation in the guinea pig." J Pharmacol Exp Ther 251(1): 199-206.

Hausdorff, W. P., M. Bouvier, et al. (1989). "Phosphorylation sites on two domains of the beta 2-adrenergic receptor are involved in distinct pathways of receptor desensitization." J Biol Chem 264(21): 12657-12665.

Heaslip, R. J., F. R. Giesa, et al. (1987). "Co-regulation of tracheal tone by cyclic AMP- and cyclic GMP-dependent mechanisms." J Pharmacol Exp Ther 243(3): 1018-1026.

Hertel, C. and J. P. Perkins (1984). "Receptor-specific mechanisms of desensitization of beta-adrenergic receptor function." Mol Cell Endocrinol 37(3): 245-256.

Hirsch, J. A., C. Schubert, et al. (1999). "The 2.8 A crystal structure of visual arrestin: a model for arrestin's regulation." Cell 97(2): 257-269.

Holgate, S. T., C. J. Baldwin, et al. (1977). "beta-adrenergic agonist resistance in normal human airways." Lancet 2(8034): 375-377.

Holloway, A. C., H. Qian, et al. (2002). "Side-chain substitutions within angiotensin II reveal different requirements for signaling, internalization, and phosphorylation of type 1A angiotensin receptors." Mol Pharmacol 61(4): 768-777.

Hoops, S., S. Sahle, et al. (2006). "COPASI--a COmplex PAthway SImulator." Bioinformatics 22(24): 3067-3074.

Householder, A. S. (1958). "Unitary Triangularization of a Nonsymmetric Matrix." Journal of the ACM 5(4).

Houslay, M. D., G. S. Baillie, et al. (2007). "cAMP-Specific phosphodiesterase-4 enzymes in the cardiovascular system: a molecular toolbox for generating compartmentalized cAMP signaling." Circ Res 100(7): 950-966.

Hu, A., G. Nino, et al. (2008). "Prolonged heterologous beta2-adrenoceptor desensitization promotes proasthmatic airway smooth muscle function via PKA/ERK1/2-mediated phosphodiesterase-4 induction." Am J Physiol Lung Cell Mol Physiol 294(6): L1055-1067.

Huang, J., Y. Sun, et al. (2004). "Distinct roles for Src tyrosine kinase in beta2-adrenergic receptor signaling to MAPK and in receptor internalization." J Biol Chem 279(20): 21637-21642.

Isogaya, M., Y. Yamagiwa, et al. (1998). "Identification of a key amino acid of the beta2-adrenergic receptor for high affinity binding of salmeterol." Mol Pharmacol 54(4): 616-622.

Iyer, V., T. M. Tran, et al. (2006). "Differential phosphorylation and dephosphorylation of beta2-adrenoceptor sites Ser262 and Ser355,356." Br J Pharmacol 147(3): 249-259.

Jack, D. (1991). "The 1990 Lilly Prize Lecture. A way of looking at agonism and antagonism: lessons from salbutamol, salmeterol and other beta-adrenoceptor agonists." Br J Clin Pharmacol 31(5): 501-514.

Janssen, L. J., T. Tazzeo, et al. (2004). "KCl evokes contraction of airway smooth muscle via activation of RhoA and Rho-kinase." Am J Physiol Lung Cell Mol Physiol 287(4): L852-858.

January, B., A. Seibold, et al. (1997). "beta2-adrenergic receptor desensitization, internalization, and phosphorylation in response to full and partial agonists." J Biol Chem 272(38): 23871-23879.

Jelsema, C. L. and J. Axelrod (1987). "Stimulation of phospholipase A2 activity in bovine rod outer segments by the beta gamma subunits of transducin and its inhibition by the alpha subunit." Proc Natl Acad Sci U S A 84(11): 3623-3627.

Johnson, M., P. R. Butchers, et al. (1993). "The pharmacology of salmeterol." Life Sci 52(26): 2131-2143.

Johnston, C. A. and D. P. Siderovski (2007). "Receptor-mediated activation of heterotrimeric G-proteins: current structural insights." Mol Pharmacol 72(2): 219-230.

Jones, B. W. and P. M. Hinkle (2005). "Beta-arrestin mediates desensitization and internalization but does not affect dephosphorylation of the thyrotropin-releasing hormone receptor." J Biol Chem 280(46): 38346-38354.

Jones, T. R., L. Charette, et al. (1993). "Interaction of iberiotoxin with beta-adrenoceptor agonists and sodium nitroprusside on guinea pig trachea." J Appl Physiol 74(4): 1879-1884.

Joost, P. and A. Methner (2002). "Phylogenetic analysis of 277 human G-protein-coupled receptors as a tool for the prediction of orphan receptor ligands." Genome Biol 3(11): RESEARCH0063.

Katsuki, S. and F. Murad (1977). "Regulation of adenosine cyclic 3',5'-monophosphate and guanosine cyclic 3',5'-monophosphate levels and contractility in bovine tracheal smooth muscle." Mol Pharmacol 13(2): 330-341.

Keighley, J. F. (1966). "Iatrogenic asthma associated with adrenergic aerosols." Ann Intern Med 65(5): 985-995.

Keith, D. E., S. R. Murray, et al. (1996). "Morphine activates opioid receptors without causing their rapid internalization." J Biol Chem 271(32): 19021-19024.

Kelly, E. (2006). "G-protein-coupled receptor dephosphorylation at the cell surface." Br J Pharmacol 147(3): 235-236.

Kenakin, T. (2002). "Drug efficacy at G protein-coupled receptors." Annu Rev Pharmacol Toxicol 42: 349-379.

Kobilka, B. K., C. MacGregor, et al. (1987). "Functional activity and regulation of human beta 2-adrenergic receptors expressed in Xenopus oocytes." J Biol Chem 262(32): 15796-15802.

Koenig, J. A. and J. M. Edwardson (1997). "Endocytosis and recycling of G protein-coupled receptors." Trends Pharmacol Sci 18(8): 276-287.

Kolakowski, L. F., Jr. (1994). "GCRDb: a G-protein-coupled receptor database." Receptors Channels 2(1): 1-7.

Komori, N., S. D. Cain, et al. (1998). "Differential expression of alternative splice variants of beta-arrestin-1 and -2 in rat central nervous system and peripheral tissues." Eur J Neurosci 10(8): 2607-2616.

Krasel, C., M. Bunemann, et al. (2005). "Beta-arrestin binding to the beta2-adrenergic receptor requires both receptor phosphorylation and receptor activation." J Biol Chem 280(10): 9528-9535.

Kristiansen, K. (2004). "Molecular mechanisms of ligand binding, signaling, and regulation within the superfamily of G-protein-coupled receptors: molecular modeling and mutagenesis approaches to receptor structure and function." Pharmacol Ther 103(1): 21-80.

Krueger, K. M., Y. Daaka, et al. (1997). "The role of sequestration in G protein-coupled receptor resensitization. Regulation of beta2-adrenergic receptor dephosphorylation by vesicular acidification." J Biol Chem 272(1): 5-8.

Krupnick, J. G. and J. L. Benovic (1998). "The role of receptor kinases and arrestins in G protein-coupled receptor regulation." Annu Rev Pharmacol Toxicol 38: 289-319.

Kurrasch-Orbaugh, D. M., V. J. Watts, et al. (2003). "Serotonin 5-hydroxytryptamine 2A receptor-coupled phospholipase C and phospholipase A2 signaling pathways have different receptor reserves." J Pharmacol Exp Ther 304(1): 229-237.

Lapetina, E. G. and R. H. Michell (1973). "A membrane-bound activity catalysing phosphatidylinositol breakdown to 1,2-diacylglycerol, D-myoinositol 1:2-cyclic phosphate an D-myoinositol 1-phosphate. Properties and subcellular distribution in rat cerebral cortex." Biochem J 131(3): 433-442.

Le Jeune, I. R., M. Shepherd, et al. (2002). "Cyclic AMP-dependent transcriptional up-regulation of phosphodiesterase 4D5 in human airway smooth muscle cells. Identification and characterization of a novel PDE4D5 promoter." J Biol Chem 277(39): 35980-35989.

Liang, W., Q. Hoang, et al. (2008). "Accelerated dephosphorylation of the beta2-adrenergic receptor by mutation of the C-terminal lysines: effects on ubiquitination, intracellular trafficking, and degradation." Biochemistry 47(45): 11750-11762.

Lim, S., A. Jatakanon, et al. (2000). "Comparison of high dose inhaled steroids, low dose inhaled steroids plus low dose theophylline, and low dose inhaled steroids alone in chronic asthma in general practice." Thorax 55(10): 837-841.

Lin, F. T., W. Chen, et al. (2002). "Phosphorylation of beta-arrestin2 regulates its function in internalization of beta(2)-adrenergic receptors." Biochemistry 41(34): 10692-10699.

Lin, F. T., K. M. Krueger, et al. (1997). "Clathrin-mediated endocytosis of the beta-adrenergic receptor is regulated by phosphorylation/dephosphorylation of beta-arrestin1." J Biol Chem 272(49): 31051-31057.

Liu, G., J. Shi, et al. (2004). "Assembly of a Ca2+-dependent BK channel signaling complex by binding to beta2 adrenergic receptor." EMBO J 23(11): 2196-2205.

Lohse, M. J., S. Andexinger, et al. (1992). "Receptor-specific desensitization with purified proteins. Kinase dependence and receptor specificity of beta-arrestin and arrestin in the beta 2-adrenergic receptor and rhodopsin systems." J Biol Chem 267(12): 8558-8564.

Lohse, M. J., J. L. Benovic, et al. (1990). "Multiple pathways of rapid beta 2-adrenergic receptor desensitization. Delineation with specific inhibitors." J Biol Chem 265(6): 3202-3211.

Lohse, M. J., J. L. Benovic, et al. (1990). "beta-Arrestin: a protein that regulates beta-adrenergic receptor function." Science 248(4962): 1547-1550.

Lohse, M. J., R. J. Lefkowitz, et al. (1989). "Inhibition of beta-adrenergic receptor kinase prevents rapid homologous desensitization of beta 2-adrenergic receptors." Proc Natl Acad Sci U S A 86(9): 3011-3015.

Lombardi, D., B. Cuenoud, et al. (2009). "Lipid membrane interactions of indacaterol and salmeterol: do they influence their pharmacological properties?" Eur J Pharm Sci 38(5): 533-547.

Loza, M. J. and R. B. Penn (2010). "Regulation of T cells in airway disease by beta-agonist." Front Biosci (Schol Ed) 2: 969-979.

Luo, J., J. M. Busillo, et al. (2008). "M3 muscarinic acetylcholine receptor-mediated signaling is regulated by distinct mechanisms." Mol Pharmacol 74(2): 338-347.

Luttrell, L. M., S. S. Ferguson, et al. (1999). "Beta-arrestin-dependent formation of beta2 adrenergic receptor-Src protein kinase complexes." Science 283(5402): 655-661.

Luttrell, L. M. and T. P. Kenakin (2011). "Refining efficacy: allosterism and bias in g protein-coupled receptor signaling." Methods Mol Biol 756: 3-35.

Luttrell, L. M., F. L. Roudabush, et al. (2001). "Activation and targeting of extracellular signal-regulated kinases by beta-arrestin scaffolds." Proc Natl Acad Sci U S A 98(5): 2449-2454.

Markham, A. and B. Jarvis (2000). "Inhaled salmeterol/fluticasone propionate combination: a review of its use in persistent asthma." Drugs 60(5): 1207-1233.

Maudsley, S., B. Martin, et al. (2005). "The origins of diversity and specificity in g protein-coupled receptor signaling." J Pharmacol Exp Ther 314(2): 485-494.

McCrea, K. E. and S. J. Hill (1993). "Salmeterol, a long-acting beta 2-adrenoceptor agonist mediating cyclic AMP accumulation in a neuronal cell line." Br J Pharmacol 110(2): 619-626.

McCrea, K. E. and S. J. Hill (1996). "Comparison of duration of agonist action at beta 1- and beta 2- adrenoceptors in C6 glioma cells: evidence that the long duration of action of salmeterol is specific to the beta 2-adrenoceptor." Mol Pharmacol 49(5): 927-937.

McDonald, N. A., C. M. Henstridge, et al. (2007). "An essential role for constitutive endocytosis, but not activity, in the axonal targeting of the CB1 cannabinoid receptor." Mol Pharmacol 71(4): 976-984.

McDonald, P. H., C. W. Chow, et al. (2000). "Beta-arrestin 2: a receptor-regulated MAPK scaffold for the activation of JNK3." Science 290(5496): 1574-1577.

McKeage, K. and S. J. Keam (2009). "Salmeterol/fluticasone propionate: a review of its use in asthma." Drugs 69(13): 1799-1828.

Mehats, C., S. L. Jin, et al. (2003). "PDE4D plays a critical role in the control of airway smooth muscle contraction." FASEB J 17(13): 1831-1841.

Menard, L., S. S. Ferguson, et al. (1997). "Synergistic regulation of beta2-adrenergic receptor sequestration: intracellular complement of beta-adrenergic receptor kinase and beta-arrestin determine kinetics of internalization." Mol Pharmacol 51(5): 800-808.

Milano, S. K., Y. M. Kim, et al. (2006). "Nonvisual arrestin oligomerization and cellular localization are regulated by inositol hexakisphosphate binding." J Biol Chem 281(14): 9812-9823.

Misior, A. M., D. A. Deshpande, et al. (2009). "Glucocorticoid- and protein kinase A-dependent transcriptome regulation in airway smooth muscle." Am J Respir Cell Mol Biol 41(1): 24-39.

Misior, A. M., H. Yan, et al. (2008). "Mitogenic effects of cytokines on smooth muscle are critically dependent on protein kinase A and are unmasked by steroids and cyclooxygenase inhibitors." Mol Pharmacol 73(2): 566-574.

Mohammad, S., G. Baldini, et al. (2007). "Constitutive traffic of melanocortin-4 receptor in Neuro2A cells and immortalized hypothalamic neurons." J Biol Chem 282(7): 4963-4974.

Moore, C. A., S. K. Milano, et al. (2007). "Regulation of receptor trafficking by GRKs and arrestins." Annu Rev Physiol 69: 451-482.

Moore, R. H., E. E. Millman, et al. (2007). "Salmeterol stimulation dissociates beta2-adrenergic receptor phosphorylation and internalization." Am J Respir Cell Mol Biol 36(2): 254-261.

Morrison, D. L., J. S. Sanghera, et al. (1996). "Phosphorylation and activation of smooth muscle myosin light chain kinase by MAP kinase and cyclin-dependent kinase-1." Biochem Cell Biol 74(4): 549-557.

Morrison, K. J., R. H. Moore, et al. (1996). "Repetitive endocytosis and recycling of the beta 2-adrenergic receptor during agonist-induced steady state redistribution." Mol Pharmacol 50(3): 692-699.

Mueller, H., H. J. Motulsky, et al. (1988). "The potency and kinetics of the beta-adrenergic receptors on human neutrophils." Mol Pharmacol 34(3): 347-353.

Napoli, S. A., C. A. Gruetter, et al. (1980). "Relaxation of bovine coronary arterial smooth muscle by cyclic GMP, cyclic AMP and analogs." J Pharmacol Exp Ther 212(3): 469-473.

Nelson, C. D., S. J. Perry, et al. (2007). "Targeting of diacylglycerol degradation to M1 muscarinic receptors by beta-arrestins." Science 315(5812): 663-666.

Nelson, H. S. (2001). "Advair: combination treatment with fluticasone propionate/salmeterol in the treatment of asthma." J Allergy Clin Immunol 107(2): 398-416.

Nelson, H. S., S. T. Weiss, et al. (2006). "The Salmeterol Multicenter Asthma Research Trial: a comparison of usual pharmacotherapy for asthma or usual pharmacotherapy plus salmeterol." Chest 129(1): 15-26.

Nials, A. T., D. I. Ball, et al. (1994). "Formoterol on airway smooth muscle and human lung mast cells: a comparison with salbutamol and salmeterol." Eur J Pharmacol 251(2-3): 127-135.

Nials, A. T., R. A. Coleman, et al. (1993). "Effects of beta-adrenoceptor agonists in human bronchial smooth muscle." Br J Pharmacol 110(3): 1112-1116.

Nino, G., A. Hu, et al. (2009). "Mechanism regulating proasthmatic effects of prolonged homologous beta2-adrenergic receptor desensitization in airway smooth muscle." Am J Physiol Lung Cell Mol Physiol 297(4): L746-757.

Nobles, K. N., K. Xiao, et al. (2011). "Distinct Phosphorylation Sites on the {beta}2-Adrenergic Receptor Establish a Barcode That Encodes Differential Functions of {beta}-Arrestin." Sci Signal 4(185): ra51.

Oakley, R. H., S. A. Laporte, et al. (2000). "Differential affinities of visual arrestin, beta arrestin1, and beta arrestin2 for G protein-coupled receptors delineate two major classes of receptors." J Biol Chem 275(22): 17201-17210.

Overington, J. P., B. Al-Lazikani, et al. (2006). "How many drug targets are there?" Nat Rev Drug Discov 5(12): 993-996.

Palczewski, K. (1997). "GTP-binding-protein-coupled receptor kinases--two mechanistic models." Eur J Biochem 248(2): 261-269.

Palczewski, K., T. Kumasaka, et al. (2000). "Crystal structure of rhodopsin: A G protein-coupled receptor." Science 289(5480): 739-745.

Palmqvist, M., G. Persson, et al. (1997). "Inhaled dry-powder formoterol and salmeterol in asthmatic patients: onset of action, duration of effect and potency." Eur Respir J 10(11): 2484-2489.

Pan, L., E. V. Gurevich, et al. (2003). "The nature of the arrestin x receptor complex determines the ultimate fate of the internalized receptor." J Biol Chem 278(13): 11623-11632.

Paterson, J. W., R. J. Evans, et al. (1971). "SElectivity of broncholidlator action of salbutamol in asthmatic patients." Br J Dis Chest 65(1): 21-38.

Penela, P., C. Ribas, et al. (2003). "Mechanisms of regulation of the expression and function of G protein-coupled receptor kinases." Cell Signal 15(11): 973-981.

Perry, S. J., G. S. Baillie, et al. (2002). "Targeting of cyclic AMP degradation to beta 2-adrenergic receptors by beta-arrestins." Science 298(5594): 834-836.

Pierce, K. L., L. M. Luttrell, et al. (2001). "New mechanisms in heptahelical receptor signaling to mitogen activated protein kinase cascades." Oncogene 20(13): 1532-1539.

Pierce, K. L., S. Maudsley, et al. (2000). "Role of endocytosis in the activation of the extracellular signal-regulated kinase cascade by sequestering and nonsequestering G protein-coupled receptors." Proc Natl Acad Sci U S A 97(4): 1489-1494.

Pippig, S., S. Andexinger, et al. (1995). "Sequestration and recycling of beta 2-adrenergic receptors permit receptor resensitization." Mol Pharmacol 47(4): 666-676.

Pontier, S. M., Y. Percherancier, et al. (2008). "Cholesterol-dependent separation of the beta2-adrenergic receptor from its partners determines signaling efficacy: insight into nanoscale organization of signal transduction." J Biol Chem 283(36): 24659-24672.

Price, D. M., C. L. Chik, et al. (2004). "Mitogen-activated protein kinase phosphatase-1 (MKP-1): >100-fold nocturnal and norepinephrine-induced changes in the rat pineal gland." FEBS Lett 577(1-2): 220-226.

Prichard, B. N. and B. Tomlinson (1986). "The additional properties of beta adrenoceptor blocking drugs." J Cardiovasc Pharmacol 8 Suppl 4: S1-15.

Qian, Y., E. Naline, et al. (1993). "Effects of rolipram and siguazodan on the human isolated bronchus and their interaction with isoprenaline and sodium nitroprusside." Br J Pharmacol 109(3): 774-778.

Rabe, K. F. (2011). "Update on roflumilast, a phosphodiesterase 4 inhibitor for the treatment of chronic obstructive pulmonary disease." Br J Pharmacol 163(1): 53-67.

Rall, T. W. and E. W. Sutherland (1962). "Adenyl cyclase. II. The enzymatically catalyzed formation of adenosine 3',5'-phosphate and inorganic pyrophosphate from adenosine triphosphate." J Biol Chem 237: 1228-1232.

Rasmussen, S. G., H. J. Choi, et al. (2007). "Crystal structure of the human beta2 adrenergic G-protein-coupled receptor." Nature 450(7168): 383-387.

Reiner, S., M. Ambrosio, et al. (2010). "Differential signaling of the endogenous agonists at the beta2-adrenergic receptor." J Biol Chem 285(46): 36188-36198.

Reiter, E. and R. J. Lefkowitz (2006). "GRKs and beta-arrestins: roles in receptor silencing, trafficking and signaling." Trends Endocrinol Metab 17(4): 159-165.

Rennard, S. I. (2004). "Treatment of stable chronic obstructive pulmonary disease." Lancet 364(9436): 791-802.

Rhodes, D. G., R. Newton, et al. (1992). "Equilibrium and kinetic studies of the interactions of salmeterol with membrane bilayers." Mol Pharmacol 42(4): 596-602.

Rinard, G. A., A. R. Rubinfeld, et al. (1979). "Depressed cyclic AMP levels in airways smooth muscle from asthmatic dogs." Proc Natl Acad Sci U S A 76(3): 1472-1476.

Rong, Y., M. Arbabian, et al. (1999). "Probing the salmeterol binding site on the beta 2-adrenergic receptor using a novel photoaffinity ligand, [(125)I]iodoazidosalmeterol." Biochemistry 38(35): 11278-11286.

Rosenbaum, D. M., V. Cherezov, et al. (2007). "GPCR engineering yields high-resolution structural insights into beta2-adrenergic receptor function." Science 318(5854): 1266-1273.

Roth, N. S., P. T. Campbell, et al. (1991). "Comparative rates of desensitization of beta-adrenergic receptors by the beta-adrenergic receptor kinase and the cyclic AMP-dependent protein kinase." Proc Natl Acad Sci U S A 88(14): 6201-6204.

Saucerman, J. J., L. L. Brunton, et al. (2003). "Modeling beta-adrenergic control of cardiac myocyte contractility in silico." J Biol Chem 278(48): 47997-48003.

Scarselli, M. and J. G. Donaldson (2009). "Constitutive internalization of G protein-coupled receptors and G proteins via clathrin-independent endocytosis." J Biol Chem 284(6): 3577-3585.

Schramm, C. M., S. T. Chuang, et al. (1995). "cAMP generation inhibits inositol 1,4,5-trisphosphate binding in rabbit tracheal smooth muscle." Am J Physiol 269(5 Pt 1): L715-719.

Schutter, E. d. (2001). Computational neuroscience : realistic modeling for experimentalists. Boca Raton, Fla., CRC Press.

Sears, M. R. (2002). "Adverse effects of beta-agonists." J Allergy Clin Immunol 110(6 Suppl): S322-328.

Seibold, A., B. G. January, et al. (1998). "Desensitization of beta2-adrenergic receptors with mutations of the proposed G protein-coupled receptor kinase phosphorylation sites." J Biol Chem 273(13): 7637-7642.

Seibold, A., B. Williams, et al. (2000). "Localization of the sites mediating desensitization of the beta(2)-adrenergic receptor by the GRK pathway." Mol Pharmacol 58(5): 1162-1173.

Shenoy, S. K., M. T. Drake, et al. (2006). "beta-arrestin-dependent, G protein-independent ERK1/2 activation by the beta2 adrenergic receptor." J Biol Chem 281(2): 1261-1273.

Shenoy, S. K., P. H. McDonald, et al. (2001). "Regulation of receptor fate by ubiquitination of activated beta 2-adrenergic receptor and beta-arrestin." Science 294(5545): 1307-1313.

Sher, E. and F. Clementi (1985). "Correlation between agonist potency, desensitization and internalization of beta adrenergic receptors in a muscle cell line." Pharmacol Res Commun 17(12): 1095-1108.

Sibley, D. R., J. L. Benovic, et al. (1987). "Regulation of transmembrane signaling by receptor phosphorylation." Cell 48(6): 913-922.

Sibley, D. R., R. H. Strasser, et al. (1986). "Phosphorylation/dephosphorylation of the beta-adrenergic receptor regulates its functional coupling to adenylate cyclase and subcellular distribution." Proc Natl Acad Sci U S A 83(24): 9408-9412.

Sitkauskiene, B. and R. Sakalauskas (2005). "The role of beta(2)-adrenergic receptors in inflammation and allergy." Curr Drug Targets Inflamm Allergy 4(2): 157-162.

Sneddon, W. B., C. E. Magyar, et al. (2004). "Ligand-selective dissociation of activation and internalization of the parathyroid hormone (PTH) receptor: conditional efficacy of PTH peptide fragments." Endocrinology 145(6): 2815-2823.

Soderling, S. H. and J. A. Beavo (2000). "Regulation of cAMP and cGMP signaling: new phosphodiesterases and new functions." Curr Opin Cell Biol 12(2): 174-179.

Song, X., S. Coffa, et al. (2009). "How does arrestin assemble MAPKs into a signaling complex?" J Biol Chem 284(1): 685-695.

Spencer, C. M. and B. Jarvis (1999). "Salmeterol/fluticasone propionate combination." Drugs 57(6): 933-940; discussion 941-933.

Spina, D. (2008). "PDE4 inhibitors: current status." Br J Pharmacol 155(3): 308-315.

Stadel, J. M., P. Nambi, et al. (1983). "Catecholamine-induced desensitization of turkey erythrocyte adenylate cyclase is associated with phosphorylation of the beta-adrenergic receptor." Proc Natl Acad Sci U S A 80(11): 3173-3177.

Stjarne, L. (2000). "Do sympathetic nerves release noradrenaline in "quanta"?" J Auton Nerv Syst 81(1-3): 236-243.

Sullivan, P., S. Bekir, et al. (1994). "Anti-inflammatory effects of low-dose oral theophylline in atopic asthma." Lancet 343(8904): 1006-1008.

Sutherland, E. W., T. W. Rall, et al. (1962). "Adenyl cylase. I. Distribution, preparation, and properties." J Biol Chem 237: 1220-1227.

Sutherland, E. W. and G. A. Robison (1966). "The role of cyclic-3',5'-AMP in responses to catecholamines and other hormones." Pharmacol Rev 18(1): 145-161.

Szczuka, A., M. Wennerberg, et al. (2009). "Molecular mechanisms for the persistent bronchodilatory effect of the beta 2-adrenoceptor agonist salmeterol." Br J Pharmacol 158(1): 183-194.

Tang, W. J. and A. G. Gilman (1991). "Type-specific regulation of adenylyl cyclase by G protein beta gamma subunits." Science 254(5037): 1500-1503.

Tian, L., L. S. Coghill, et al. (2004). "Distinct stoichiometry of BKCa channel tetramer phosphorylation specifies channel activation and inhibition by cAMP-dependent protein kinase." Proc Natl Acad Sci U S A 101(32): 11897-11902.

Tohgo, A., K. L. Pierce, et al. (2002). "beta-Arrestin scaffolding of the ERK cascade enhances cytosolic ERK activity but inhibits ERK-mediated transcription following angiotensin AT1a receptor stimulation." J Biol Chem 277(11): 9429-9436.

Tolkovsky, A. M. and A. Levitzki (1981). "Theories and predictions of models describing sequential interactions between the receptor, the GTP regulatory unit, and the catalytic unit of hormone dependent adenylate cyclases." J Cyclic Nucleotide Res 7(3): 139-150.

Torphy, T. J., W. B. Freese, et al. (1982). "Cyclic nucleotide-dependent protein kinases in airway smooth muscle." J Biol Chem 257(19): 11609-11616.

Torphy, T. J., B. J. Undem, et al. (1993). "Identification, characterization and functional role of phosphodiesterase isozymes in human airway smooth muscle." J Pharmacol Exp Ther 265(3): 1213-1223.

Torphy, T. J., H. L. Zhou, et al. (1991). "Role of cyclic nucleotide phosphodiesterase isozymes in intact canine trachealis." Mol Pharmacol 39(3): 376-384.

Touretzky, D. S. (1989). Advances in neural information processing systems. San Mateo, CA, Morgan Kaufmann Publishers: v.

Tran, T. M., J. Friedman, et al. (2007). "Characterization of beta2-adrenergic receptor dephosphorylation: Comparison with the rate of resensitization." Mol Pharmacol 71(1): 47-60.

Tran, T. M., J. Friedman, et al. (2004). "Characterization of agonist stimulation of cAMP-dependent protein kinase and G protein-coupled receptor kinase phosphorylation of the beta2-adrenergic receptor using phosphoserine-specific antibodies." Mol Pharmacol 65(1): 196-206.

Tran, T. M., R. Jorgensen, et al. (2007). "Phosphorylation of the beta2-adrenergic receptor in plasma membranes by intrinsic GRK5." Biochemistry 46(50): 14438-14449.

Trendelenburg, A. U., E. G. Gaiser, et al. (1999). "Mouse postganglionic sympathetic neurons: primary culturing and noradrenaline release." J Neurochem 73(4): 1431-1438.

Trester-Zedlitz, M., A. Burlingame, et al. (2005). "Mass spectrometric analysis of agonist effects on posttranslational modifications of the beta-2 adrenoceptor in mammalian cells." Biochemistry 44(16): 6133-6143.

Vallabhajosyula, R. R., V. Chickarmane, et al. (2006). "Conservation analysis of large biochemical networks." Bioinformatics 22(3): 346-353.

Van Metre, T. E., Jr. (1969). "Adverse effects of inhalation of excessive amounts of nebulized isoproterenol in status asthmaticus." J Allergy 43(2): 101-113.

Vaughan, D. J., E. E. Millman, et al. (2006). "Role of the G protein-coupled receptor kinase site serine cluster in beta2-adrenergic receptor internalization, desensitization, and beta-arrestin translocation." J Biol Chem 281(11): 7684-7692.

Vayttaden, S. J. and U. S. Bhalla (2004). "Developing complex signaling models using GENESIS/Kinetikit." Sci STKE 2004(219): pl4.

Vayttaden, S. J., J. Friedman, et al. (2010). "Quantitative modeling of GRK-mediated beta2AR regulation." PLoS Comput Biol 6(1): e1000647.

Violin, J. D., L. M. DiPilato, et al. (2008). "beta2-adrenergic receptor signaling and desensitization elucidated by quantitative modeling of real time cAMP dynamics." J Biol Chem 283(5): 2949-2961.

Violin, J. D. and R. J. Lefkowitz (2007). "Beta-arrestin-biased ligands at seven-transmembrane receptors." Trends Pharmacol Sci 28(8): 416-422.

Violin, J. D., X. R. Ren, et al. (2006). "G-protein-coupled receptor kinase specificity for beta-arrestin recruitment to the beta2-adrenergic receptor revealed by fluorescence resonance energy transfer." J Biol Chem 281(29): 20577-20588.

Vishnivetskiy, S. A., J. A. Hirsch, et al. (2002). "Transition of arrestin into the active receptor-binding state requires an extended interdomain hinge." J Biol Chem 277(46): 43961-43967.

Vishnivetskiy, S. A., C. L. Paz, et al. (1999). "How does arrestin respond to the phosphorylated state of rhodopsin?" J Biol Chem 274(17): 11451-11454.

Vishnivetskiy, S. A., C. Schubert, et al. (2000). "An additional phosphate-binding element in arrestin molecule. Implications for the mechanism of arrestin activation." J Biol Chem 275(52): 41049-41057.

Vroling, B., M. Sanders, et al. (2011). "GPCRDB: information system for G protein-coupled receptors." Nucleic Acids Res 39(Database issue): D309-319.

Waage, P. (1864). ""Experiments for Determining the Affinity Law"." Forhandlinger i Videnskabs-Selskabet i Christiania.

Waage, P. and C. M. Guldberg (1864). ""Studies Concerning Affinity"."
Forhandlinger: Videnskabs-Selskabet i Christiana

Waage, P. and C. M. Guldberg. (2000 (Translation)). "Studies Concerning Affinity."
2011, from http://chimie.scola.ac-
paris.fr/sitedechimie/hist_chi/text_origin/guldberg_waage/Concerning-Affinity.htm.

Wei, H., S. Ahn, et al. (2004). "Stable interaction between beta-arrestin 2 and
angiotensin type 1A receptor is required for beta-arrestin 2-mediated activation of
extracellular signal-regulated kinases 1 and 2." J Biol Chem 279(46): 48255-48261.

Wei, H., S. Ahn, et al. (2003). "Independent beta-arrestin 2 and G protein-mediated
pathways for angiotensin II activation of extracellular signal-regulated kinases 1
and 2." Proc Natl Acad Sci U S A 100(19): 10782-10787.

Weinberger, M. and L. Hendeles (1996). "Theophylline in asthma." N Engl J Med
334(21): 1380-1388.

Whaley, B. S., N. Yuan, et al. (1994). "Differential expression of the beta-
adrenergic receptor modifies agonist stimulation of adenylyl cyclase: a quantitative
evaluation." Mol Pharmacol 45(3): 481-489.

Whistler, J. L. and M. von Zastrow (1998). "Morphine-activated opioid receptors
elude desensitization by beta-arrestin." Proc Natl Acad Sci U S A 95(17): 9914-
9919.

Williams, B. R., R. Barber, et al. (2000). "Kinetic analysis of agonist-induced down-regulation of the beta(2)-adrenergic receptor in BEAS-2B cells reveals high- and low-affinity components." Mol Pharmacol 58(2): 421-430.

Wisler, J. W., S. M. DeWire, et al. (2007). "A unique mechanism of beta-blocker action: carvedilol stimulates beta-arrestin signaling." Proc Natl Acad Sci U S A 104(42): 16657-16662.

Witherow, D. S., T. R. Garrison, et al. (2004). "beta-Arrestin inhibits NF-kappaB activity by means of its interaction with the NF-kappaB inhibitor IkappaBalpha." Proc Natl Acad Sci U S A 101(23): 8603-8607.

Wong, S. K. and C. K. Buckner (1978). "Studies on beta-adrenoceptors mediating changes in mechanical events and adenosine 3',5'-monophosphate levels. Guinea-pig trachea." Eur J Pharmacol 47(3): 273-280.

Woo, A. Y., T. B. Wang, et al. (2009). "Stereochemistry of an agonist determines coupling preference of beta2-adrenoceptor to different G proteins in cardiomyocytes." Mol Pharmacol 75(1): 158-165.

Wooldridge, A. A., J. A. MacDonald, et al. (2004). "Smooth muscle phosphatase is regulated in vivo by exclusion of phosphorylation of threonine 696 of MYPT1 by phosphorylation of Serine 695 in response to cyclic nucleotides." J Biol Chem 279(33): 34496-34504.

Xin, W., T. M. Tran, et al. (2008). "Roles of GRK and PDE4 activities in the regulation of beta2 adrenergic signaling." J Gen Physiol 131(4): 349-364.

Xu, T. R., G. S. Baillie, et al. (2008). "Mutations of beta-arrestin 2 that limit self-association also interfere with interactions with the beta2-adrenoceptor and the ERK1/2 MAPKs: implications for beta2-adrenoceptor signalling via the ERK1/2 MAPKs." Biochem J 413(1): 51-60.

Yan, H., D. A. Deshpande, et al. (2011). "Anti-mitogenic effects of beta-agonists and PGE2 on airway smooth muscle are PKA dependent." FASEB J 25(1): 389-397.

Yu, S. S., R. J. Lefkowitz, et al. (1993). "Beta-adrenergic receptor sequestration. A potential mechanism of receptor resensitization." J Biol Chem 268(1): 337-341.

Yuan, N., J. Friedman, et al. (1994). "cAMP-dependent protein kinase and protein kinase C consensus site mutations of the beta-adrenergic receptor. Effect on desensitization and stimulation of adenylylcyclase." J Biol Chem 269(37): 23032-23038.

Zhang, J., L. S. Barak, et al. (1997). "A central role for beta-arrestins and clathrin-coated vesicle-mediated endocytosis in beta2-adrenergic receptor resensitization. Differential regulation of receptor resensitization in two distinct cell types." J Biol Chem 272(43): 27005-27014.

Zhou, H. L., S. J. Newsholme, et al. (1992). "Agonist-related differences in the relationship between cAMP content and protein kinase activity in canine trachealis." J Pharmacol Exp Ther 261(3): 1260-1267.

Zhou, X. B., C. Arntz, et al. (2001). "A molecular switch for specific stimulation of the BKCa channel by cGMP and cAMP kinase." J Biol Chem 276(46): 43239-43245.

Vita

Sharat received his Bachelor of Science in 1999 from the University of Mangalore, India and his Master of Science in 2001 from Kerala University, India. He joined the Graduate School of Biomedical Sciences at the University of Texas Health Science Center at Houston in the Fall of 2005. Sharat joined the Cell and Regulatory Biology program and will graduate with his Doctorate of Philosophy in December of 2011.